Reference Site Conditions for Floating Wind Arrays in the United States

Michael Biglu, Matthew Hall, Ericka Lozon, and Stein Housner

National Renewable Energy Laboratory

NREL is a national laboratory of the U.S. Department of Energy
Office of Energy Efficiency & Renewable Energy
Operated by the Alliance for Sustainable Energy, LLC

This report is available at no cost from the National Renewable Energy Laboratory (NREL) at www.nrel.gov/publications.

Contract No. DE-AC36-08GO28308

Technical Report
NREL/TP-5000-89897
August 2024

Reference Site Conditions for Floating Wind Arrays in the United States

Michael Biglu, Matthew Hall, Ericka Lozon, and Stein Housner

National Renewable Energy Laboratory

Suggested Citation
Biglu, Michael, Matthew Hall, Ericka Lozon, and Stein Housner. 2024. *Reference Site Conditions for Floating Wind Arrays in the United States*. Golden, CO: National Renewable Energy Laboratory. NREL/TP-5000-89897.
https://www.nrel.gov/docs/fy24osti/89897.pdf

NREL is a national laboratory of the U.S. Department of Energy
Office of Energy Efficiency & Renewable Energy
Operated by the Alliance for Sustainable Energy, LLC

This report is available at no cost from the National Renewable Energy Laboratory (NREL) at www.nrel.gov/publications.

Contract No. DE-AC36-08GO28308

Technical Report
NREL/TP-5000-89897
August 2024

National Renewable Energy Laboratory
15013 Denver West Parkway
Golden, CO 80401
303-275-3000 • www.nrel.gov

NOTICE

This work was authored by the National Renewable Energy Laboratory, operated by Alliance for Sustainable Energy, LLC, for the U.S. Department of Energy (DOE) under Contract No. DE-AC36-08GO28308. Funding provided by the U.S. Department of Energy Office of Energy Efficiency and Renewable Energy Wind Energy Technologies Office. The views expressed herein do not necessarily represent the views of the DOE or the U.S. Government.

Cover Photos by Dennis Schroeder: (clockwise, left to right) NREL 51934, NREL 45897, NREL 42160, NREL 45891, NREL 48097, NREL 46526.

Acknowledgments

The authors would like to thank Nicola Bodini (National Renewable Energy Laboratory) for providing offshore wind reanalysis data and Carlos Garcia-Moreno (Scripps Institution of Oceanography) for helping with access of the high-frequency radar surface current data.

List of Acronyms and Abbreviations

API	American Petroleum Institute
BOEM	Bureau of Ocean Energy Management
ERA-5	European Centre for Medium Range Weather Forecasts 5 Reanalysis
GEBCO	General Bathymetric Chart of the Oceans
GW	gigawatt
HFRNet	High Frequency Radar Network
IEA Wind TCP	International Energy Agency Wind Technology Collaboration Programme
IEC	International Electrotechnical Commission
IOOS	Integrated Ocean Observing System
ISO	International Organization for Standardization
km	kilometer
m	meter
metocean	meteorological ocean
m/s	meter per second
MDA	maximum dissimilarity algorithm
nm	nautical mile
NCEI	National Centers for Environmental Information
NDBC	National Data Buoy Center
NOAA	National Oceanic and Atmospheric Administration
NOW-23	20223 National Offshore Wind dataset
NREL	National Renewable Energy Laboratory
OCS	Outer Continental Shelf
R&D	research and development

Executive Summary

This report presents site condition information that was developed to represent four U.S. areas where floating offshore wind energy development is likely. Floating wind farm design is highly site-specific, so information about the site conditions in a project area is key to performing realistic design studies. However, specific site condition data for potential (floating) offshore wind projects in the United States are very limited in the public domain. Relevant individual data sources exist but there are gaps and numerous challenges to collecting and combining the data into a cohesive dataset for a given site. This report describes how the authors addressed those challenges and developed representative site condition datasets for four floating offshore wind energy areas in the United States. These datasets can facilitate future site-specific floating wind research endeavors.

In this work, we first reviewed existing literature on site condition data, processing, and characterization methods. The most important site condition data for floating wind farm engineering designs can be divided into two categories:

- Meteorological ocean (metocean) conditions: Characteristics of the meteorological and oceanographic climate, especially measures of wind, wave, and current characteristics
- Seabed conditions: Geophysical characteristics of the seabed including the bathymetry, seismic activity, and seabed features, and geotechnical characteristics of the soils and rocks on-site.

We selected the following four regions for providing representative site condition data:

- Humboldt Bay: An area in Northern California with two lease areas
- Morro Bay: An area in Southern California with three lease areas
- Gulf of Maine: An area being considered for a research-oriented wind farm as well as lease areas
- Gulf of Mexico: An area southwest of current lease areas that is in deeper waters.

Bathymetry data for each site are based on rectangular gridded depth values from the National Centers for Environmental Information Digital Elevation Model Global Mosaic, interpolated to a uniform grid with a 200-, 500- and 1000-meter horizontal resolution. The soil characteristics at each site are based on an average Folk classification (i.e., the fraction of soil that is mud, sand, or muddy sand) at each site's centroid based on a spatially weighted average of surrounding measurement points from the usSEABED database.

We gathered metocean data at each site from a combination of metocean buoys, wind resource reanalysis data, and radar-based current measurements. National Data Buoy Center measurement data are used as the primary measurement dataset for wave data. The buoy wind measurements a few meters above the water surface had too much uncertainty in scaling up to hub height and the availability of ocean current measurement data is too intermittent. Therefore, we used two additional data sources to fill these gaps: wind data from the 2023 National Offshore Wind dataset and ocean surface measurements from the Integrated Ocean Observing System High Frequency Radar Network. We processed and merged these data sources for wind, wave, and currents into one homogenous hourly time series dataset for each site. We then used these hourly time series as a basis for analyzing metocean distributions and extreme conditions.

We calculated metocean extreme values for strength load cases and joint probabilities for fatigue load cases using the combined and processed time series. Extreme parameters of wind, wave, and currents for a range of return periods were computed using a distribution fitting process. These results include extreme return-period values for wind speed, wave height, and current speed, along with corresponding expected values of directions of each, and wave peak period. Conditional values for each wind speed bin are also provided. These extreme metocean results are based on all data points in the time series and do not include specific assessment of extreme events such as hurricanes, which may be of particular relevance for the Gulf of Mexico. The joint distribution of metocean parameters is represented by a clustering approach, providing 100 probability-weighted metocean conditions that can be used for fatigue loads analyses.

The combined site condition datasets provide ready-to-use inputs for floating wind research and development endeavors that need realistic and representative data for several U.S. regions. Metocean extreme values and fatigue bin cases provide inputs for loads analyses while curated hourly time series provide input for logistics analyses or power production simulations. Although preexisting sources provide a good basis for research, the applicability for a comprehensive offshore wind farm design might be limited. Therefore, developing a single, publicly available dataset containing all the metocean data needed to design a (floating) offshore wind farm is an important contribution to site-specific floating wind research and development in the United States.

Table of Contents

List of Figures

List of Tables

1 Introduction

The design of floating offshore wind turbines and floating wind farms is highly dependent on local site conditions. Wind conditions determine the maximum possible annual energy production of the farm, including the degree of wake losses depending on the array layout. Individual floating wind turbine systems are designed and sized to provide good stability across the range of meteorological ocean (metocean) conditions and to ensure survivability and safe operations in extreme conditions. The wind, wave, and current characteristics therefore must be well-characterized to design floating wind systems that strike the right balance between cost-effectiveness and survivability. Metocean conditions also affect installation and maintenance processes; offshore operations can only be done in mild conditions, so more severe metocean conditions reduce the availability of "weather windows" in which operations can be conducted. The water depth dictates the types of mooring systems that can be used, and the seabed soil type dictates which anchor types can be used. These seabed factors can vary considerably between lease areas as well as within a lease area. Seabed variations and exclusion areas constrain the positioning of anchors and potentially the array layout. For example, while gentle slopes are no obstacle for most anchor types, steep slopes should generally be avoided. Therefore, detailed knowledge of the site conditions is key to successfully addressing the design considerations described earlier.

Site condition data for potential floating wind energy locations in the United States are limited. The most applicable data on wind, wave, and currents are spread across several sources with varying degrees of availability and completeness. Data for seabed depth (bathymetry) at a low resolution are available from a central source with global coverage, but available data for soil conditions generally lack the spatial resolution or the measurement parameters needed for floating wind farm design. This lack of complete and collated site condition data presents a considerable obstacle to analyzing floating wind turbines and arrays in U.S. site conditions.

The floating wind energy industry is still at an early stage and engaged in significant research and development (R&D) activities, especially for dealing with the large range of water depths of U.S. locations and for optimizing designs for serial production and supply-chain compatibility. Despite the significant experience of the oil-and-gas industry with floating structures and the European wind industry with fixed-bottom offshore wind turbines, the floating wind industry faces unique challenges related to the economical large-scale deployment of many floating structures in deep water. These challenges prompt many ongoing R&D efforts, which often require assumptions about site conditions but do not have the resources of a project developer to conduct independent site condition measurements. Therefore, there is a need for organized, open-source site condition data to support numerous floating wind R&D activities. As part of the Floating Wind Array Design project, the National Renewable Energy Laboratory (NREL) set out to gather and process the available site condition data for several regions to generate combined and ready-to-use datasets of representative U.S. site conditions for use in floating wind energy R&D projects. This report describes the data sources and methods we used to generate those

representative site condition datasets, and provides a summary of the datasets. The datasets can be downloaded from the NREL data catalog (Biglu et al. 2024)[1].

This effort is in alignment with Task 49 of the International Energy Agency Wind Technology Program (IEA Wind TCP): Integrated Design of Floating wind Arrays. The authors developed the U.S. reference site conditions in coordination with Task 49 Work Package 1, which developed reference site conditions for floating wind arrays for a set of 10 locations around the globe. That work package also identified requirements of metocean datasets for floating wind arrays, which informed our selection of parameters and processing methods in the present work (IEA Wind TCP Task 49 2021).

1.1 Existing Site Conditions Data Sources and Studies

In this work, we reviewed existing literature on site condition data, processing, and characterization methods. The most important site condition data for floating wind farm engineering design purposes can be divided into two categories:

- Metocean conditions: combined characteristics of the meteorological (weather-related) and oceanographical (ocean-related) conditions, especially measures of wind, wave, and current characteristics
- Seabed conditions: Geophysical characteristics of the seabed including the bathymetry, seismic activity, and seabed features, and geotechnical characteristics of the soils and rocks on-site.

Most available global metocean data are available for locations where oil-and-gas fields are located. International standards, such as from the American Petroleum Institute (API) and International Organization for Standardization (ISO) (API 2014b; ISO 2015), provide basic metocean data for some of these locations. The project to establish a System of Industry Metocean data for the Offshore and Research Communities (SIMORC) covers more than 7,700 datasets from major oil companies containing wind, waves, currents, and sea levels (MARIS et al. n.d.)[2], among others in the Gulf of Mexico.

The same applies for the Unites States, in which most data are available where the oil-and-gas industry operates. At most potential U.S. offshore wind energy sites, no offshore construction has been performed previously, with the exception of the Gulf of Mexico, leading to a lack of physical site condition data at those locations (Bailey et al. 2015). Knowledge about the local soil and marine conditions is key to successfully developing offshore wind farms (Bailey et al. 2015). However, although there might be metocean site condition data available at some locations as a result of offshore oil-and-gas developments, the datasets may not be sufficient for the design of offshore wind turbines. For example, the wind speed at hub height and respective wind speed conditioned data are mostly not available.

[1] https://data.nrel.gov/submissions/241
[2] Mariene Informatie Service "MARIS" BV (MARIS), www.maris.nl

1.1.1 Metocean Site Conditions

Metocean site condition data for potential (floating) offshore wind project sites are limited in the public domain. None of the few sources available provide an easily accessible and complete metocean dataset that contains all required parameters for the design of an offshore wind farm.

In the offshore wind energy industry, metocean measurement data are often unavailable for a sufficiently long period to accurately characterize the metocean conditions. While offshore wind projects are being developed, developers often install metocean buoys and floating lidar buoys at their lease areas. Lidar buoys are used to measure hub-height wind speeds, because metocean buoys typically measure wind speeds at only around a 3-meter (m) height. These metocean measurements typically only begin a few years before the actual offshore construction and installation activities start, which is far too late to gather enough measurements for the basic design and they usually don't contain accurate information on turbulence.

Initial load assessments are therefore often based on hindcast or reanalysis data, which are based on simulations calibrated to historical measurements. These synthetic data sources can have large uncertainties, so best practice is to calibrate or verify them against measurement data gained in the immediate geographical vicinity (ISO 2015).

Both synthetic and measurement data sources exist for U.S. metocean conditions. The National Oceanic and Atmospheric Administration's (NOAA's) National Data Buoy Center (NDBC) deployed more than 100 moored weather buoys in U.S. coastal and offshore waters, many of them operating since the early 1980s (NDBC 1971), providing measurement time series up to 40 years. Depending on each buoy's sensors, the data can include wave, wind, and current measurements. However, the data coverage and consistency are somewhat variable, meaning that considerable effort may be required to use the data reliably.

Data from NDBC buoys were also used in standards and recommended practices, such as by API and ISO (API 2014b; ISO 2015), to provide metocean conditions on the Californian coast and Gulf of Mexico. It is therefore a proven approach to base metocean assessments on the measurement data provided by these stations. However, the conditions of the reference site should be similar in water depth, fetch limits, and overall climate (ISO 2015).

Stewart et al. used data from 23 NDBC buoys to create a metocean database for use in U.S. offshore wind energy research (Stewart et al. 2016)[3].The dataset provides conditional probability functions for the following metocean parameters: wind speed, significant wave height, wave-peak-spectral period, wind direction, and wave direction. However, for a comprehensive metocean site assessment, it is crucial to consider extreme events, accurate wind speeds at hub height, and ocean currents, and provide time series as well, which are not included in the aforementioned dataset. Other important design parameters include wind turbulence, shear, and coherence; however, these are often not available in the public domain.

The predominant source for synthetic metocean data combining both wind and waves is the European Centre for Medium Range Weather Forecasts 5 Reanalysis (ERA5) dataset (Hersbach

[3] The dataset is available here: https://www.nrel.gov/wind/nwtc/metocean-data.html.

et al. 2020), which is the fifth generation of such a model and output from an atmospheric reanalysis of the global climate since 1940. The ERA5 dataset is beneficial because it provides a vast and consistent set of distributed wind and wave estimates at an hourly resolution. However, its estimates have high levels of uncertainty and often considerable disparities with local metocean buoy measurements.

NREL has produced reanalysis results for wind velocities at the hub heights of offshore wind turbines in U.S. regions. NREL released the 2023 National Offshore Wind dataset (NOW-23), which focuses on the offshore wind resource and provides 5-minute (min) velocity data for key offshore wind regions in the United States (Bodini et al. 2020, 2024). However, this dataset does not consider shear, turbulence intensity, or coherence. It replaces the offshore component of the WIND toolkit (Draxl et al. 2015), published some 10 years ago and currently one of the main resources for stakeholders carrying out wind resource assessments on the continental United States.

An important U.S. data source for water surface current measurements is the High Frequency Radar Network (HFRNet) operated by the U.S. Integrated Ocean Observing System (IOOS) (NOAA n.d.). By using multiple radar measurements of wave velocities and comparing with expected wave speeds for the given wavelength, the radar network can estimate surface current velocities over a wide area of ocean surface. These velocity data are available at hourly intervals over a large portion of the U.S. coast including Hawaii and Puerto Rico and with a spatial resolution of 6 kilometers (km) or finer. This data source is notable because measurements of currents are not included in ERA5 and are only available from some NDBC buoys.

Considering the previously mentioned sources of metocean data, no single dataset provides the required information for floating wind turbine analysis with sufficient quality. Therefore, obtaining a reliable set of site conditions requires selecting, processing, and combining data from multiple sources.

1.1.2 Seabed Site Conditions

Data characterizing the seabed for offshore wind regions in the United States can be divided into geophysical and geotechnical data. In general, geophysical survey data are more commonly available than specific geotechnical survey data, mainly because geotechnical data are specific to a particular location, whereas geophysical data cover large areas. For general applicable site conditions, the most important element of geophysical conditions is the spatially varying seabed depth, or bathymetry. The Coastal Relief Model, provided by NOAA's National Centers for Environmental Information (NCEI 2023), provides gridded elevation/depth data in the U.S. coastal zone including the continental United States, Alaska, Hawaii, and Puerto Rico at a resolution of 1 arc-second[4]; however, it has limited coverage of the Gulf of Maine and Gulf of Mexico, and very little coverage of the West Coast. The NCEI Digital Elevation Models Global Mosaic provides more complete coverage of U.S. coasts at a resolution of 3 arc seconds (NCEI 2024). In addition, the General Bathymetric Chart of the Oceans (GEBCO) (GEBCO

[4] 1 arc second " at equatorial sea level = 1852m/60 = 30.86666667m

Compilation Group 2023) provides gridded bathymetry data for the entire globe at a resolution of 15 arc seconds.

Geotechnical site data are very important for floating wind projects as well, as they affect anchor compatibility and holding capacity. Data on the stratification, geological characteristics, and geotechnical properties of the soils and rocks on-site are typically obtained from geotechnical surveys involving taking cores (depthwise soil samples) at key locations where anchors will be placed (International Society for Soil Mechanics and Geotechnical Engineering 2005). These surveys are often done by developers for specific projects; however, there are limited geotechnical data available from public datasets and specific publications.

The usSEABED dataset provides the largest public data of sediment samples and other observations within the U.S. Exclusive Economic Zone (Buczkowski et al. 2020). It comprises more than 300,00 georeferenced data points and includes information about grain size, sediment texture, mineral type, and more. These data can be used to classify soil types into established qualitative categories. However, the data points are sparse relative to the size of an offshore wind lease area so they are not suitable for identifying soil variations within a lease area. The International Ocean Discovery Program (IODP) provides detailed geotechnical data recorded from cores and including charts and measurement values, providing information on seabed sediments, rocks, and subseafloor environment for many drilling locations around the world (International Ocean Discovery Program 2023). However, those sites are few and mostly not in the immediate vicinity of offshore wind energy areas. Publicly available datasets often contain only one or a few data types that provide good information on a specific subject area. Furthermore, postprocessing of the data is required in many cases to better understand seabed conditions in a particular area, and it is often necessary to combine and analyze several sources, such as is done in desktop studies. The Bureau of Ocean Energy Management (BOEM) commissioned several site-specific desktop studies, such as for the West Coast, including Humboldt Bay (Tajalli Bakhsh et al. 2020, 2023). These reports summarize publicly available geophysical, geological, and geotechnical data to provide a better understanding of potential geohazards in the vicinity of currently planned floating offshore wind farms. Publicly available geophysical and geotechnical data for the Gulf of Mexico and East Coast, including the Gulf of Maine, that include seafloor and near-seafloor conditions relevant to offshore wind energy developments were provided by Fugro (Trandafir et al. 2022). Another desktop study was conducted for an offshore wind research array in the Gulf of Maine that provided detailed site-specific assessments, including seabed-related data, as well as other topics such as vessel traffic and marine mammals (State of Maine 2021). NOAA offers a publicly accessible Gulf of Mexico Data Atlas that includes many types of information, including bathymetry and soil data as well as economic and environmental information (NOAA 2011).

In summary, bathymetric data are available for all floating wind energy locations in the United States, whereas the availability of suitable site-specific geotechnical and geophysical data is very limited.

1.2 Objectives and Scope

For the Floating Offshore Wind Array Design project, our objective was to create site condition datasets representing key U.S. regions for floating offshore wind energy development. This work was conducted using existing publicly available data sources and did not involve running models

to generate new data. Our main tasks included identifying data sources, processing and integrating the data, computing metocean metrics for loads analysis, and publishing the combined datasets for easy access and use. These datasets will support the emerging floating offshore wind industry in the United States by providing a well-organized and processed collection of reference site data that can be easily utilized in R&D projects and industry. Typical applications of this data include inputs for modeling software tools used in various research studies on floating wind system power production, performance, logistics, and technoeconomics.

When selecting reference site locations, we considered data availability, relevance to near-term floating wind energy development, and a desire to include a range of characteristics so that the datasets could be used to evaluate technologies and designs over a range of conditions. These considerations were also informed by analyses from IEA Wind Task 49 that looked at key site condition metrics for around 50 sites worldwide. Ultimately, we selected the following four locations to serve as the geographic reference points that our site condition datasets should represent:

- Humboldt Bay: An area in Northern California with deep water (from 550 to 1,300 m) and two existing commercial lease areas with a combined potential capacity near 2 gigawatts (GW)

- Morro Bay: An area in Southern California with deep water (from 900 to 1,400 m) and three existing commercial lease areas with a combined potential capacity near 4 GW

- Gulf of Maine: A region of long-standing interest for floating wind energy development, and a specific location being considered for a research-oriented wind farm (with a water depth of just under 200 m)

- Gulf of Mexico: A region of general interest for offshore wind energy development with hurricane conditions[5], and a specific location southwest of current fixed-bottom offshore wind lease areas (with a water depth of 80 m, as suitable for floating wind turbines).

The site condition datasets are tailored to include the most relevant information for floating wind farm research and development activities, within the limits of available data. The included site characteristics are as follows:

- Metocean data
    - Hourly time series of the following channels
        - Wind direction at 10 m above the water surface
        - Wind speed at 10 m above the water surface
        - Wind direction at hub height (150 m)
        - Wind speed at hub height (150 m)
        - Mean wave direction
        - Significant wave height

[5] We do not specifically assess hurricane events in our analysis, but extreme metocean conditions are included in general.

        - Peak wave period
        - Surface current direction
        - Surface current speed
        - Air temperature at 10 m above the water surface
        - Water temperature
    - Processed extreme values
        - Unconditional extreme values of hub-height wind speed, significant wave height, and current speed for return periods from 1 to 500 years
        - Extreme values of significant wave height and current speed conditioned to wind speed in 2 meter per second (m/s) increments
        - Expected values of wind/wave/current direction and peak wave period associated with the extreme values
    - Metocean fatigue bins
        - One hundred bins of hub-height wind velocity and wave conditions with associated probabilities and standard deviation measures generated by a clustering method to represent the joint wind-wave probability distribution
- Seabed data
    - Bathymetry
        - Seabed depth over a rectangular grid with a 200-m, 500-m and 1000-m resolution
    - Soil characteristics
        - Folk classification (e.g., sand, clay, mud fractions)
        - Grain size as Krumbein phi scale.

Wind speed near the surface (e.g., at 10 m height) is relevant for determining the limits of marine operations during installation and maintenance phases. Wind speed and direction are most relevant for turbine performance and farm energy production. Wind shear and veer, which are of secondary importance, are left for future more detailed data processing. Wind turbulence information was not available from the existing data but can be estimated from other studies or standards. The wind, wave, and current direction data allows for analysis of misalignment effects. Wave direction, significant wave height, and peak spectral period provide the most fundamental parameters for floating system loads analysis. Water surface current speed and direction represent the most dominant current drag force on floating systems, and profiles can be assumed to estimate current speeds at depth. Tidal variations in sea level, which are most relevant for shallow water and tension-leg platforms, are not included. Other types of site information are also important when designing floating wind farms, such as transmission infrastructure, the local power grid condition, other marine space uses, local infrastructure, and socio-economic and political factors. In this report we only focus on the metocean and seabed parameters listed above.

In the remainder of the report, Section 2 describes the methodology for producing the reference site conditions, including data sources and analysis methods for the metocean data. Section 3 presents the resulting site conditions for the four selected areas. Section 4 provides a conclusion and discusses the limitations and possible future work with the site conditions. Appendices provide the full set of computed metocean parameters that can be used for floating wind turbine design load cases, as well as additional listings about data sources and references.

2 Methodology

The process of developing the reference site conditions can be divided into three parts: gathering and processing metocean data, computing extreme and fatigue load case parameters from the metocean data, and gathering seabed data. Because of the limited and dispersed nature of existing data sources, a large part of the effort involved gathering, checking, and combining data for each site. This process was especially demanding for the metocean data, for which many sources exist but there are difficulties related to spatial and temporal coverage as well as data reliability. Analyzing the data to produce parameters for load cases was also challenging because practical methods are not widely shared and agreed upon. In contrast, gathering and using the seabed data is relatively straightforward; the main challenge is simply that there is little data available for soil conditions.

2.1 Metocean Data Collection and Processing

As described in Section 1.1.1, the metocean data required for analyzing a floating wind turbine or farm are not available in a complete and ready-to-use form from any single existing source. Therefore, we surveyed a wide range of possible metocean data sources to find those that are the most suitable for obtaining metocean parameters. We then checked and processed the data to compile different data sources into the same format and replace erroneous measurement values with alternative sources to produce consistent and continuous metocean data time series.

Our gathering and processing of metocean conditions for the four sites draws from three data sources:

- Metocean buoy measurements of wave and current conditions
- Hindcast atmospheric reanalysis results of wind data
- High-frequency radar measurements of surface ocean current data.

These three data sources and the methods taken to process them are covered in the following subsections.

2.1.1 National Data Buoy Center (NDBC) Metocean Buoys

NOAA's NDBC oversees more than 100 metocean buoys in coastal and offshore U.S. waters, many of them operating since the early 1980s (NDBC 1971). It is the most extensive metocean buoy measurement network in the United States, with buoy locations shown in Figure 1.

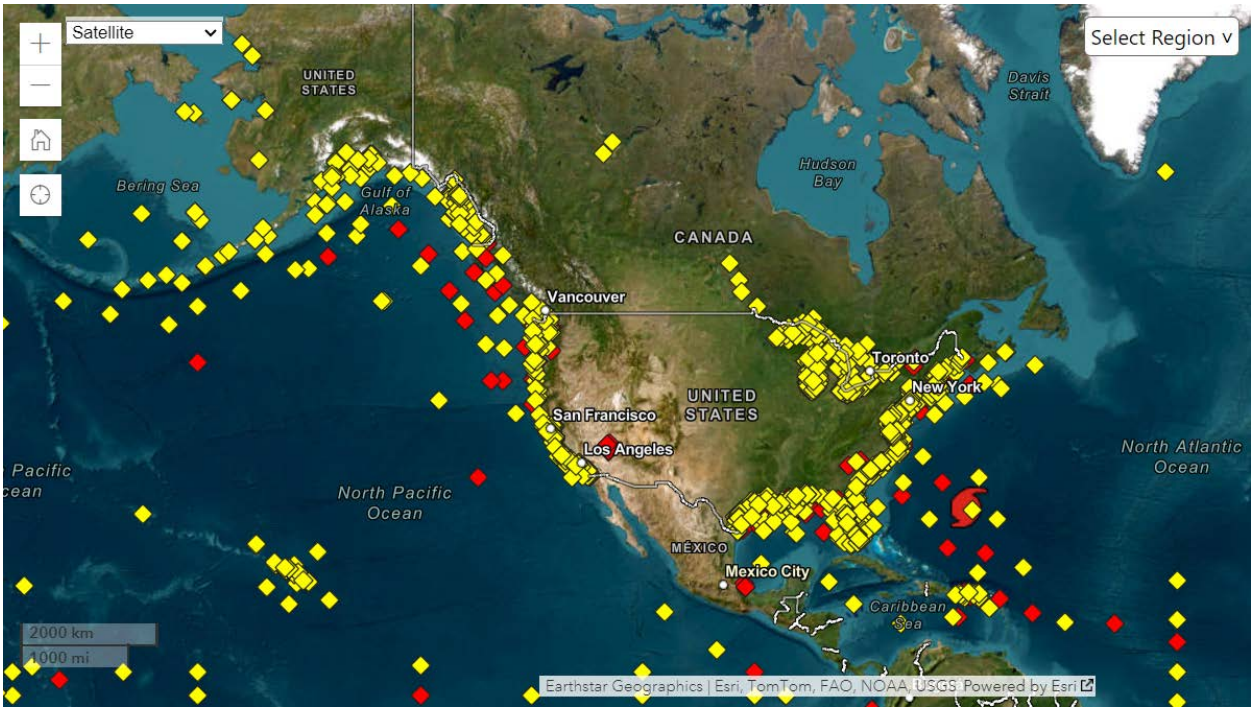

Figure 1. NDBC metocean observation sites located off U.S. coasts. ***Image from the National Data Buoy Center***

Metocean buoys are thought to be the most accurate source of wave measurements, so the NDBC buoys were our primary source for wave data. Their wave measurement data—including significant wave height, peak wave period, and mean wave direction—are available typically in time series with between 30-minute and hourly intervals. In some cases, there is also ocean current data available, including depth profiles. However, there is often only a few years of reliable current data available, and some readings appear to be incorrect. Therefore, we used the ocean current data provided by the NDBC buoys when other ocean current measurements were unavailable.

The metocean buoys typically include wind measurements (wind speed and direction) at a height of 3.2 m to 4.1 m above the water surface, depending on the specific buoy. These measurements are available typically with between 10-minute and hourly intervals. Extrapolation to hub height would be very sensitive to assumptions about the wind shear factor, and could underpredict extreme wind speeds due to shielding effects of large storm waves (BOEM 2020). Therefore, we used NOW-23 data for wind velocities at 10 m above the water surface and at hub height.

The process for gathering the NDBC data involved downloading individual data files for specific buoys from the NDBC website and then combining and processing the data. We then combined the data from the files to create a single dataset for the metocean readings at each buoy. We combined the various time series into a single hourly time series by averaging the data over each

1-hour interval. We calculated the averages for wave direction and peak period by weighting them according to significant wave height, ensuring that the average direction within a given period reflects the primary direction of energy. The measurement intervals for each parameter vary depending on the specific year, buoy type and location. The data files sometimes had changes in format or number of channels across different years, so this step also involved making manual adjustments for these inconsistencies. We also had to check the data because of missing and faulty entries. Due to the large amount of available data, we decided to discard missing entries instead of interpolating them, which was already done by Stewart et al. (2016). Missing entries were common for wave, and ocean current data, predominantly for directional values. A summary of the covered time period per parameter is provided in Appendix F.

Appendix G provides some supplementary reference information about the NDBC buoy data including a description of the metocean parameters in the data files, links to access the data, and information on measurement accuracy of different NDBC sensors. This information could help others looking to use the NDBC data directly.

2.1.2 *National Offshore Wind (NOW-23) Dataset Atmospheric Hindcasts*

The NOW-23 dataset was generated using version 4.2.1 of the Weather Research and Forecasting model, initialized with the ERA5 reanalysis dataset (Bodini et al. 2024). The model is configured with an initial horizontal grid of 6 km and a nested internal domain that refines the spatial resolution to 2 km. The model runs with 61 vertical levels, of which 12 levels are in the lower 300 m of the atmosphere and extend from a 5-to 45-m height. For all regions, the NOW-23 dataset begins on January 1, 2000. For the Hawaii and North Pacific regions, NOW-23 extends to December 31, 2019. For the South Pacific region, the model runs until December 31, 2022. For all other regions, the model runs until December 31, 2020. The NOW-23 data consists of time series at a 5-min resolution, and are made available as HDF5 files (Bodini et al. 2020), which is a file format using hierarchical structure for storing an managing scientific data. The covered regions are shown in Figure 2.

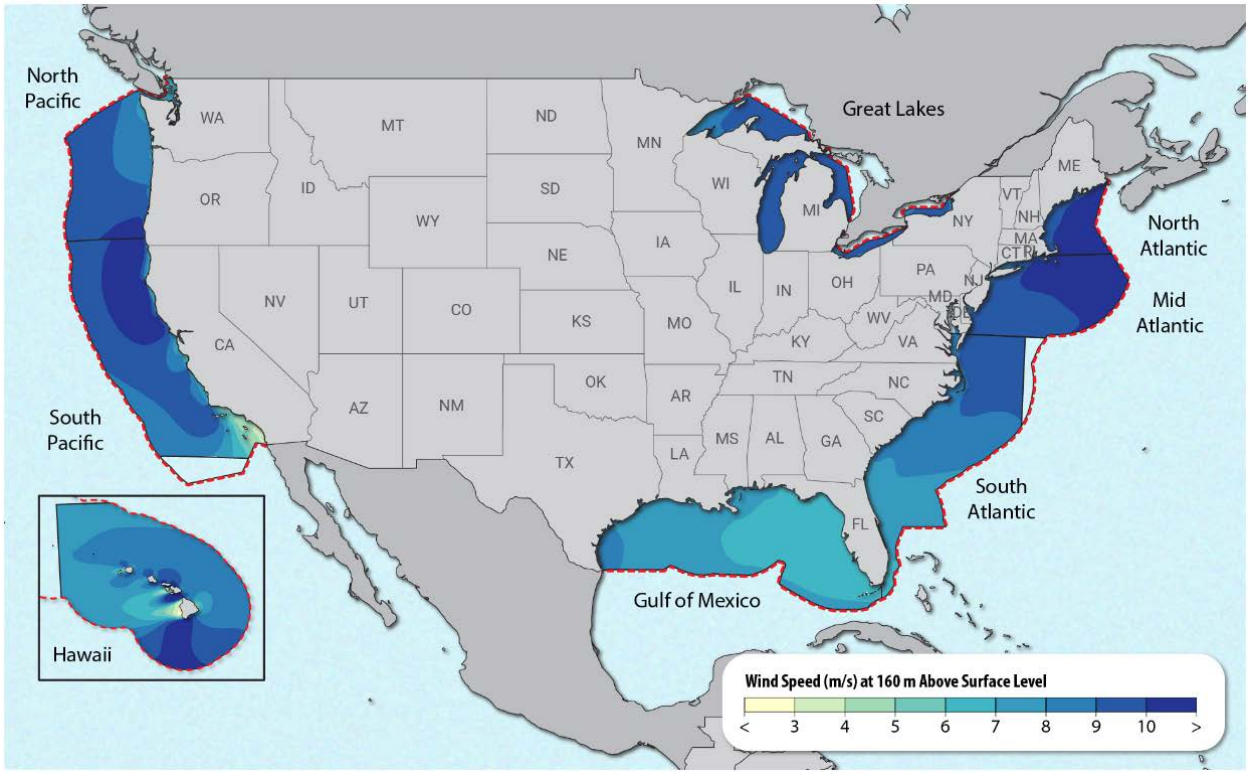

Figure 2. NOW-23 map of the contiguous United States plus Hawaii, outlining the domain of each region's offshore wind zones. ***Image from Bodini et al. (2024)***

We used the NOW-23 dataset to determine the wind inflow conditions at each reference site over the duration of the dataset. NOW-23 provides wind speed and direction at different heights: starting at 10 m, then in 20-m intervals between a 20- and 300-m height and values at 400- and 500-m heights. We converted the 5-min intervals of the NOW-23 dataset into hourly intervals by calculating the average values over one-hour periods. This ensures that the data are aligned with other metocean parameters up to a height of 400 m and interpolated the wind velocity at the x-y coordinates of interest for each site, until reaching a height of 400 m to support different wind turbine hub heights. It should be noted that this is an interpolated velocity as opposed to a rotor-averaged velocity. The latter is more accurate for power assessment as it takes into account the entire rotor surface and the rotor characteristics, whereas interpolation only takes into account the speeds at two heights. Our choice was simpler and did not require assumptions about the turbine rotor, making it more suitable for providing basic site condition data. We calculated the wind speed and direction at hub height (150 m) via linear interpolation between data at 140 m and 160 m, which we consider to be a more representative estimate than choosing between 140 m and 160 m due to the wind velocity distribution over height. However, it should be noted that wind speed profiles are not linear.

The wind shear factor at 150 m could be computed from the wind speeds at different heights; however, the turbulent flow in the dataset results in variations if the exponential shear factor is computed based on wind speeds at vertically adjacent points. Other methods, such as fitting a logarithmic profile to the wind speeds over the height of a full rotor, could provide more representative time-domain shear results. Wind shear relationships that are based on wind speed

and direction computed over the entire dataset could also be developed. However, given the objective of providing a simple and clearly defined dataset, we avoided making wind shear estimates and the assumptions they require.

The NOW-23 dataset does not include values for turbulence. Calculating turbulence intensity from a time series requires a sample rate of at least 1 Hertz (Manwell et al. 2009), so it could not be done by postprocessing 5-minute wind-velocity time series of the NOW-23 dataset.

Wind shear factors and turbulence intensities can be estimated by users according to their needs and preferred methods, taking into account the limitations of the current dataset. One of the easiest approaches for each parameter is to use an existing distribution that provides a shear factor α and turbulence intensity as a function of wind speed and direction. In our usage of the dataset, we followed the American Bureau of Shipping's *Floating Offshore Wind Turbines* guide recommendations with a shear factor of 0.14 for normal conditions and 0.11 for extreme conditions (American Bureau of Shipping 2020). For turbulence intensity, we assumed values that were provided by IEA Wind Task 49 based on a full-scale turbulence model that accounts for surface roughness effects due to waves (Santos et al. 2023). These turbulence intensity values are listed in Appendix E. Further information—and a list of all included parameters—can be found in Appendix G.2.

2.1.3 High Frequency Radar Network (HFRNet) Current Measurements

HFRNet operates shore-mounted radar units that measure ocean surface current velocities over a wide area with a range of up to 200 km and resolution of 6 km or finer (NOAA 2024). The network is operated by IOOS, a national-regional partnership (NOAA n.d.), and its ocean surface current data are provided by NDBC in collaboration with the Scripps Institution of Oceanography Coastal Observing Research and Development Center (Hervey and Petraitis 2015). Figure 3 shows the spatial coverage, which is very extensive in some areas such as the West Coast but limited in others. Most of the Gulf of Mexico, Southeast Coast, and Gulf of Maine are not covered. The high-resolution data shows that the Outer Banks, a line of islands off the coast of North Carolina, have probably some of the highest current speeds.

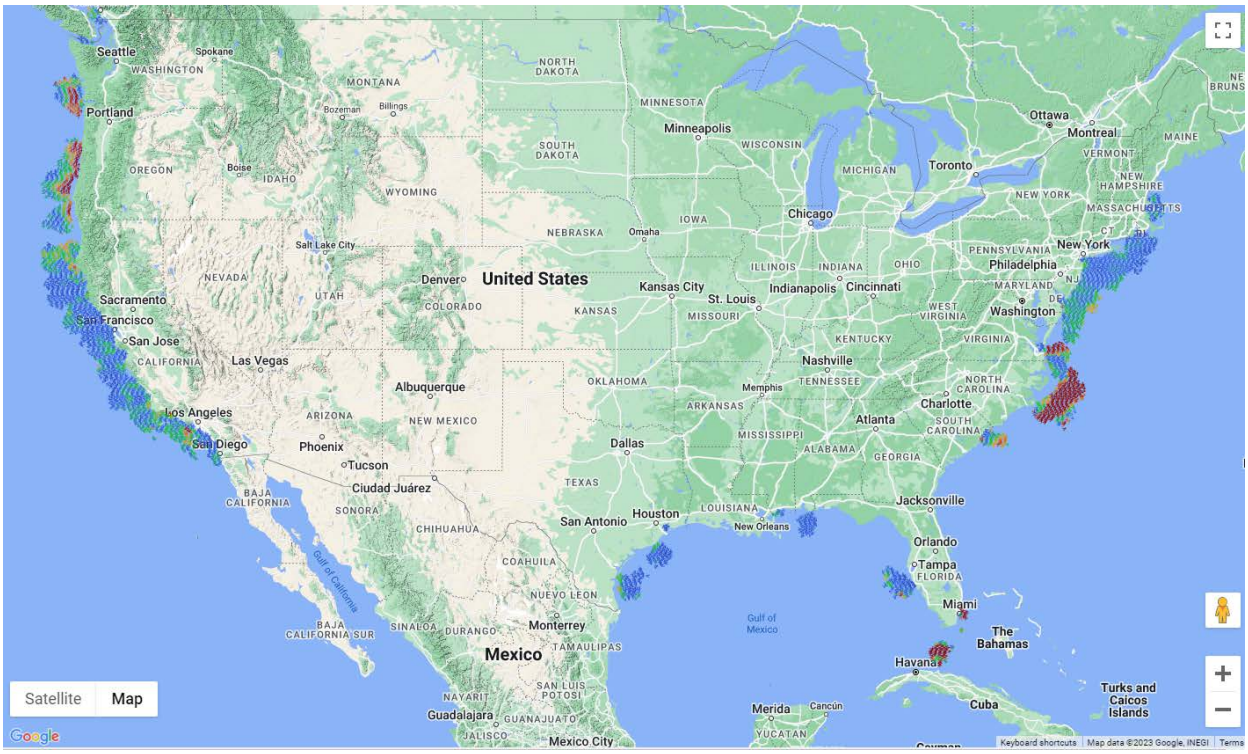

Figure 3. Ocean surface currents High Frequency Radar Network coverage around U.S. coasts at a 6-km resolution. *Image from https://cordc.ucsd.edu/projects/hfrnet/.*

Note: Colors represent current speeds, from low (blue) to high (red).

The HFRNet dataset contains hourly time series up to 20 years, depending on the location. Because of the nature of the measurement method, the measured velocities reflect conditions in the upper 0.3 to 2.5 meters of the ocean, depending on the operating frequency and the water column's vertical velocity profile (Hervey and Petraitis 2015). Further information about the data access and a list of all included parameters can be found in Appendix G.3.

2.1.4 Metocean Data Integration

After gathering the metocean data for a site, it needs to be combined into a single time-series dataset so that the correlations between different metocean parameters can be accounted for in any subsequent analyses. The main goal is to create one metocean time series dataset for each site with consistent time steps and clean data. As the main measurement data source for wave conditions at sea level, we used the metocean buoys operated by the NDBC. Data gaps, especially for wave-related parameters, can be filled with data from adjacent buoys. We took wind-related data at a 10 m height and at turbine hub height from the NOW-23 dataset. Due to the limited data coverage of ocean current measurements from NDBC buoys, we used measurements from HFRNet where possible.

We included only surface-level current data in the reference site conditions for several reasons. First, the HFRNet dataset was by far the most consistent and extensive data source for currents in the areas of interest. Surface currents are a clear and well-defined quantity, whereas considering currents at depth introduces many variables related to current profiles and potential directional variations with depth. In our experience, most of the effect from currents on a floating wind

turbine design comes from current drag loads on the floating platform (as opposed to the mooring lines or power cables), and surface currents provide a good approximation of the currents acting over the submerged part of a shallow-drafted platform. For platforms with deep drafts such as spars, a current profile could be assumed to scale down the surface current velocities with depth, based on additional analysis of the site's current characteristics. As with wind shear, we did not include such an analysis in our scope and leave such methods and assumptions to users to suit their specific needs. For these reasons, we only include surface current data, even when using acoustic Doppler current profiler measurements from NDBC buoys that include current velocities at multiple depths.

The time span of the available time series data varies per location and data source. For the NDBC buoy data, the time series often go back to the 1970s, whereas the NOW-23 dataset time series starts in 2000 and the HFRNet ocean current data starts in 2012. Detailed information about the time ranges, data coverage, and links to the respective sources can be found in Appendix F. To provide a homogenous metocean dataset with both wind and wave data available for most of the time span, we used a time range from 2000 to 2020 (21 years) when creating the combined time series.

The time steps of all data sources vary, as typical time steps are in 5-minute intervals for the NOW-23 data, 20 minutes for NDBC wave data, and 1 hour for HFRNet ocean current data. We processed the various time series into a combined time series with hourly resolution, leading to a homogeneous, combined file for each reference site. For this purpose, all values were averaged over a period of 1 hour. In the case of the wave- and current-related directional data and wave peak period, we computed the average as a weighted average, wherein the weighting for current direction is current speed and the weighting for wave heading and peak period is significant wave height. This approach ensures that the average direction calculated within a specific period represents the main direction of energy. For all other parameters, we calculated a classical mean value. Missing or faulty values are marked as NaN (not a number) in the data files and were not included in the averaging.

The resulting metocean data files contain hourly time series of all the considered parameters, which are shown in Table 1. All directions are in compass headings measured in degrees clockwise from geographic north. Wind, wave and current directions are given as the heading from which the wind/wave/current is coming. This direction convention deviates from the common convention in which current directions are typically defined as the heading the current is flowing towards. We defined all directions the same way to make the dataset easier to use.

Table 1. List of Metocean Parameters Contained in the metocean1h File

Data Type	Parameter Key	Unit	Description	Data Source
Time	YY	yr	Year	
	MM	mo	Month, from 1 to 12	
	DD	dy	Day of month, from 1	
	hh	hr	Hour, from 0 to 23	
Wind Data	WDIR10m	deg	Wind direction at 10 m (“from”)	2023 National Offshore Wind dataset (NOW-23)
	WSPD10m	m/s	Wind speed at 10 m	
	WDIR150m	deg	Wind direction at 150 m (“from”)	
	WSPD150m	m/s	Wind speed at 150 m	
Waves	MWD	deg	Mean wave direction (“from”)	National Data Buoy Center (NDBC)
	WVHT	m	Significant wave height	
	DPD	sec	Peak wave period	
Ocean Currents	CDIR	deg	Surface current direction (“from”) at 0 m	High Frequency Radar Network (HFRNet)
	CSPD	m/s	Surface current speed at 0 m	
Temperature	ATMP10m	deg C	Air temperature at 10 m	NOW-23
	WTMP	deg C	Water temperature	NDBC

2.2 Metocean Analysis

After combining the hourly metocean time series (as described in Section 2.1.4), we used these combined time series for analysis of extreme metocean conditions and analysis of the joint probability distribution. These results are typically used when setting up design load cases for simulations that evaluate extreme and fatigue loads, respectively.

2.2.1 Extreme Values

The extreme value analysis is focused on estimating the most extreme metocean conditions that can be expected to occur within certain return periods to account for extreme events during the service lifetime of an offshore structure. A return period indicates the time span in which a certain extreme value is expected to occur; for example, a 50-year wave height is the wave

height that is expected to occur on average once every 50 years, which is equivalent to a probability of occurrence of 0.02 in any given year.

Extreme values are generally estimated by fitting a probability distribution to a set of existing data, and then reading values off the probability distribution at probabilities that correspond to the desired return period. The quality of results depends heavily on the time span of the input data, and how a distribution is fit to it. ISO 19901-1 recommends using a time series of at least 25 years to obtain accurate estimates of extreme events with up to a 100-year return period (ISO 2015). Different standards require different return periods. A return period of 50 years is common (International Electrotechnical Commission [IEC] 2019a, 2019b), but some standards specify 100 or even 500 years to account for extreme events such as hurricanes (ABS 2020; API 2014a; DNV 2021; DNV GL 2018; IEC 2019a).

The most important metocean parameters for obtaining extreme values are wind speed, significant wave height, wave peak period, and current speed. The most probable directions corresponding to these extreme values should also be identified. Wind, wave, and current extreme values are typically assumed to be uncorrelated and can be computed independently (ISO 2015). However, in reality the wave and wind climate are often correlated, because waves are often wind generated (DNV GL 2018). Wave height and period are closely related, so their extreme values should not be computed separately. One approach is to construct a joint probability distribution of wave height and period, and then pick points on the probability contour of the desired return period. The choice of which height-period point to use along a contour can be made based on what is the most severe load for the design in question, or multiple values can be used in a loads analysis. An alternative approach is to focus solely on the extreme value of wave height, and then use the most probable wave peak period that corresponds to that height. For simplicity and avoiding decisions about specific wave peak periods, we used the latter approach, recognizing that the respective significant wave height is connected to a range of possible peak periods (ISO 2015).

Several methods exist for determining the extreme parameter values. Michelen and Coe (2015) compared the following most applicable methods when dealing with loads from waves:

- Weibull fit to all peaks: Peaks are identified from the entire time series (with some threshold for minimum spacing) and then a Weibull distribution is fit to all of them. It uses the most data but includes data that may not be relevant to the high-return-period extremes. This approach can be modified to just fit to the tail of the distribution to prioritize the high-return-period data points.

- Block maxima: This approach divides the data into regular blocks (such as monthly or yearly), finds the maxima of each block, and provides a generalized extreme value fit to these maxima. It provides a more direct estimation of extremes, but typically has fewer data points so it can be less robust for shorter datasets.

- Peaks over threshold: This approach considers all peaks above a chosen threshold value and fits a Pareto distribution to them. The idea is to only fit the distribution to peaks that are high enough to be considered an extreme event. The results can be sensitive to the choice of threshold.

When dealing with data of varying lengths and qualities, we tried several methods and selected one that seemed to provide the most trustworthy results on a case-by-case basis. In general, the block maxima approach with monthly blocks gave reliable results when the data quality and quantity were high. When using yearly blocks or when the data quality was poor, the method led to overly large extreme values. When dealing with lower-quality data, the Weibull fit to the peaks generated more reasonable results; however, there was some variability depending on the distance threshold used when finding peaks. Figure 4 shows the probability distributions fit to wave data for one of the sites to illustrate the difference between the approaches.

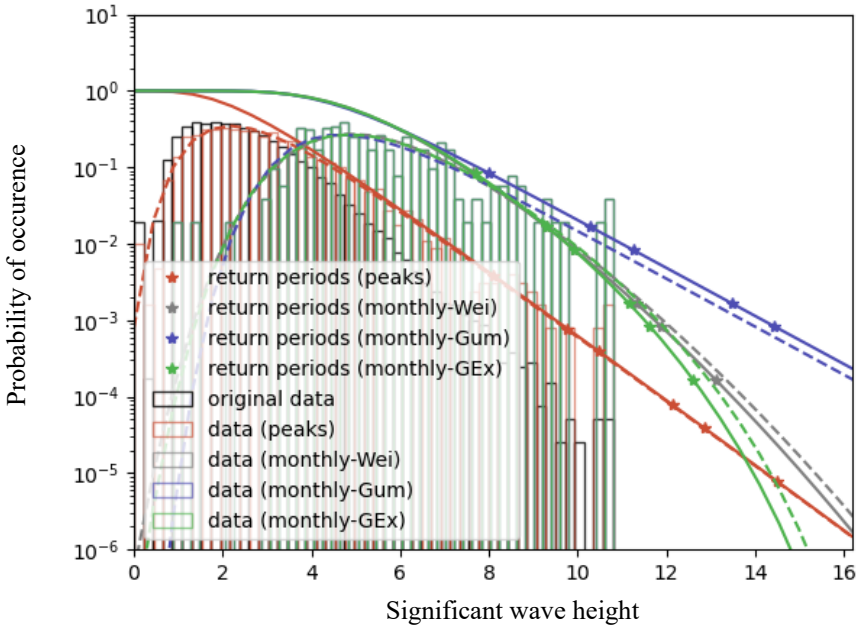

Figure 4. Example probability distribution fits for significant wave height data.

Note: "Wei" stands for Weibull, "Gum" stands for Gumbel and "GEx" stands for generalized extreme value.

In the figure, the bars indicate the histograms of the original data, the processed block maxima, or the peaks. The dashed lines indicate the probability distribution fits. The solid lines indicate the survival functions from which the extreme values can be read. A survival function is defined as:

$$SF(x) = 1 - CDF(x) \tag{1}$$

where CDF is the cumulative distribution function and x is the parameter in question. Once a distribution has been fitted, we find the extreme value for a given return period by locating where the survival function intercepts the probability corresponding to the return period:

$$SF(x) = \frac{1}{n\,f} \tag{2}$$

where n is the return period and f is a factor determined based on which method is used:

$$f = \begin{cases} 12, & \text{monthly block-maxima approach} \\ n_{peaks}/T, & \text{peaks approach} \end{cases} \quad (3)$$

where n_{peaks} is the number of identified peaks and T is the data time span in years. The x location of the intersection is the corresponding extreme value. We note the method used for each case when the results are presented in Section 3.

To estimate the most likely direction that corresponds with the extreme wind speed, wave height, or current speed, we extracted the direction coinciding with each peak or block-maxima speed/height data point, and then took a weighted average of these directions (weighted according to the amplitude measurement). This approach provides more accurate direction estimates by weighting the higher loads stronger. We did not consider a more detailed approach because the directions were not strongly correlated with the amplitudes.

To estimate the most likely wave period corresponding to an extreme wave height, we used a curve fit approach because there tends to be a correlation between significant wave height and peak wave period. Following the guidance of IEC 61400 3-1 (IEC 2019a), we used a square root fit:

$$T_p = a \cdot \sqrt{\frac{H_s}{g}} \quad (4)$$

where T_p is the peak wave period, a is the fitting coefficient, H_s is the significant wave height, and g is acceleration due to gravity (9.81 m/s²).

Some IEC load cases require using conditioned extreme values, such as for wave conditions that are more likely to appear at a certain wind speed. Unconditioned extreme values tend to be more conservative because they are calculated according to each separate parameter; they do not account for correlation between different parameters. For conditional extreme values, we filtered the wave and current time series into 2-m/s-wide wind speed bins before doing the monthly maxima, after which we used the same process as before on the subset of data that falls in each wind speed bin.

2.2.2 Joint Probability Distributions and Fatigue Bins

To evaluate fatigue loads of floating systems, a set of metocean conditions must be defined that represents the joint probability distribution of the metocean conditions at the site. This set can then be used to run simulations that model the fatigue damage that occurs within each metocean condition. The lifetime fatigue damage can then be found by summing damage across the cases and weighting by probability.

The set of metocean conditions, sometimes called fatigue bins, can be obtained in various ways. A simple approach is to follow IEC 61400 3-1 (IEC 2019a), which specifies that the designer may consider the most probable wave parameters for each wind speed bin. This method, however, does not capture the variation in wave height, period, and direction within each wind speed bin. Additionally, the method to consider wind direction in this approach is not clear.

A more thorough approach is to divide the full metocean parameter space into a rectangular grid. IEC 61400 3-1 (IEC 2019a) specifies the recommended maximum bin widths to use for analyzing joint probability distributions as follows: 2 m/s for wind speed, 0.5 m for significant wave height, 0.5 s for wave period, and 30 degrees for directions.

Using this rectangular-grid approach results in a large number of bins. Our calculations showed that adhering to the recommended maximum bin sizes would lead to an excessive number of bins and, consequently, an excessive number of simulations for each site. This would be prohibitively computationally expensive for many R&D projects. An alternative approach that can represent the distribution of metocean conditions with fewer bins is clustering, wherein the full set of metocean parameter data points is grouped into clusters, and each cluster is reduced to a single representative point at its centroid. The clusters are determined based on the proximity between data points and do not need to follow a rectangular pattern, allowing for much more efficient coverage of the data distribution. Kanner et al. (2018) demonstrated the use of clustering for metocean conditions of floating wind turbines and showed that clustering can provide comparable fatigue results while reducing the amount of analysis points by multiple orders of magnitudes compared to rectangular binning.

Given the massive difference in the number of bins required for a grid versus clustering approach, we used a clustering approach to characterize the joint probability distributions of each site and produce a corresponding list of fatigue cases that can be simulated. Representing the joint probability with fewer bins takes less computing time when evaluating fatigue loads for the site conditions.

A variety of methods exist for clustering data. The K-means clustering method was introduced more than 50 years ago and is designed to divide data into K clusters, wherein each cluster has a similar degree of variance (Steinley 2006). Furthermore, this method exchanges data between clusters to reduce the within-cluster variance and has been used to bin environmental data (Vogel et al. 2016). Self-organizing maps are another option, with the goal of minimizing the distance from the data vectors to the centroid vector within a given cluster. Another option, the maximum dissimilarity algorithm (MDA), creates new clusters by maximizing the dissimilarity between new samples and the existing clusters. Camus et al. (2011) compared the three methods and found that the self-organizing maps resulted in cluster centroids that were the closest together, whereas the MDA method resulted in centroids that were spaced the furthest apart. The K-means method was a middle ground between the other two methods.

Kanner et al. (2017, 2018) applied the MDA method to multivariate metocean data to conduct an efficient fatigue analysis. They showed the algorithm can be used to input a multidimensional time series—for example, with wind speed, direction, wave height, and wave period—and produce a set of discrete bins with associated probabilities. They demonstrated the tool on data from the Borsele Wind Farm Zone and compared the results with a standard grid binning method, finding that the MDA method could maintain the same error margin with a far smaller number of bins.

Building on the success of the approach of (Kanner et al. 2018), we implemented an MDA-based clustering algorithm that follows many of the same steps. It follows an iterative approach to

forming the clusters, beginning with assigning a single data point to a cluster and ending when all data points are assigned. The general process for each iteration is as follows:

- Iteratively add a specified number of new clusters:
  - Compute distances from unassigned data points to existing cluster centroids
  - Assign the most distant data point to be the centroid of a new cluster
- Assign all data points within a distance threshold to the nearest cluster centroid
- Calculate each updated cluster's centroid as the mean of its assigned data points.

We conducted several comparison studies to check the effectiveness of the MDA clustering approach and determine the parameters and number of bins required to accurately characterize fatigue loads. We focused on the fatigue loads of mooring lines because they are particularly sensitive to loading direction. This study used the metocean data from the Humboldt Bay site (discussed further in Section 3.1) so the findings may not apply as well to other sites.

First, we compared the MDA method to the standard regular grid method with uniform bin sizes. For this analysis, we considered only the wave height, wave period, and wave direction to reduce the number of parameters and simplify the comparison. We ran OpenFAST simulations of the VolturnUS-S 15-megawatt semisubmersible reference floating wind turbine with a generic mooring system for every bin. Table 2 shows the total fatigue damage for each mooring line calculated across the bins, for both binning methods. As shown, the MDA method's prediction of fatigue damage is similar to the prediction from using standard grid bins, but with much fewer bins. We took this as confirmation that the MDA method could adequately represent the metocean joint probability for fatigue loading.

Table 2. Fatigue Damage Compared for Standard Binning and MDA Approaches for Wave-Only Data

	L1 Damage	L2 Damage	L3 Damage
207 Standard Grid Bins	0.152	0.366	0.318
910 Standard Grid Bins	0.129	0.333	0.295
20 MDA Bins	0.103	0.297	0.277
40 MDA Bins	0.113	0.316	0.282
60 MDA Bins	0.117	0.319	0.286

Next, we evaluated the effect of currents on the fatigue prediction. We generated 100 MDA bins with seven parameters: wind speed, wind direction, wave height, wave period, wave direction, current speed, and current direction. We ran OpenFAST simulations of the 100 bins twice: once with current and once without. All other parameters were identical between the two cases. The total fatigue damage is shown in Table 3. The fatigue damage is within 1%, with and without current. Based on this result, we concluded that current can be excluded from the fatigue bins, thereby removing two variables from the parameter space and allowing greater accuracy for binning the remaining five parameters.

Table 3. Fatigue Damage for 100 MDA Bins With and Without Current

	L1 Damage	L2 Damage	L3 Damage
100 Bins With Current	0.773	1.033	0.501
100 Bins Without Current	0.779	1.037	0.499
% difference	0.7%	0.4%	-0.4%

Finally, we investigated the required number of bins when using the MDA clustering method. We applied the MDA to make clusters of wind speed, wind direction, wave height, wave period, and wave direction data for different numbers of bins. Table 4 presents the results, showing the fatigue damage for each mooring line when computed using 100, 200, 300, and 600 bins. The results have noticeable variability and lack a clear trend with respect to the number of bins. For example, the results with 100 bins are closer to the results with 600 bins than the results with 200 bins. We believe this variability is due to the randomness inherent in the binning method. A more extensive study with more bin counts would likely reveal a trend of convergence in the damage estimates as bin count increases. However, our focus is simply to determine a method to produce a minimal number of fatigue bins that can adequately approximate the fatigue loads for given metocean conditions. Considering that the predicted fatigue values were similar over four binning levels ranging from 100 to 600 (the largest difference being 25%), we concluded that using 100 bins provides acceptable fatigue estimates relative to the general uncertainty levels of modeling fatigue.

Table 4. Fatigue Damage for MDA for a Varied Number of Bins

	L1 Damage	L2 Damage	L3 Damage
100 Bins	0.966	1.234	0.522
200 Bins	0.768	1.071	0.499
300 Bins	0.842	1.165	0.532
600 Bins	0.903	1.217	0.547

To summarize our findings from these analyses, we concluded the following for this site dataset:

- The MDA approach can provide similar fatigue estimate as the regular rectangular binning approach with significantly fewer simulations.
- Current speed and direction can be omitted from the fatigue bins, leaving only five parameters: wind speed, wind direction, wave height, wave period, and wave direction.
- With these five parameters, 100 clusters are enough bins to approximate fatigue damage within the general level of uncertainty of the rest of the data.

These analyses were limited in scope and focused on quickly confirming a suitable approach for fatigue bins for the reference site conditions. Other applications or sites could have different requirements, which could call for differences in which metocean parameters are binned or the method and granularity of the binning. In the interest of efficiency, we followed the use of 100 wind-wave bins in the fatigue bin creations in our site datasets. These bins are defined by the wind speed, wind direction, significant wave height, wave period, wave direction, and probability of occurrence. These parameters can then be used to set up a simulation of each bin, determine the probability-weighted fatigue damage in that bin, and then sum across the 100 bins to determine the lifetime damage. Additionally, the hourly metocean time series included with

the reference site conditions can be used for alternative binning approaches or further investigation.

2.3 Seabed Data Collection and Processing

Geophysical information includes data on subsurface conditions such as rock layers, fault lines, and seismic activity. Within this category, bathymetric data describes the underwater topography, meaning the water depths and seabed contours. Geotechnical information focuses on soil properties, including strength, composition, and stability. Soil conditions from geotechnical studies detail the composition and behavior of sediments on and below the seabed. Together, these data sets are essential for understanding both surface and subsurface conditions in offshore environments.

There are a few databases that provide geophysical and geotechnical data on a global or at least U.S. scale, which are described in the following sections. Bathymetric data is available for all areas of interest. Soil condition data is much more limited, with U.S.-wide datasets having very few data points within the areas of interest. For more detailed information on the soil conditions of a particular site, local seabed investigation reports can be a good source of information, such as the site investigation reports commissioned by BOEM (Tajalli Bakhsh et al. 2020; Trandafir et al. 2022).

2.3.1 National Centers for Environmental Information Digital Elevation Model Global Mosaic

We used the NCEI Digital Elevation Model Global Mosaic (NCEI 2024) as the source for bathymetry data because it provides data at a high resolution of 3 arc seconds and covers all of the areas we considered for reference sites. We extracted the bathymetry data around each area of interest using the NCEI Bathymetric Data Viewer,[6] which helps select a rectangular region and then downloads the data in the geotiff format, which is a raster format gridded over longitude and latitude.

To provide a convenient format for the bathymetry data, we converted from the original geotiff raster data into a rectangular grid of depth values for each reference site, wherein the grid is measured in meters relative to the site's reference location. This conversion involves interpolating from the original geographic coordinate system into a local rectangular coordinate system. To accommodate varying needs, we generated files for each reference site at three different grid resolution sizes: 200 m, 500 m, and 1,000 m. We share these data in plain text files following the MoorDyn bathymetry input file format for easy use.

2.3.2 General Bathymetric Chart of the Oceans (GEBCO)

GEBCO could serve as an alternative source for bathymetry data. It has been in operation since 1903, and aims to provide the most authoritative publicly available bathymetry of the world's oceans (GEBCO Bathymetric Compilation Group 2023). Its gridded dataset comes from a global terrain model for ocean and land, with terrain data as positive values and water depths as negative values. The global bathymetry grid can be downloaded as netCDF, geotiff, or Esri

[6] https://www.ncei.noaa.gov/maps/bathymetry

ASCII raster files. Alternatively, specific locations can be selected and downloaded with the map interface, as shown in Figure 5. These easily accessible data formats make it convenient for further data processing.

Although NCEI Digital Elevation Model Global Mosaic is limited to American waters, GEBCO offers bathymetry data for the whole world. However, the resolution of 15 arc seconds is significantly lower compared to the respective NCEI data.

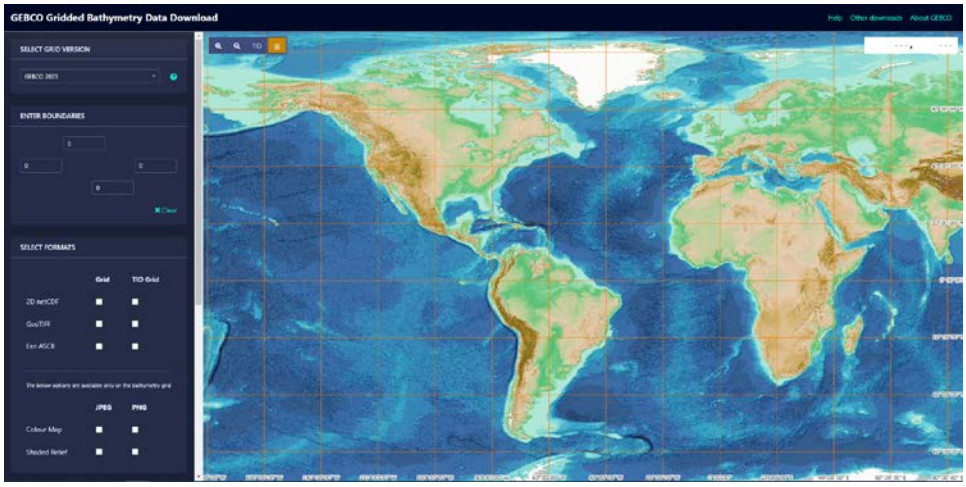

Figure 5. GEBCO gridded bathymetry data download. *Image from GEBCO*[7]

2.3.3 usSEABED

The usSEABED project provides an extensive database containing soil data within the United States Exclusive Economic Zone (Buczkowski et al. 2020a). It is a collaboration between the U.S. Geological Survey and University of Colorado, among others, and provides integrated sediment data at georeferenced locations from different sources around the U.S. coasts (Buczkowski et al. 2020a). It is the largest, publicly available database on seabed data for U.S. coasts, Figure 6 shows the web interface. The usSEABED database contains the following:

- Extracted lab data from analyzed soil samples,
- Parsed information based on qualitative descriptions, and
- Calculated data as results from the dbSEABED software.

The data are available from the database in one combined file, US9_ONE (Buczkowski et al. 2020a and 2020b), which we used data from in the present assessment. The list of parameters that the file contains is shown in Appendix J.

Among other parameters, such as the grain size, the database provides information about the soil classification according to Folk's classification scheme (Folk 1980), which is one of the most used systems by sedimentologists (Williams et al. 2006). The system is based on two triangular

[7] https://download.gebco.net/

diagrams with 21 categories, depending on the ratios of gravel, sand, and mud, as well as the ratios of sand, silt, and clay, as shown in Figure 7.

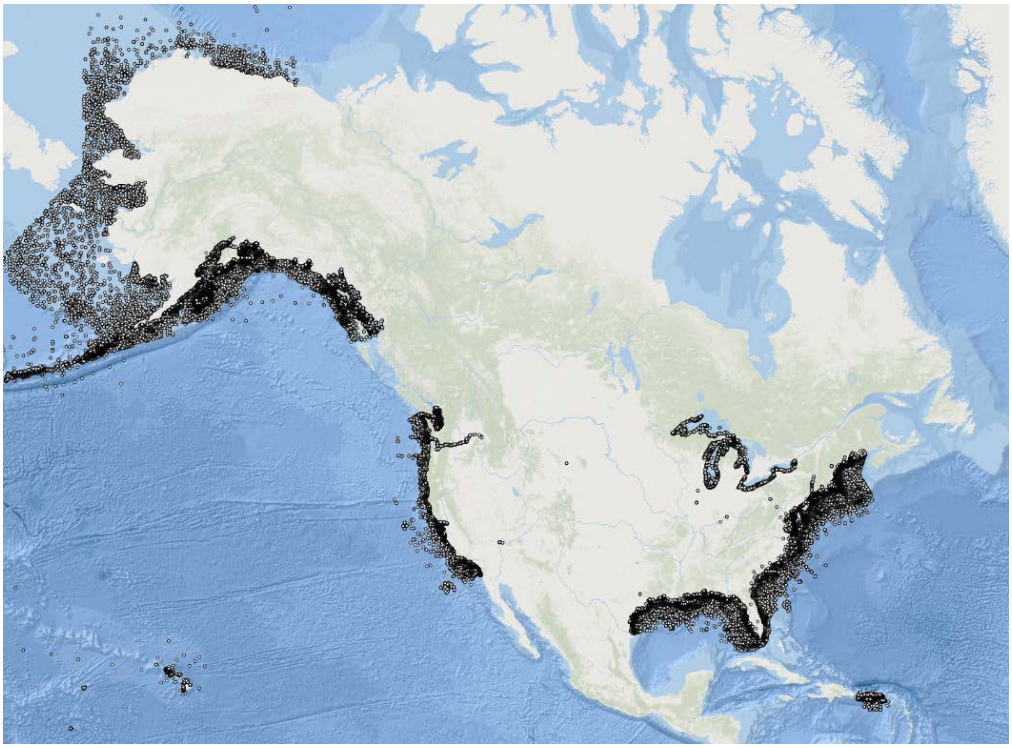

Figure 6. usSEABED map interface. ***Image from https://cmgds.marine.usgs.gov/usseabed/.***

Note: Data locations, including extracted, parsed and calculated are represented by the dots.

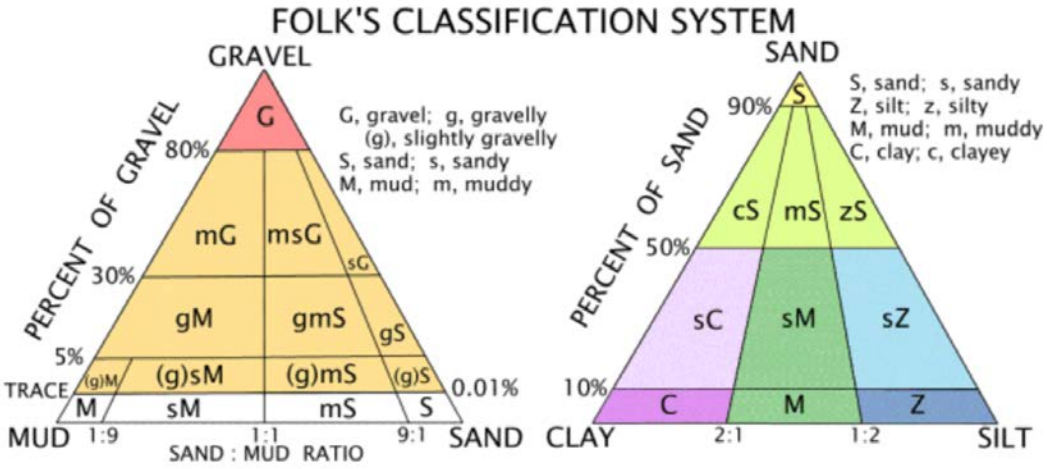

Figure 7. Folk's classification system. ***Image from Williams et al. (2006)***

The spatial density of the usSEABED data points is very coarse, so it is only practical to get soil characteristics that represent an average for a large area, such as an offshore wind energy lease area. However, it should be noted that soil conditions are highly local and can vary within a small area depending on the specific site, so using a spatial average is a significant approximation.

In this work, we selected all existing data points within a 50 km by 50 km square centered around each reference site area's centroid. We chose this size because it covers most of the leased areas. We used the normalized proximity of each data point from the center location to weight the respective data point, with 1 for the closest data point and 0 for the most distant one. Next, we calculated the soil ratios for gravel, sand, and mud in percent by first calculating the distance-weighted values per data point, then computing the average per ratio across all data points, and finally scaling the ratios so that the sum is again 100%. The respective equations can be found in Appendix K. Based on the resulting soil ratios, the Folk classification can be estimated, as shown in Figure 7.

3 Reference Site Conditions

In this section we present the results of the four selected reference sites.

3.1 Humboldt Bay

The Humboldt Bay reference site is based on conditions that are representative of the Humboldt Bay lease areas. BOEM awarded five offshore wind leases off the coast of California (BOEM 2023a): OCS-P0561 to OCS-P0565, two lease areas are located near Humboldt Bay and three near Morro Bay. The Humbold Bay lease areas (OCS-P0561 and OCS-P0562) and bathymetry are shown in Figure 8 and were chosen for the creation of site-specific metocean conditions due to the current development activities. The two combined lease areas have a steep seafloor gradient over a distance of 12 nautical miles (nm), with the water depth ranging from approximately 550 m at the eastern boundary to approximately 1,200 m at the western boundary.

3.1.1 Metocean Site Conditions

The target location (40.928, -124.708) is the centroid of the western lease area and was chosen for the NOW-23 data analysis because it is located further offshore (25 nm to shore) and in deeper waters than the eastern lease area. We selected all other data sources based on their proximity to this location and the data coverage of their respective stations.

We used NDBC station 46022 (12.5 nm to the target location) as the primary source for wave data. The station is moored at a water depth of 419 m and located 17 nm off Humboldt Bay. We used NDBC station 46244 (110 m water depth, 8 nm to shore) to fill wave data gaps of station 46022, especially for wave directions, because roughly only 9 years of directional wave data were available from that station. The distance between these stations is 12 nm.

The closest available HFRNet current measurements grid point was found at the boundary of the eastern lease area (8.5 nm off the target location), which provides more than 5 years of almost continuous ocean current measurements in the period from 2012 to 2023. NDBC station 46022 provided 2 years of discontinuous current measurements, so the HFRNet measurements are the better choice for the present application. Table 5 summarizes basic information of the data sources used, including the location, depth, and distance to shore per data source.

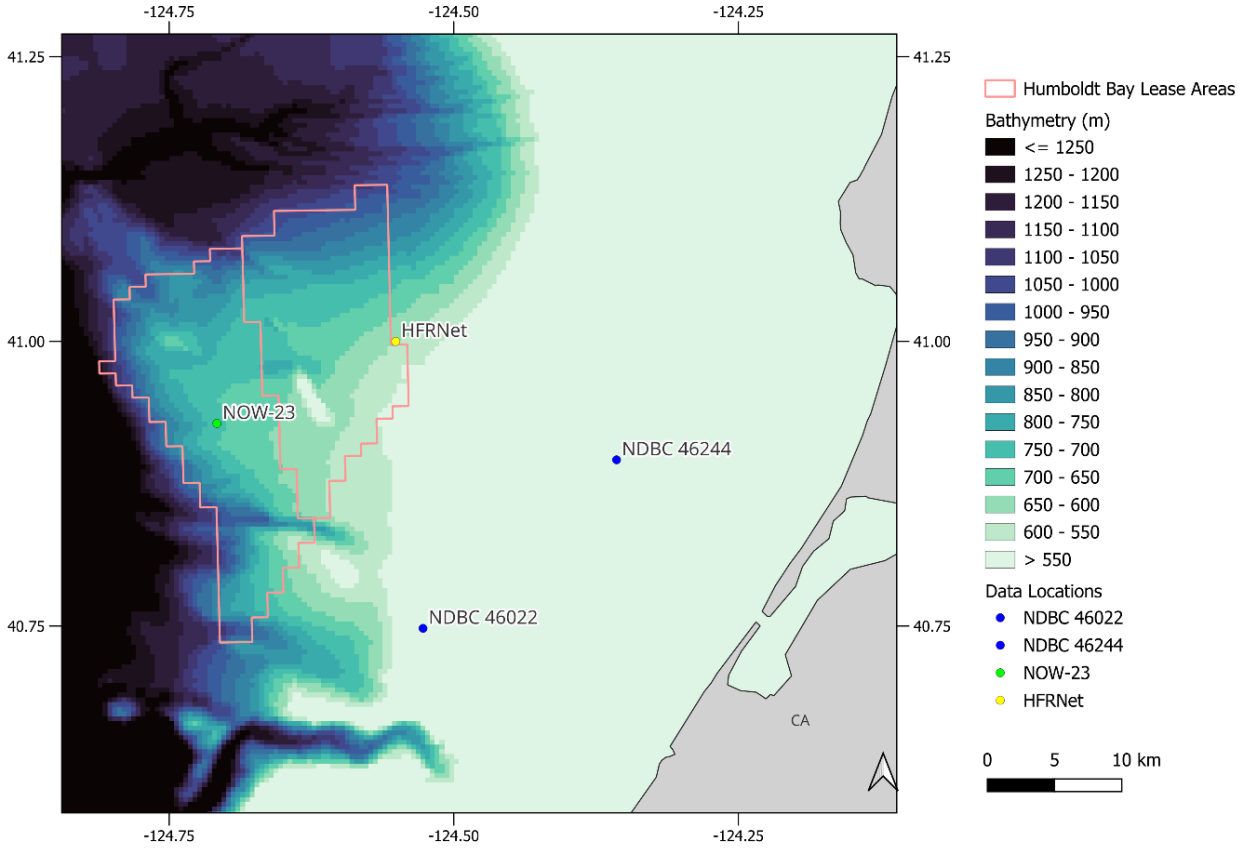

Figure 8. Humboldt Bay bathymetry and metocean data source locations.

Note: Lease areas (contours) from west to east: OCS-P0561 and OCS-P0562. Bathymetry data source: NCEI (2024).

Table 5. Humboldt Bay Locations of Data Sources

Type	Station ID	Latitude (deg)	Longitude (deg)	Water Depth (m)	Distance to Shore (nm)
Waves	46022	40.748	-124.527	419	12
	46244	40.896	-124.357	110	8
Wind	NOW-23	40.928	-124.708	800	25
Currents	HFRNet	41	-124.551	600	20

The speed and directional distributions of wind, waves, and current data are shown in Figure 9. For waves, significant wave height is plotted.

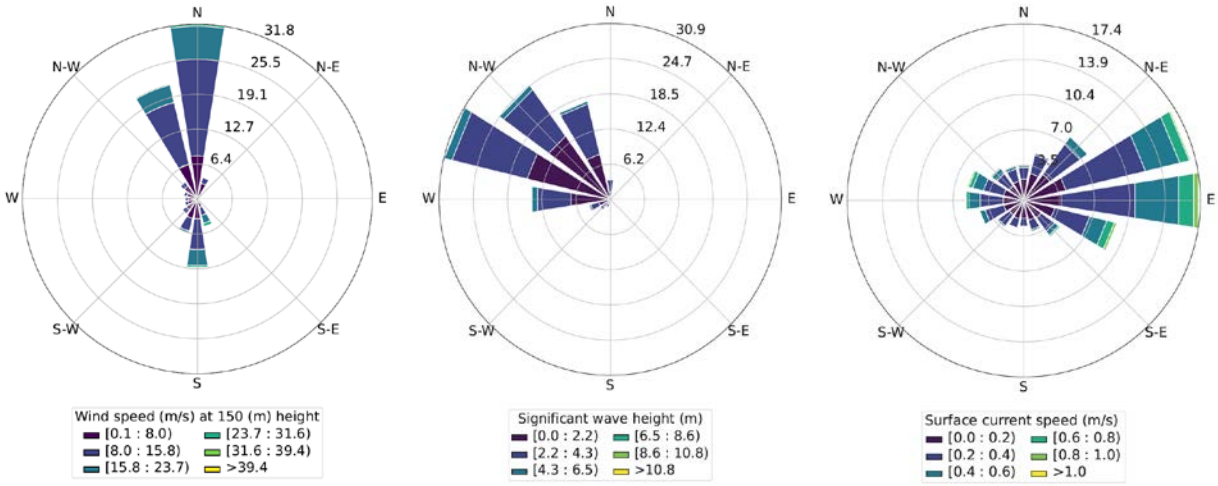

(a) Wind (b) Wave (c) Current

Figure 9. Humboldt Bay wind, wave, and current roses.

Note: 0° corresponds to coming from the north.

Extreme wind, wave, and current parameters for return periods ranging from 1 to 500 years are shown in Table 6. The mean directions of the peaks used for the extrapolation are 339° for wind, 302° for waves, and 84° for currents. Conditional values of wave height, wave period, and current speed for wind speed bins of every 2 m/s are provided in Appendix A.

Table 6. Extreme Metocean Parameters for Humboldt Bay

Return Period (years)	Wind Speed (m/s)	Significant Wave Height (m)	Peak Wave Period (s)	Current Speed (m/s)
1	31.0	8.5	16.8	0.92
5	34.9	9.8	18.1	1.09
10	36.4	10.4	18.6	1.15
50	39.4	11.8	19.8	1.28
100	40.6	12.4	20.3	1.33
500	43.0	13.7	21.4	1.44

Following the method discussed in Section 2.2.2, we used the maximum dissimilarity algorithm to generate 100 clusters of the hourly metocean data points, which represent 100 fatigue bins that can be used for fatigue loads analysis. Figure 10 shows the data points and cluster centroids for these 100 bins. The parameters of these bins are also provided in Appendix A.

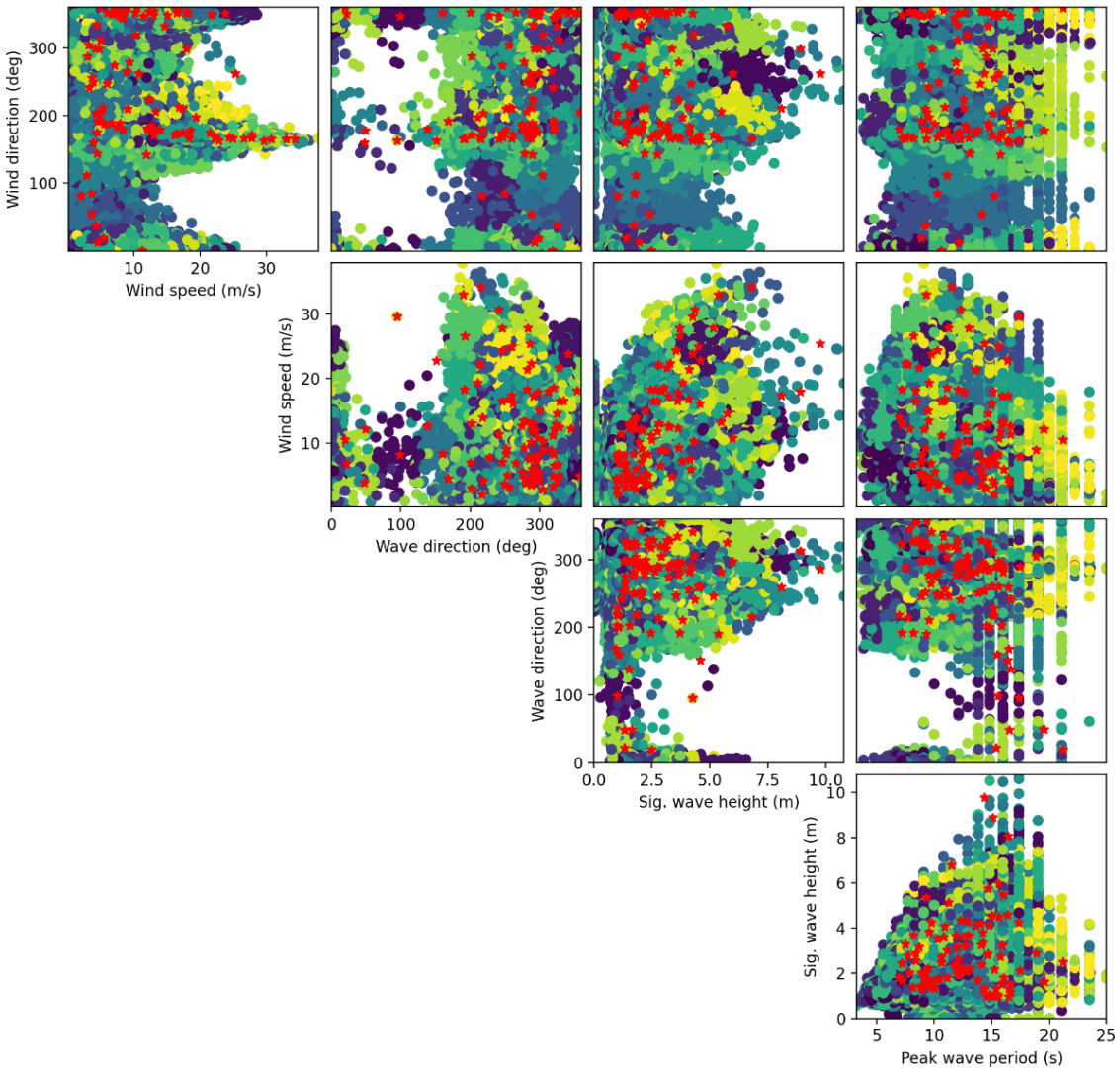

Figure 10. Humboldt Bay metocean fatigue bin clusters.

Note: Clusters represented by different colors, centroids marked in red.

3.1.2 Seabed Conditions

We processed bathymetry data from the NCEI Digital Elevation Model Global Mosaic for a rectangular area that is 60 km wide and 80 km long around the reference area (marked as NOW-23 in Figure 8). These interpolated data are available at three discretization levels in the data repository. Figure 11 shows the grid with 1,000-m resolution, which is easiest to see.

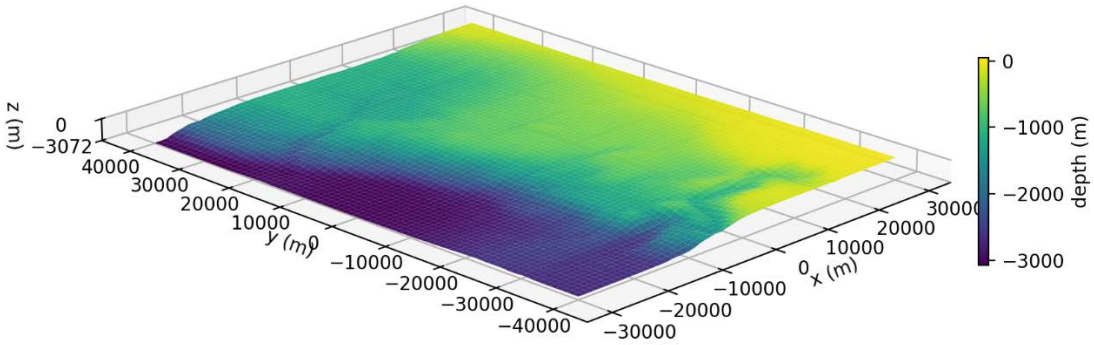

Figure 11. Humboldt Bay reference site bathymetry at a 1,000-m resolution

Based on 237 data points from the usSEABED database within a 50 km by 50 km square area centered at the target location, as shown in Figure 12, the sediment in this area can be classified as sandy mud (sM). The results are shown in Table 7, and Figure 13 confirms this observation. In addition, the grain size (phi) of 6.08 characterizes it as fine silt, which is unconsolidated soil. However, data from a more detailed study from Goldfinger et al. (2014), shown in Figure 13, indicates that there are certain areas with hard soils, such as bedrock.

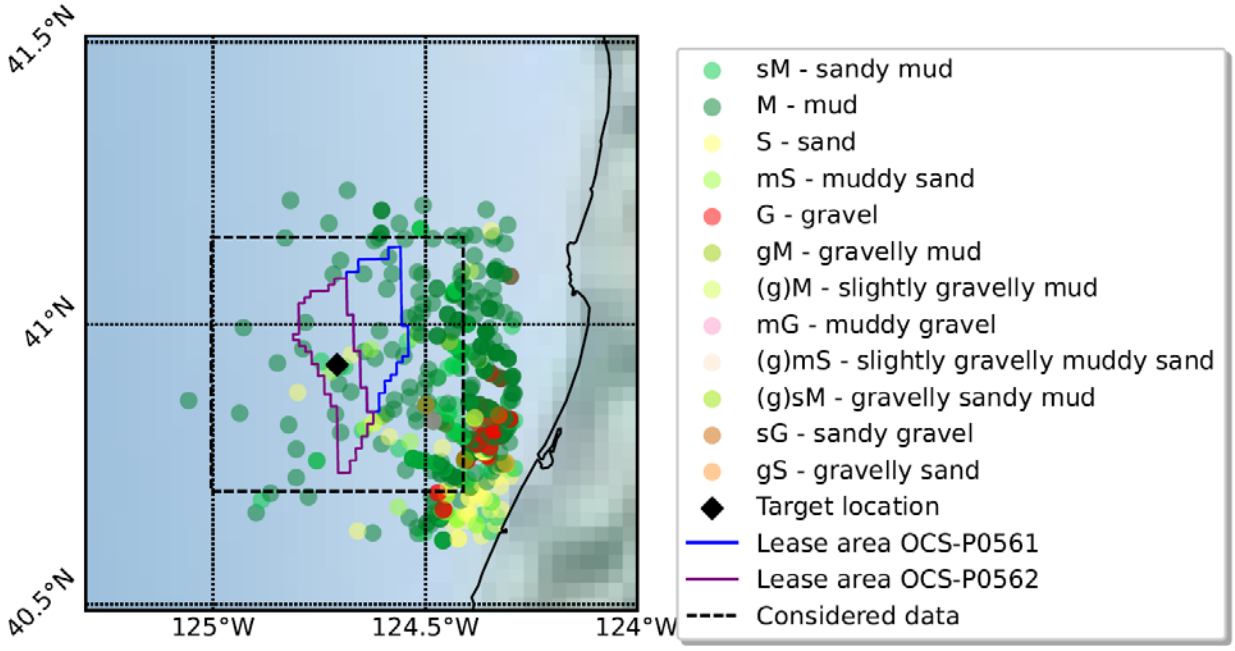

Figure 12. usSEABED soil data points at the Humboldt Bay lease area location

Table 7. Humboldt Bay Seabed Sediment Classification at Site

Latitude (deg)	Longitude (deg)	Gravel (%)	Sand (%)	Mud (%)	Grain Size (phi)	Folk Class
40.702 to 41.154	-125.004 to -124.410	0.94	13.99	85.07	6.08	Sandy mud (sM)

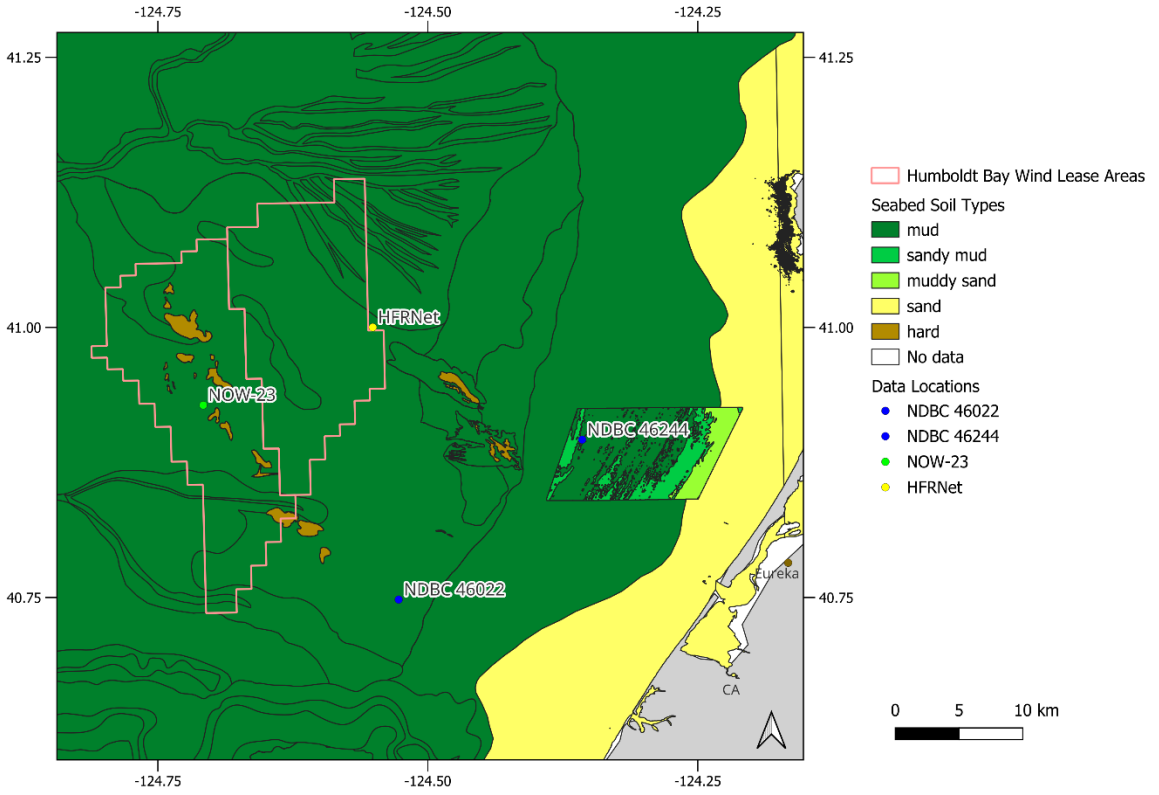

Figure 13. Soil type of the Humboldt Bay lease area and surrounding region. *Data from Goldfinger et al. (2014)*

3.2 Morro Bay

The Morro Bay lease areas (OCS-P0563, OCS-P0564, and OCS-P0565), shown in Figure 14, were chosen as the location for the second reference site because they also are an area of offshore wind development and their metocean conditions contrast from those of Humboldt Bay. The three combined Morro Bay lease areas have a steep depth gradient over a distance of 18 nm, with the water depth ranging from approximately 900 m at the eastern boundary to approximately 1,300 m at the western boundary.

3.2.1 Metocean Site Conditions

The target location (35.569, -121.845) is the centroid of the middle lease area (approximately 1,050-m water depth) and was chosen for the NOW-23 data analysis because it is considered representative for all three lease areas. All other data sources were chosen based on the distance to this location and the data coverage of respective stations. NDBC station 46028 (a 12.6-nm distance to the target location) was used as the primary source for wave data. The station is moored at a water depth of 1,154 m, 55 nm off the coast. No other NDBC stations were available in the vicinity to fill data gaps.

The closest available HFRNet current measurement grid point was found north of the western lease area, at 14 nm north of NDBC station 46028 and 26.4 nm away from the target location. The HFRNet data at this location provides 8 years of almost continuous ocean current measurements from 2012 to 2020. No NDBC station measuring ocean currents was available in

the vicinity of this location. Table 8 summarizes basic information of the data sources, providing the location, depth at these locations, and the distance to shore per data source.

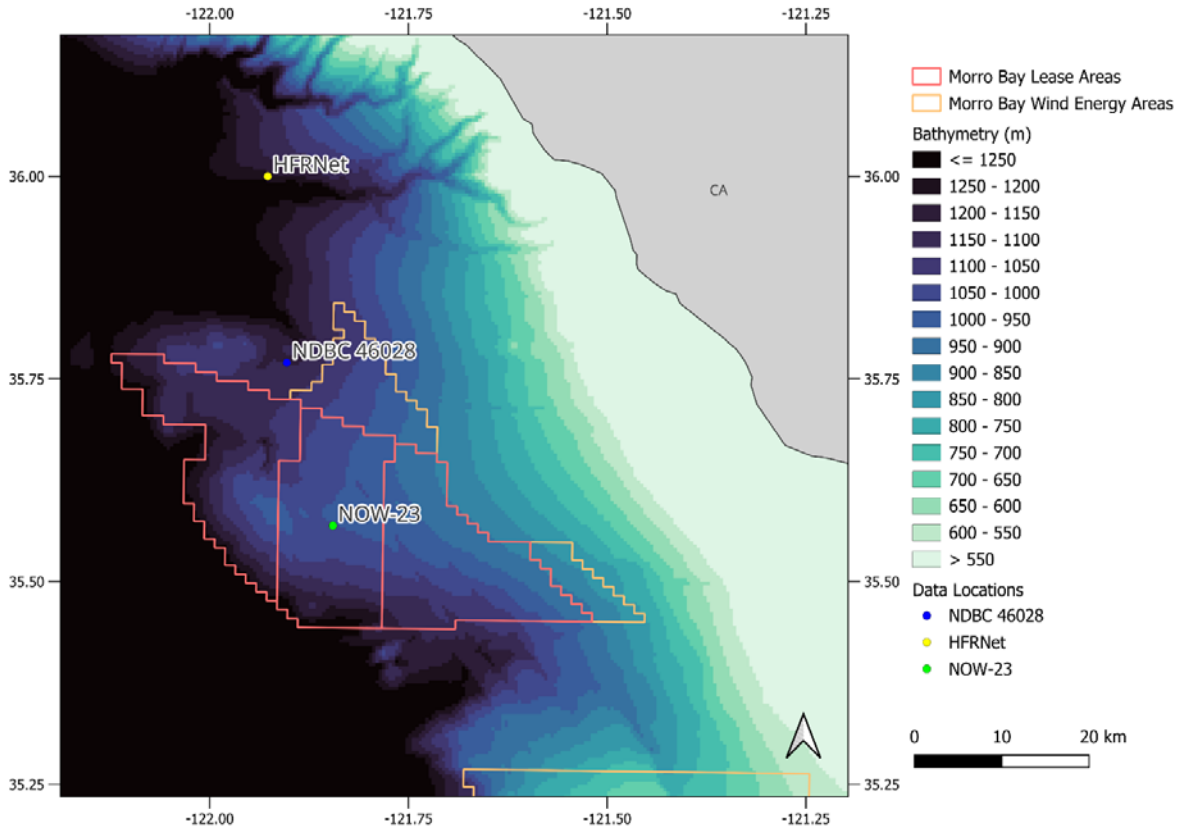

Figure 14. Morro Bay bathymetry and metocean data source locations.

Note: Lease areas (contours) from west to east: OCS-P0563, OCS-P0564, and OCS-P0565. Bathymetry data source is NCEI (2024).

Table 8. Morro Bay Locations of Data Sources

Type	Station ID	Latitude (deg)	Longitude (deg)	Water Depth (m)	Distance to Shore (nm)
Waves	46028	35.77	-121.903	1,154	23
Wind	NOW-23	35.569	-121.845	1,050	27
Currents	HFRNet	36	-121.927	1,300	16

The speed and directional distributions of wind, waves, and current data are shown in Figure 15. For waves, significant wave height is plotted in place of wind or current speed.

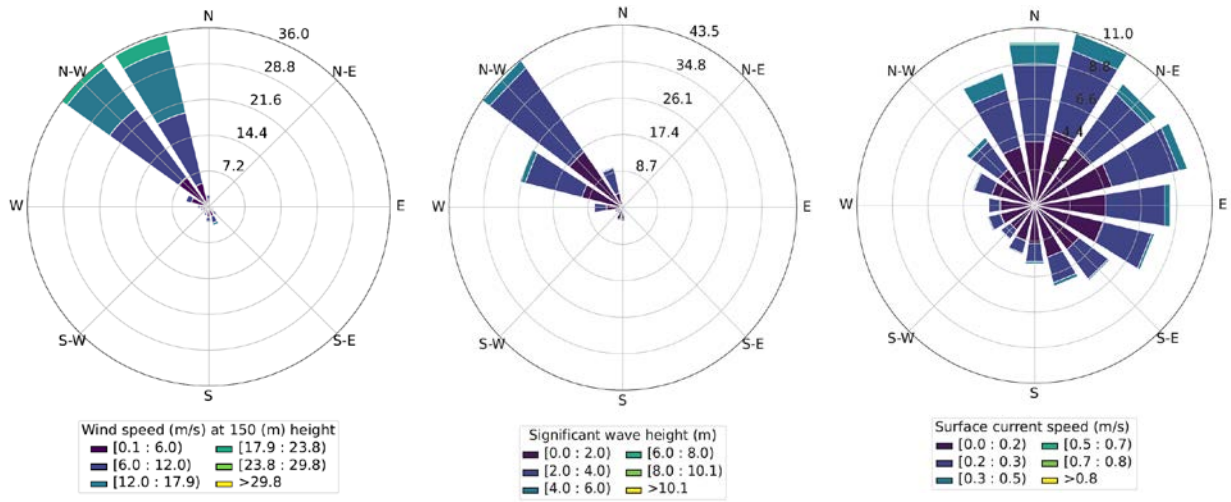

(a) Wind (b) Wave (c) Current

Figure 15. Morro Bay wind, wave, and current roses.

Note: 0° corresponds to North.

Extreme wind, wave, and current parameters for return periods ranging from 1 to 500 years are shown in Table 9. The mean directions of the peaks used for the extrapolation are 321° for wind, 300° for waves, and 45° for currents.

Table 9. Extreme Metocean Parameters for Morro Bay

Return Period (years)	Wind Speed (m/s)	Significant Wave Height (m)	Peak Wave Period (s)	Current Speed (m/s)
1	24.6	6.9	15.7	0.68
5	26.7	8.5	17.5	0.81
10	27.5	9.2	18.2	0.87
50	28.9	10.7	19.6	0.99
100	29.4	11.3	20.1	1.04
500	30.4	12.7	21.3	1.16

Conditional values of wave height, wave period, and current speed for wind speed bins of every 2 m/s are provided in Appendix B.

We generated 100 metocean clusters for fatigue bins from the hourly metocean data, which are visualized in Figure 16. The 100 bins are listed in Appendix B.

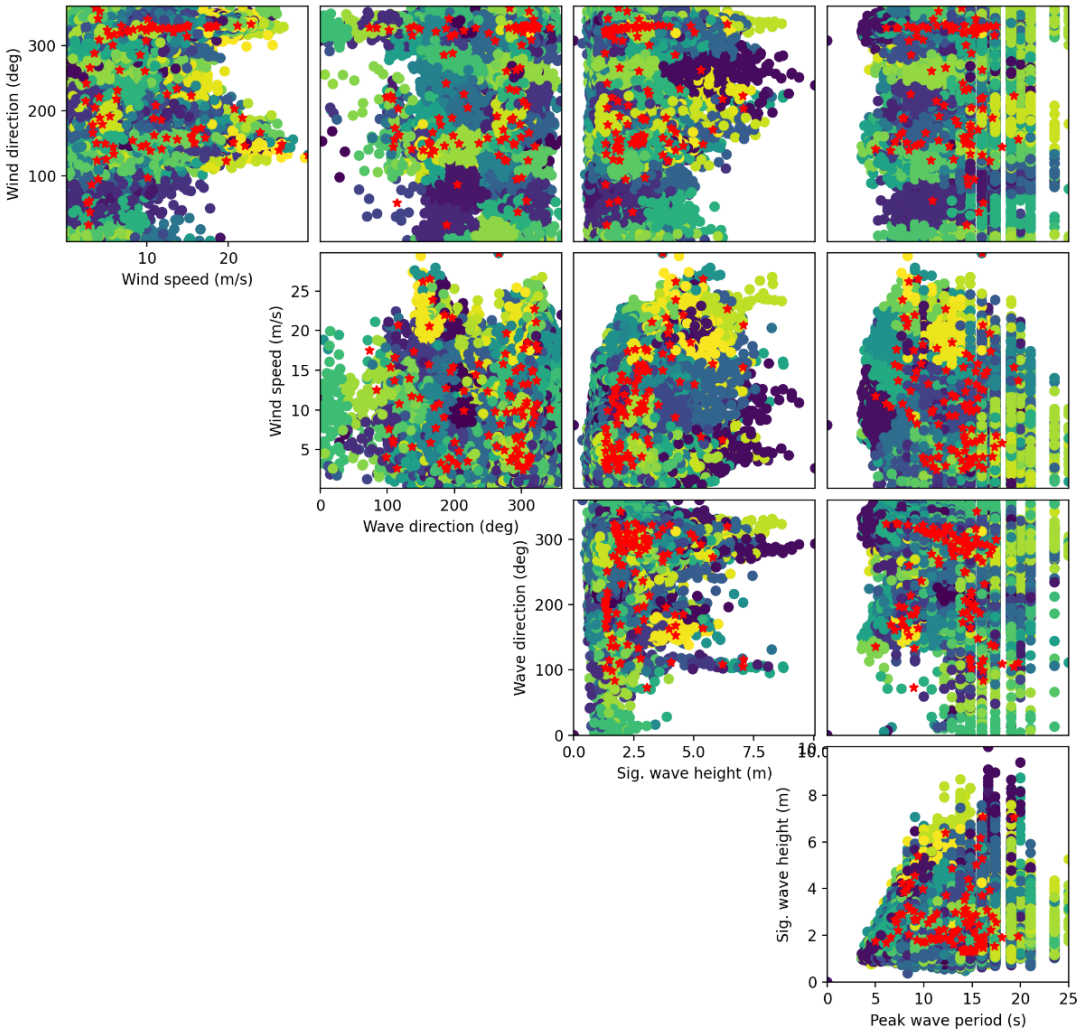

Figure 16. Morro Bay metocean fatigue bin clusters.

Note: Clusters represented by different colors, centroids marked in red.

3.2.2 Seabed Conditions

We processed bathymetry data from the NCEI Digital Elevation Model Global for a rectangular area that is 80 km wide and 60 km long around the reference area (marked as NOW-23 in Figure 14). These interpolated data are available at three discretization levels in the data repository. Figure 17 shows the grid with a 1,000-m resolution.

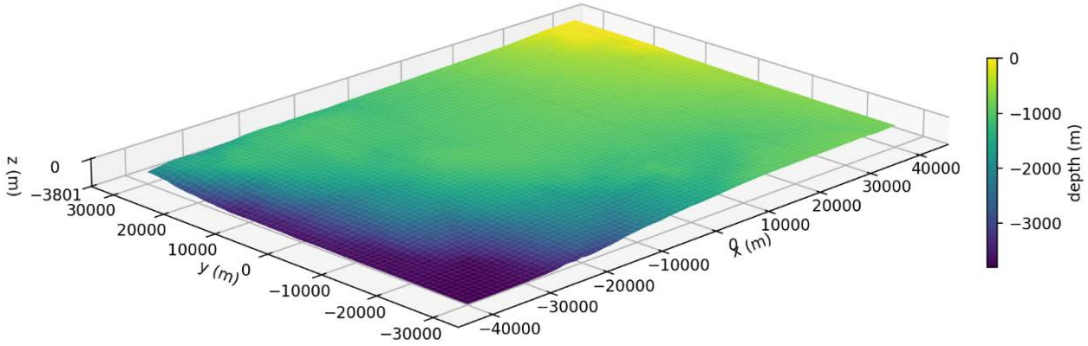

Figure 17. Morro Bay reference site bathymetry at a 1,000-m resolution

Based on 26 data points from the usSEABED database that are within a 50-km square area centered around the target location (Figure 18), the sediment in this area can be classified as mud (M) or sandy mud (sM). Results of the seabed sediment classification are shown in Table 10. The grain size (phi) of 6.04 characterizes the soil as fine silt or mud, which falls under unconsolidated soils and aligns according to a recent study (Tajalli Bakhsh et al. 2020).

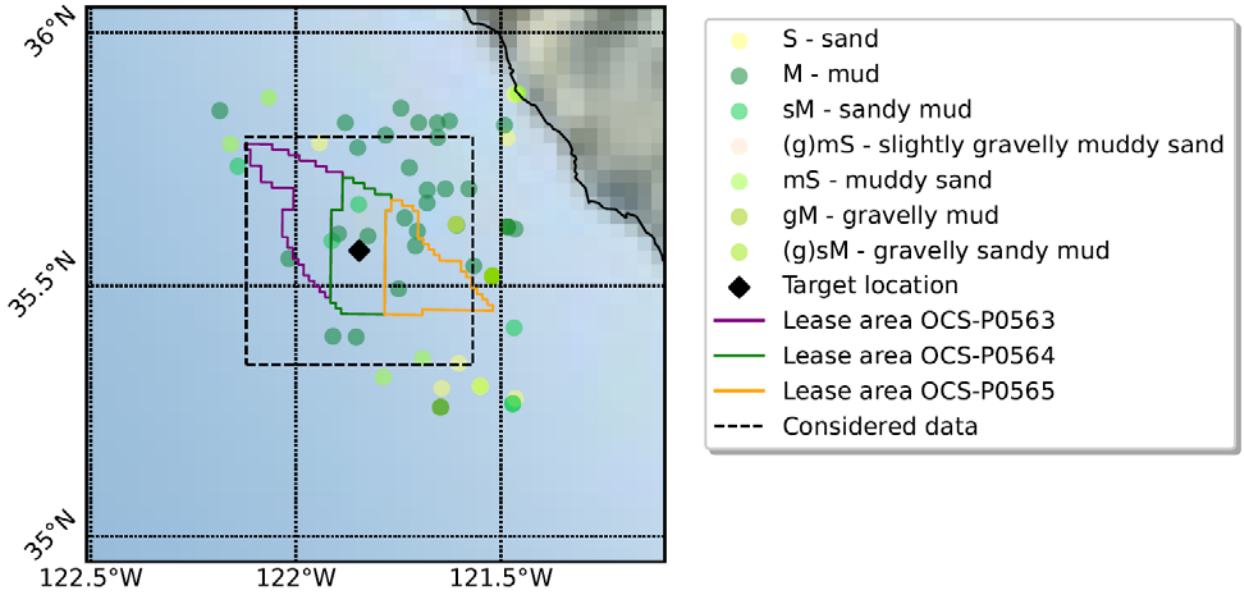

Figure 18. usSEABED soil data points at the Morro Bay lease area location

Table 10. Morro Bay Seabed Sediment Classification at Site

Latitude (deg)	Longitude (deg)	Gravel (%)	Sand (%)	Mud (%)	Grain Size (phi)	Folk Class
40.702 to 41.154	-125.004 to -124.410	0	10.22	89.78	6.04	Mud (M) to sandy mud (sM)

3.3 Gulf of Maine

The Gulf of Maine reference site is intended to represent conditions at the Maine Research Array location, as shown in Figure 19. The Gulf of Maine has two major ocean streams flowing into it: the northern Labrador Current (cold water) and the Gulf Stream (warm water) (Gulf of Maine Research Institute 2023) and is adjacent to the Bay of Fundy, which is known for having the highest tides in the world (NOAA 2023), with corresponding strong currents.

For more than 10 years there have been efforts to establish a floating offshore wind demonstration project in the Gulf of Maine. More recently, the University of Maine has planned a research array of multiple turbines, and BOEM has identified proposed lease areas for a larger auction (BOEM 2023b).

3.3.1 Metocean Site Conditions

We used NDBC station 44005 (43.2, -69.127) as the primary source for wave data, due to its proximity to the proposed Maine Research array site (15 nm) and its data availability, as shown in Figure 19. The station is moored at a water depth of 176.8 m, 43 nm off the coast. We used NOW-23 data at the same location, and consider this to be the target location of the reference site.

We used NBDC station 44098 to fill wave data gaps of station 44005, especially because 44005 provides approximately 5 years of directional wave measurements between 2016 and 2022 only. Station 44098 is located in water that is 80 deep m and 40 nm offshore, which is 51 nautical miles away from 44005. The Gulf of Maine is not covered by IOOS, meaning that there are no HRFNet current measurements available for that area. Therefore, we obtained current measurements from NDBC station 44032 (E01), which is located in water that is 100 m deep, 10 nm off the coast. This station is operated and maintained by the Northeastern Regional Association of Coastal Ocean Observing Systems, as part of the University of Maine Ocean Observing System, and which provided up to 22 years of current measurements. The data are not directly accessible via NDBC, and had to be reformatted into the standard NDBC format (University of Maine n.d.). Another alternative buoy is 44037 (M01), which is located northeast of the main location of interest, in the Jordan Basin. This buoy is closer to the Bay of Fundy and experiences higher currents than expected in the target area.

Table 11 summarizes basic information of each data source for locations in the Gulf of Maine, including the location, depth, and distance to shore.

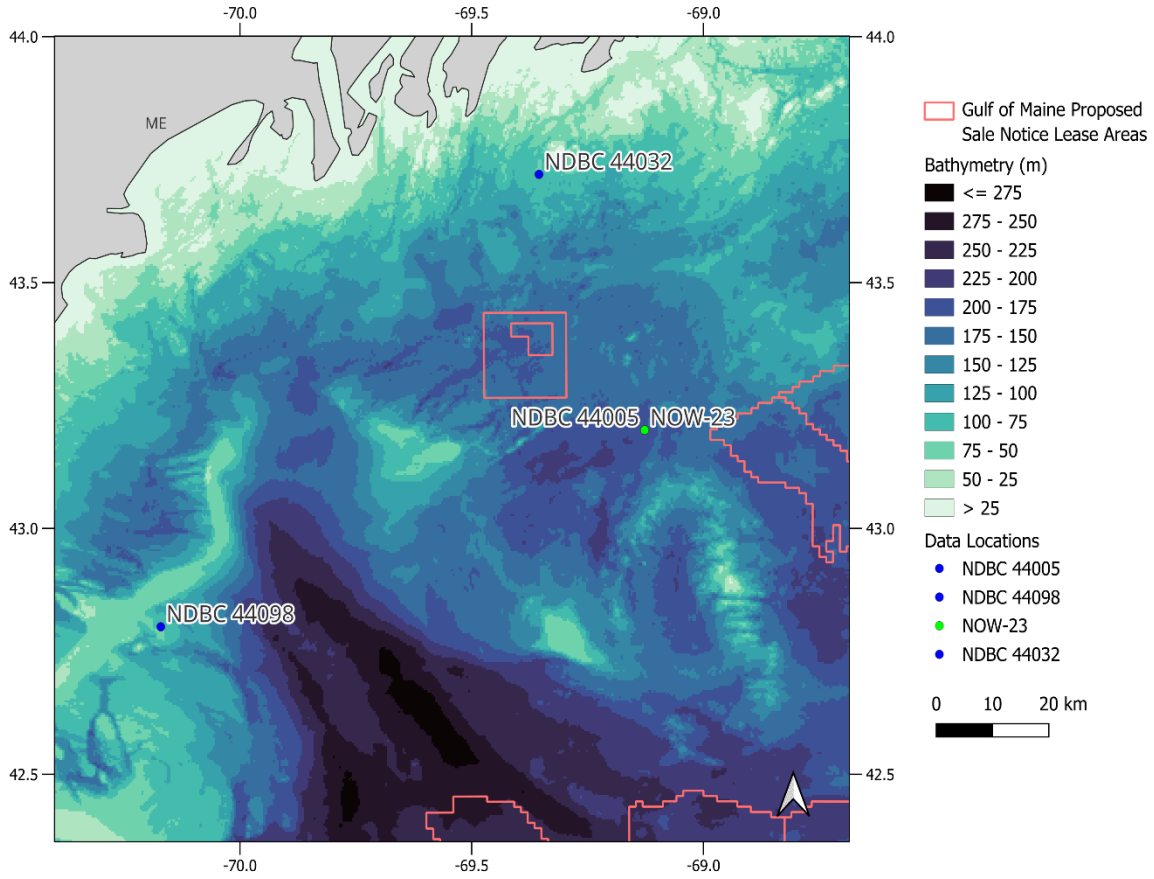

Figure 19. Gulf of Maine bathymetry and metocean data source locations.

Note: Contours are current Request for Competitive Interest areas. Bathymetry data source: (NCEI 2024).

Table 11. Data Sources for Gulf of Maine Locations

Type	Station ID	Latitude (deg)	Longitude (deg)	Water Depth (m)	Distance to Shore (nm)
Waves	44005	43.2	-69.127	176.8	43
	44098	42.8	-70.171	80	22
Wind	NOW-23	43.2	-69.127	176.8	43
Currents	44032	43.72	-69.355	100	10

The speed and directional distributions of wind, waves, and current data are shown in Figure 20. For waves, significant wave height is plotted in place of wind or current speed.

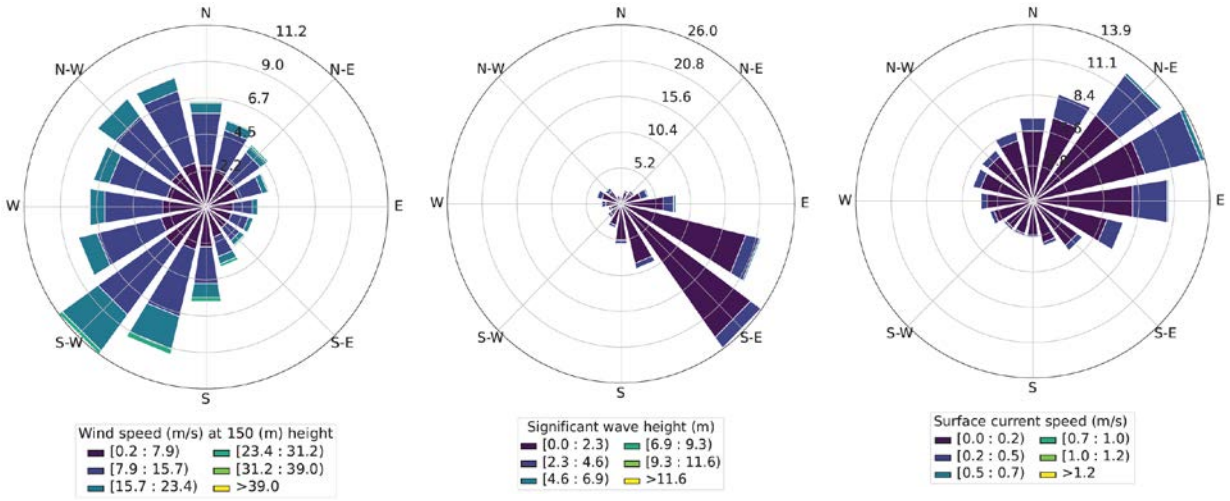

(a) Wind (b) Wave (c) Current

Figure 20. Gulf of Maine wind, wave, and current roses.

Note: 0° corresponds to North.

Extreme wind, wave, and current parameters for the Gulf of Maine for return periods ranging from 1 to 500 years are shown in Table 12. The mean directions of the peaks used for the extrapolation are 253° for wind, 134° for waves, and 44° for currents.

Table 12. Extreme metocean parameters for Gulf of Maine

Return Period (years)	Wind Speed (m/s)	Significant Wave Height (m)	Peak Wave Period (s)	Current Speed (m/s)
1	33.39	7.07	12.17	0.71
5	37.01	9.2	13.87	0.88
10	38.25	10.04	14.49	0.94
50	40.59	11.86	15.75	1.11
100	41.41	12.59	16.23	1.18
500	42.96	14.19	17.23	1.34

Conditional values of wave height, wave period, and current speed for wind speed bins of every 2 m/s are provided in Appendix B, as are the parameters for 100 fatigue bins generated with the maximum dissimilarity algorithm. Figure 21 shows the data points and cluster centroids for the 100 bins.

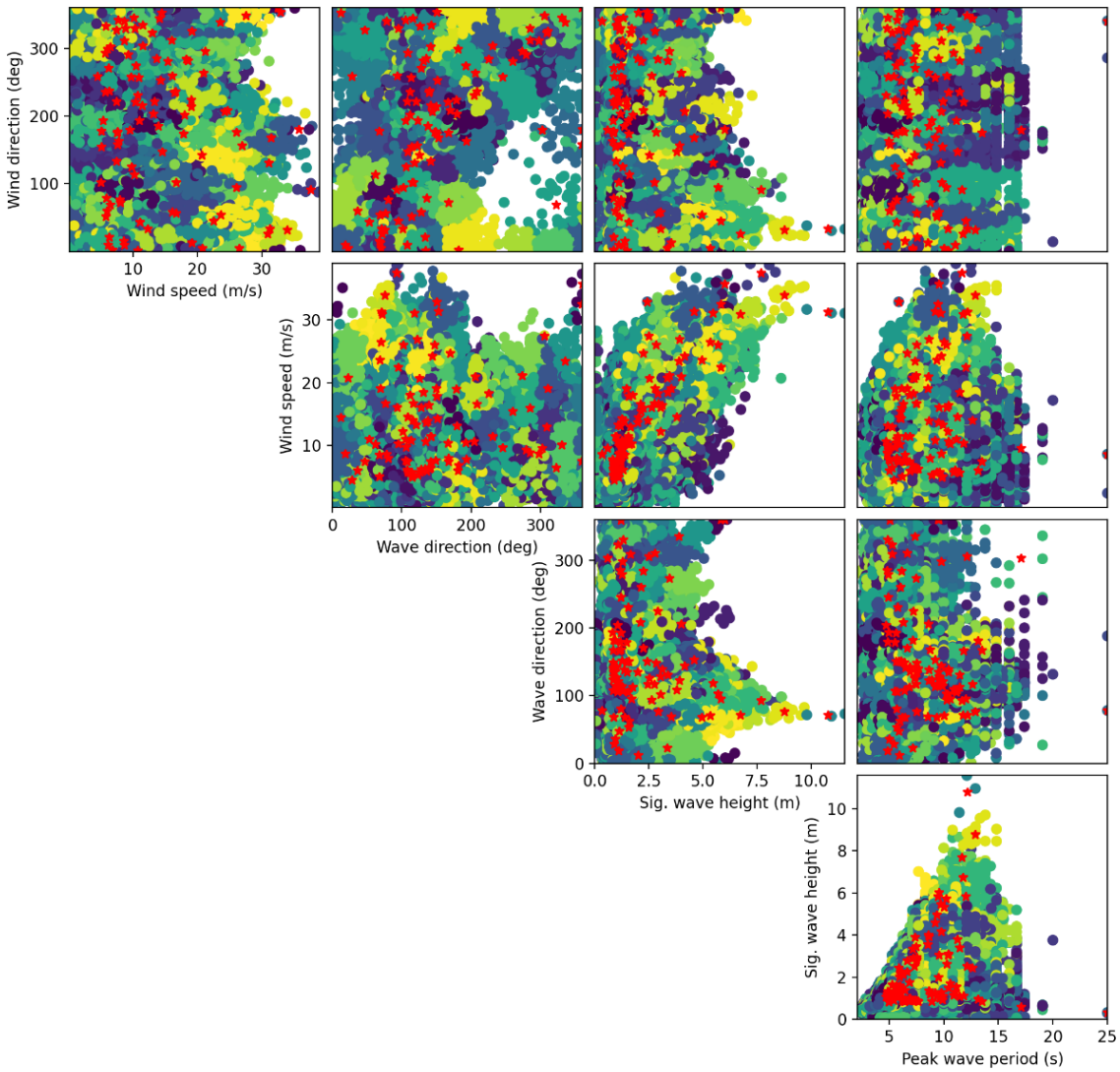

Figure 21. Gulf of Maine metocean data and fatigue bin clusters.

Note: Clusters represented by different colors, centroids marked in red.

3.3.2 Seabed Conditions

As with the Humboldt Bay and Morro Bay areas, we processed bathymetry data from the NCEI Digital Elevation Model Global Mosaic for a rectangular area that is 60 km wide and 80 km long around the reference area (marked NOW-23 in Figure 19) and produced MoorPy-style bathymetry files at three discretization levels. Figure 22 shows the grid with a 1,000-m resolution. The shallowness of the area means that the depth variation is barely perceptible relative to the horizontal extent of the area.

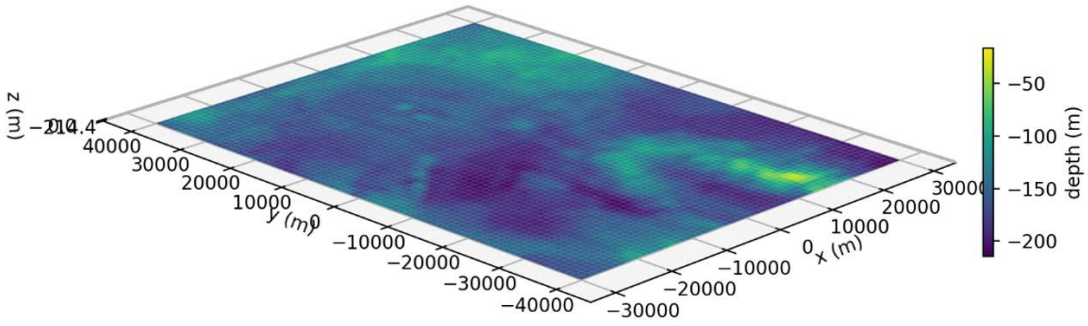

Figure 22. Gulf of Maine reference site bathymetry at a 1,000-m resolution

Based on 85 data points from the usSEABED database that are located in a 50-km square area around the target area (as shown in Figure 23), the sediment in this area can be classified as slightly gravelly sandy mud ((g)sM). The results of the seabed sediment classification are shown in Table 13. According to the grain size (phi) of 5.91, which is characterized as medium to fine silt.

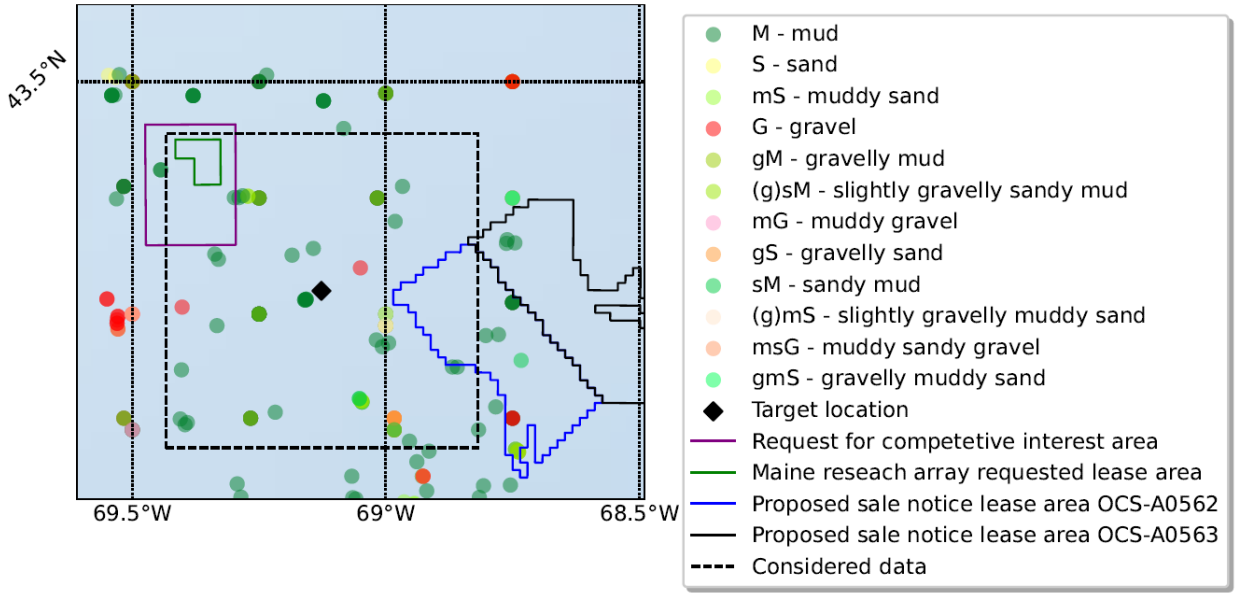

Figure 23. usSEABED soil data points at the proposed lease area locations in the Gulf of Maine

Table 13. Gulf of Maine Seabed Sediment Classification at Site

Latitude (deg)	Longitude (deg)	Gravel (%)	Sand (%)	Mud (%)	Grain Size (phi)	Folk Class
42.974 to 43.426	-68.818 to -69.434	4.39	14.69	80.91	5.91	slightly gravelly sandy mud ((g)sM)

3.4 Gulf of Mexico

The Gulf of Mexico is known for oil-and-gas production and it is now being considered for offshore wind energy development. The locations of the considered data sources and the Gulf of Mexico wind energy area are shown in Figure 24.

The rather slow wind speeds, combined with extreme events like hurricanes, make it challenging to deploy offshore wind energy in the Gulf of Mexico. We have not conducted an assessment of hurricanes, although this would be necessary to achieve a more detailed analysis of extreme events in this region.

The shallow water depth of approximately 20 m led us to focus primarily on offshore wind turbines with fixed foundations. However, with the advancement of floating offshore wind technologies, deeper water could become a point of interest in future.

3.4.1 Metocean Site Conditions

For the metocean assessment in deeper waters that are compatible with floating wind energy (at least 50 m), we chose the location of NDBC station 42019 as the target area, as shown in Figure 24. This buoy provides sufficient wave data and is located in a water depth suitable for the development of floating offshore wind turbines (83.5 m). It is located at (27.91, -95.345), which is southwest of the lease area OCS-G37336, as shown in Appendix F. All other data sources were chosen based on their proximity to this location and the data coverage of respective stations.

We used NDBC station 42019 as the primary source for wave data. The station is located in water that is 83.5 m deep and 50 nm off the coast. No other station was available in the vicinity to fill data gaps. We used NOW-23 data from the same location for hub-height wind speeds.

As a data source for ocean currents, we used the NDBC station 42049 (TABS W), which is maintained by Texas A&M University. The buoy is located in water 21 m deep and is located approximately 43 nm from NDBC station 42019. It provides approximately 8.45 years of ocean current measurements. The HFRNet current dataset includes the vicinity of this location but we had difficulty accessing the data so instead used the NDBC buoy measurements.

Table 14 summarizes basic information of the data sources for locations in the Gulf of Mexico, including the location, depth, and distance to shore.

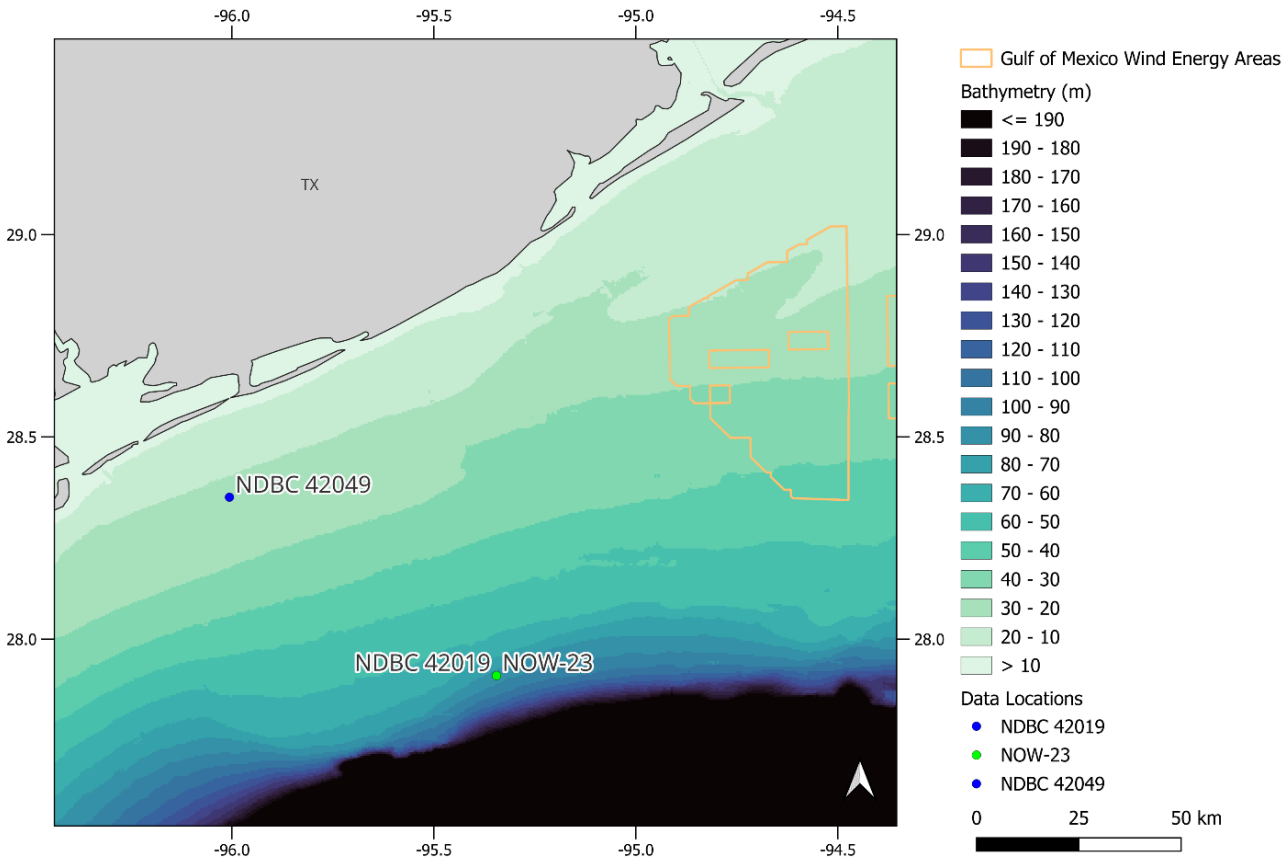

Figure 24. Gulf of Mexico bathymetry and metocean data source locations.

Note: Wind energy areas are shown as contours. Bathymetry data source: (NCEI 2024).

Table 14. Data Sources of Gulf of Mexico locations

Type	Station ID	Latitude (deg)	Longitude (deg)	Water Depth (m)	Distance to Shore (nm)
Waves	42019	27.91	-95.345	83.5	50
Wind	NOW-23	27.91	-95.345	83.5	50
Currents	42049	28.351	-96.006	21	15

The speed and directional distributions of wind, waves, and current data are shown in Figure 25. For waves, significant wave height is plotted in place of wind or current speed.

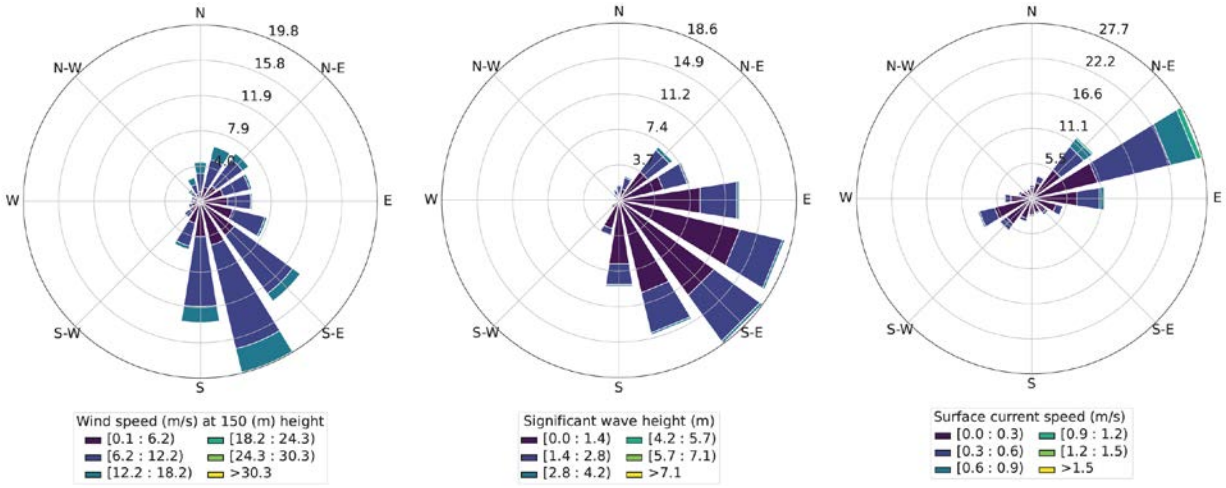

(a) Wind (b) Wave (c) Current

Figure 25. Gulf of Mexico wind, wave, and current roses.

Note: 0° corresponds to North.

Extreme wind, wave, and current parameters for return periods ranging from 1 to 500 years are shown in Table 15. The mean directions of the peaks used for the extrapolation are 125° for wind, 111° for waves, and 69° for currents.

Table 15. Extreme Metocean Parameters for the Gulf of Mexico

Return Period (years)	Wind Speed (m/s)	Significant Wave Height (m)	Peak Wave Period (s)	Current Speed (m/s)
1	23.9	4.9	10.1	1.0
5	27.0	5.8	11.1	1.3
10	28.0	6.1	11.4	1.5
50	29.8	6.8	11.9	1.7
100	30.4	7.0	12.1	1.8
500	31.5	7.4	12.5	2.1

Conditional values of wave height, wave period, and current speed for wind speed bins of every 2 m/s are provided in Appendix D, as are the parameters for 100 fatigue bins generated with the maximum dissimilarity algorithm. Figure 26 shows the data points and cluster centroids for the 100 bins.

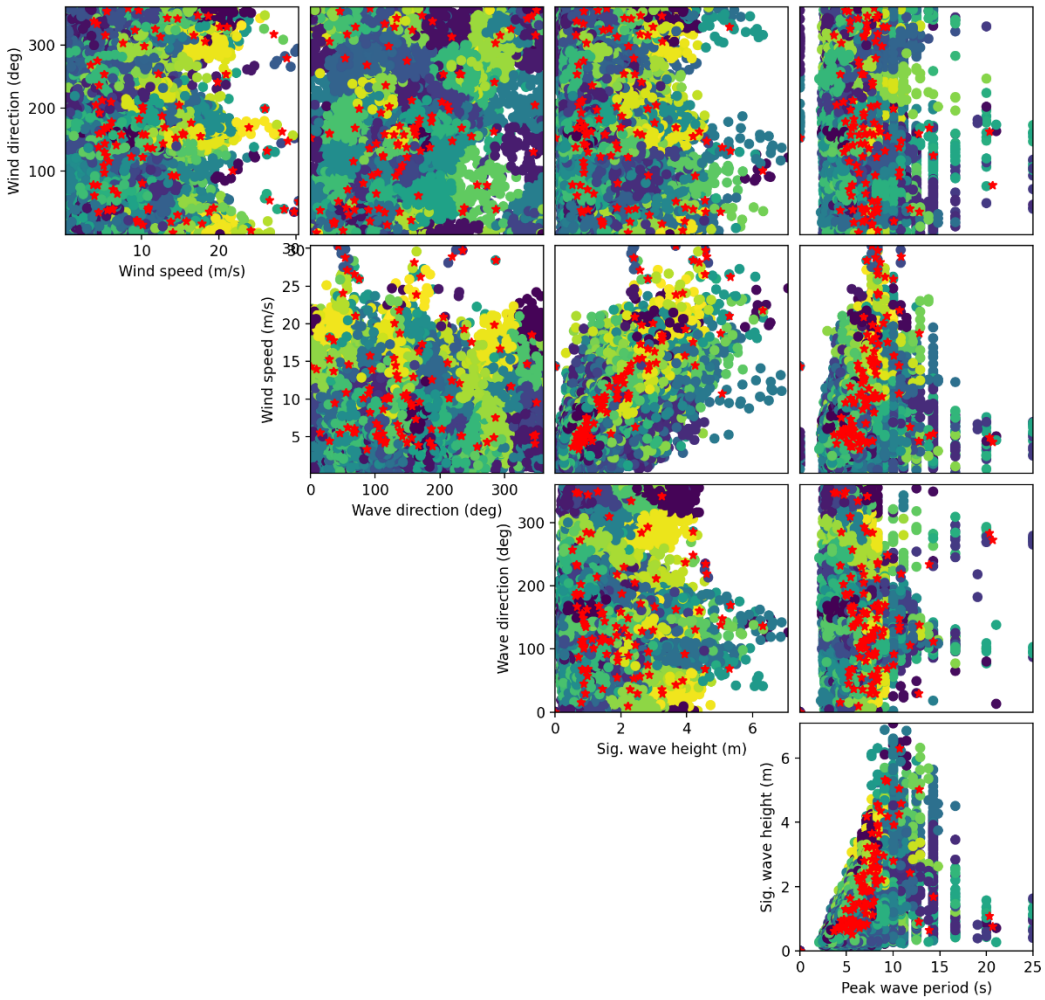

Figure 26. Gulf of Mexico metocean data and fatigue bin clusters.

Note: Clusters represented by different colors, centroids marked in red.

3.4.2 Seabed Conditions

We generated bathymetry grid files from the NCEI Digital Elevation Model Global Mosaic for a rectangular area that is 60 km wide and 80 km long around the reference area (marked as NOW-23 in Figure 24) at three discretization levels. Figure 27 shows the grid with a 1,000-m resolution, where the reference location is in a relatively smooth and shallow sloping area just north of a steep drop-off.

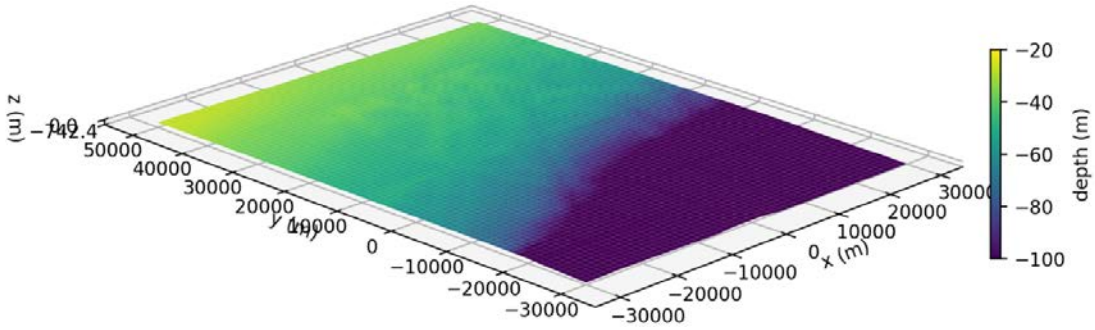

Figure 27. Gulf of Mexico reference site bathymetry at a 1,000-m resolution

Based on 15 data points of the usSEABED database that are located in a 50-km square area around the target area, as shown in Figure 28, the sediment in this area can be classified as gravelly mud (gM). The results of the seabed sediment classification are shown in Table 16. According to the grain size (phi) of 4.17, which is characterized as coarse silt or mud.

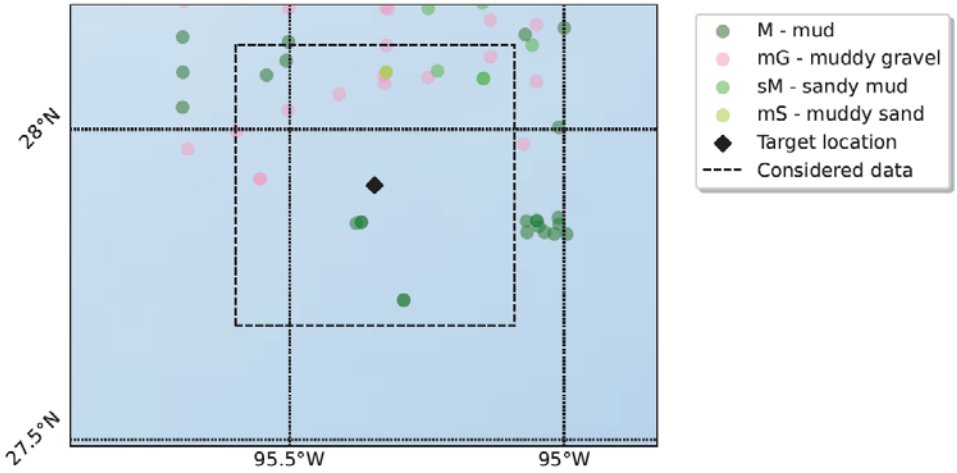

Figure 28. usSEABED soil data points at the Gulf of Mexico lease area location

Table 16. Gulf of Mexico Seabed Sediment Classification at Site

Latitude (deg)	Longitude (deg)	Gravel (%)	Sand (%)	Mud (%)	Grain Size (phi)	Folk Class
27.684 to 28.136	-95.599 to -95.090	21.12	4.93	73.95	4.17	Gravelly mud (gM)

4 Conclusions

Information about the specific site conditions in the vicinity of a wind energy area is key to a successful offshore wind farm design. However, publicly available, site-specific data for potential floating offshore wind project sites in the United States are very limited. To address this need, we collected data, including metocean, geophysical, and sediment data, on four U.S. locations that represent areas of interest for floating wind energy development:

- Humboldt Bay: An area in Northern California with two lease areas
- Morro Bay: An area in Southern California with three lease areas
- Gulf of Maine: An area being considered for a research-oriented wind farm as well as potential future lease areas
- Gulf of Mexico: An area southwest of current lease areas that is in deeper waters

We obtained the geophysical and sediment data from publicly available sources. In the case of sediment data, which were based on the usSEABED database, we estimated the resulting Folk classification for a specific location by taking the weighted average of the surrounding data points.

The process of getting the right metocean data for a specific site, which can be used for offshore wind turbine design, required data from multiple sources. We used NDBC metocean buoy measurement data as the primary source for wave data and a secondary source for current data. Using this data involved significant effort for combining disparate data files and dealing with erroneous values and data inconsistencies. We used surface current measurements from the HFRNet dataset when possible, and substituted current measurements from nearby NDBC buoys when necessary due to coverage or data access limitations. We used wind data from the NOW-23 dataset, which is the most recently updated offshore wind hindcast for the United States and is considered more accurate than other available data sources. Merging the data from different sources into one homogenous dataset for each site involved a large data processing effort. The resulting hourly time series can be used for a wide variety of site-specific analysis tasks.

Using the combined hourly time series, we conducted additional analyses to compute metocean parameters for use in extreme and fatigue loads analyses. Extreme parameters of wind, wave, and currents for a range of return periods were computed using a distribution fitting process. These results include extreme return-period values for wind speed, wave height, and current speed, along with corresponding expected values of direction and wave peak period. The joint distribution of metocean parameters is represented by a clustering approach, providing 100 probability-weighted metocean conditions that can be used for fatigue loads analyses.

The processed datasets provide reference site conditions for the four sites that can support U.S. site-specific offshore wind energy research endeavors. Although more extensive data is needed for developing real projects, the collected reference site datasets are a significant step forward by providing unified, publicly available data containing all the metocean and bathymetric information needed for typical floating wind array research studies and technology development activities.

4.1 Recommendations and Future Work

The presented reference site conditions are limited to four sites and do not represent all U.S. regions of interest for floating wind development. The work presented here could be replicated to create similar reference site conditions for other U.S. regions. The development of the presented reference site conditions has shown that there are a variety of different publicly available data sources, many of which also cover other locations. Relevant locations for additional reference sites could be selected based on areas where future lease areas are established, especially if their metocean or seabed characteristics are very different from those of the existing reference sites.

The largest data gap is with seabed geotechnical information. The only data source for seabed sediment that covers all areas is usSEABED, and it did not include soil strength profile information and it had very sparse spatial coverage in the areas of interest. Of the four reference sites, only the Humboldt Bay site had available survey data that provided distinction of different ground conditions within the area (in this case, between clay and rock). This survey data at the necessary spatial resolution is not available for many areas of interest, and it lacks quantitative geotechnical information so still entails making significant assumptions. There is a significant need for geotechnical data that can provide quantitative soil strength profiles at a spatial resolution that captures variations within lease areas. In addition, the sediment depth should be characterized to understand the site-specific feasibility of certain anchor types.

Each category of metocean data could be further improved with more data or more advanced analysis methods. For wind data, the NOW-23 dataset provides the best currently-available wind speeds and directions at various heights for a period of around 21 years. We did not include wind shear and veer in our analysis due to limited time. However, with some additional effort they could be estimated based on the velocity profiles in the time series. A key limitation of the NOW-23 dataset is that it does not include turbulence intensity and coherence, which are important parameter for wind turbine behavior. The 5-minute temporal resolution of the dataset is not high enough to compute turbulence intensity from. Either expanding the NOW-23 dataset to include turbulence intensity or developing an estimation method for it would improve the usability of the dataset for wind system design.

The presented sea state data—significant wave heights, peak wave periods, and mean wave directions—could be expanded by including spectral wave data that is available for many NDBC buoys, including the estimation of a separate time series for the JONSWAP peak enhancement factors. While the JONSWAP spectrum is not universally ideal across all U.S. waters (such as those dominated by long-period swell on the West Coast), it could be a good fit for fetch-limited regions along the East Coast and Gulf Coast, where wind-driven waves dominate. However, unlike the Pierson-Moskowitz spectrum, which assumes fully developed seas, the JONSWAP spectrum includes additional parameters like the peak enhancement factor, making it more adaptable to a wider range of real-world conditions, particularly in growing or fetch-limited seas.

In addition, further analysis of the data to directly calculate joint probability distributions including directionality could provide a more complete picture of the sea conditions on site. Wind and wave alignment is crucial because when wind and waves are aligned, vessels and offshore structures experience reduced motion, making navigation and operations safer and more efficient. Misalignment between wind and waves, however, can increase stress on structures, lead to more challenging sea conditions, and heighten the risk of accidents or damage.

The presented ocean current data consists of surface current velocities. This approach neglects how the currents could vary with depth, and these currents can cause additional loading on subsea structures and seabed scouring around anchors and cables. Furthermore, the existing current data was limited spatially (in some cases the measurement buoys were relatively far from the areas of interest) and temporally (long-term ocean current data were rarely available and there were often large periods of missing or faulty data in buoy measurements). Additional long-term and depth-spanning current data through numerical modeling or new acoustic Doppler current profiler measurements would allow currents to be included at the same quality level as wind and wave data.

There are various ways that the analysis of the processed metocean time series could be improved and expanded. Data coverage of all metocean parameters could be increased by applying methods to fill data gaps, for example by combining different measurement sources with hindcast data. A more thorough study of extreme value extrapolation methods would improve confidence in the extreme value predictions. Some critical load cases require return periods of more than 500 years, which requires longer time series with high data coverage and very reliable extrapolation methods. Special analysis methods may be necessary for accurately estimating extreme values in areas subject to hurricanes, as well as to account for climate-change-related trends in the severity of these events.

Our use of a clustering approach to represent the joint probability distributions has limitations and was not vetted for all sites. Fully assessing the accuracy of various fatigue binning methods and discretization levels requires more intensive computations than we performed here. Our sensitivity study on fatigue binning was confined to hundreds of simulations (as practical for many R&D applications), whereas a precise assessment would require establishing a baseline high-confidence fatigue estimate using a regular grid approach with several orders of magnitude more bins. Furthermore, more site-specific assessment would be warranted to confirm if our assumptions about number of bins and neglecting current are applicable for other areas.

References

ABS. 2020. *Guide for Building and Classing Floating Offshore Wind Turbines*. https://ww2.eagle.org/content/dam/eagle/rules-and-guides/current/offshore/fowt-guide-july20.pdf.

API. 2014a. *API RP 2A WSD - Planning, Designing, and Constructing Fixed Offshore Platforms—Working Stress Design* (Version 22). API Publishing Services.

API. 2014b. *API RP 2MET - Derivation of Metocean Design and Operating Conditions* (Version 1). American Petroleum Institute (API).

Bailey, B. H., M. Filippelli, and M. Baker. 2015. *Metocean Data Needs Assessment for U.S. Offshore Wind Energy* (5372FTR). AWS Truepower LLC., Albany, NY (United States). https://doi.org/10.2172/1338823.

Biglu, Michael, Matthew Hall, Ericka Lozon, and Stein Housner. 2024. "Reference Site Condition Datasets for Floating Wind Arrays in the United States." NREL Data Catalog. Golden, CO: National Renewable Energy Laboratory. DOI: 10.7799/2425969. https://data.nrel.gov/submissions/241.

Bodini, N., M. Optis, M. Rossol, A. Rybchuk, S. Redfern, J. K. Lundquist, D. Rosencrans. 2020. *2023 National Offshore Wind data set (NOW-23)* (4500) [dataset]. DOE Open Energy Data Initiative; National Renewable Energy Laboratory, Golden, CO (United States). https://doi.org/10.25984/1821404.

Bodini, N., M. Optis, S. Redfern, D. Rosencrans, A. Rybchuk, J. K. Lundquist, V. Pronk, S. Castagneri, A. Purkayastha, C. Draxl, R. Krishnamurthy, E. Young, B. Roberts, E. Rosenlieb, W. Musial. 2024. "The 2023 National Offshore Wind data set (NOW-23)." *Earth System Science Data*, *16*(4), 1965–2006. https://doi.org/10.5194/essd-16-1965-2024.

Bureau of Ocean Energy Management. 2020. *Information Guidelines for a Renewable Energy Construction and Operations Plan (COP)* (Version 4). https://www.boem.gov/sites/default/files/documents/about-boem/COP%20Guidelines_Technical_Corrections.pdf

___. 2023a. "California Activities." https://www.boem.gov/renewable-energy/state-activities/california.

___. 2023b. "Gulf of Maine." https://www.boem.gov/renewable-energy/state-activities/maine/gulf-maine.

Buczkowski, B., J. A. Reid, P. N. Schweitzer, V. A. Cross and C. J. Jenkins. 2020a. *usSEABED: Offshore surficial-sediment database for samples collected within the United States Exclusive Economic Zone* [Csv]. U.S. Geological Survey. https://doi.org/10.5066/P9H3LGWM.

Buczkowski, B., J. A. Reid and C. J. Jenkins. 2020b. *Sediments and the sea floor of the continental shelves and coastal waters of the United States—About the usSEABED integrated sea-floor-characterization database, built with the dbSEABED processing system: U.S. Geological Survey*. Open-File Report 2020–1046, 14 p. https://doi.org/10.3133/ofr20201046.

Camus, P., F. J. Mendez, R. Medina, and A. S. Cofiño. 2011. "Analysis of clustering and selection algorithms for the study of multivariate wave climate." *Coastal Engineering*, *58*(6), 453–462. https://doi.org/10.1016/j.coastaleng.2011.02.003.

Conservation Biology Institute. 2020. *US Pacific Coast Seafloor Sediment (usSEABED) | CA Offshore Wind Energy Gateway*. https://caoffshorewind.databasin.org/datasets/c9117302f7be44cba2aa0b4182e84dc7/.

DNV. 2021. *DNV-ST-0437 Loads and site conditions for wind turbines*. https://www.dnv.com/energy/standards-guidelines/dnv-st-0437-loads-and-site-conditions-for-wind-turbines/

DNV GL. 2018. *Metocean Characterization Recommended Practices for U.S. Offshore Wind Energy*. Bureau of Ocean Energy Management (BOEM). https://www.boem.gov/sites/default/files/environmental-stewardship/Environmental-Studies/Renewable-Energy/Metocean-Recommended-Practices.pdf.

Draxl, C., A. Clifton, B. M. Hodge, and J. McCaa. 2015. "The Wind Integration National Dataset (WIND) Toolkit." *Applied Energy*, *151*, 355–366. https://doi.org/10.1016/j.apenergy.2015.03.121

Folk, R. L. 1980. *Petrology of Sedimentary Rocks*. Hemphill Publishing Company. http://hdl.handle.net/2152/22930.

GEBCO Bathymetric Compilation Group 2023. 2023. The GEBCO_2023 Grid - a continuous terrain model of the global oceans and land. NERC EDS British Oceanographic Data Centre NOC. https://doi.org/doi:10.5285/f98b053b-0cbc-6c23-e053-6c86abc0af7b.

Goldfinger, C., S. K. Henkel, C. Romsos, A. Havron, and B. Black. 2014. *Benthic Habitat Characterization Offshore the Pacific Northwest Volume 1: Evaluation of Continental Shelf Geology* (OCS Study BOEM 2014-662; p. 161). U.S. Department of the Interior, Bureau of Ocean Energy Management, Pacific OCS Region. https://espis.boem.gov/final%20reports/5453.pdf.

Gulf of Maine Research Institute. 2023. *Gulf of Maine, Explained: Causes & Impacts of Rapid Warming*. https://www.gmri.org/stories/gulf-of-maine-explained-causes-impacts-of-rapid-warming/.

Hersbach, H., B. Bell, P. Berrisford, S. Hirahara, A. Horányi, J. Muñoz-Sabater, J. Nicolas, C. Peubey, et al. 2020. "The ERA5 global reanalysis." *Quarterly Journal of the Royal Meteorological Society*. https://doi.org/10.1002/qj.3803.

Hervey, R. V., and D. Petraitis. 2015. *Near-real-time surface ocean velocities derived from HF radar stations located along coastal waters of North Slope Alaska, Puerto Rico/Virgin Islands, eastern US/Gulf of Mexico, Hawaii and western US* [dataset]. https://www.ncei.noaa.gov/access/metadata/landing-page/bin/iso?id=gov.noaa.nodc:NDBC-HFRadarRTVector.

International Society for Soil Mechanics and Geotechnical Engineering. 2005. *Geotechnical and Geophysical Investigations for Offshore and Nearshore Developments*. . https://www.kivi.nl/uploads/media/58a3570951450/Investigations%20for%20developments.pdf.

International Energy Agency. 2021. "IEA Wind TCP Task 49." https://iea-wind.org/task49/

International Electrotechnical Commission. 2019a. *IEC 61400-3-1, Wind turbines – Part 3-1: Design requirements for fixed offshore wind turbines*. ANSI

___. 2019b. *IEC 61400-3-2:2019 Wind energy generation systems – Part 3-2: Design requirements for floating offshore wind turbines* (Version 1). ANSI.

International Ocean Discovery Program. 2023. *International Ocean Discovery Program—Exploring the Earth Unter the Sea*. https://iodp.org/.

International Organization for Standardization. 2015. *ISO 19901-1: 20015: Petroleum and natural gas industries – Specific requirements for offshore structures – Part 1: Metocean design and operating considerations* (Version 1)

Kanner, S., A. Aubault, A. Peiffer, &and B. Yu. 2017. *Efficient Algorithm for Discretization of Metocean Data Into Clusters of Arbitrary Size and Dimension*. ASME 2017 36th International Conference on Ocean, Offshore and Arctic Engineering. https://doi.org/10.1115/OMAE2017-62077.

Kanner, S., A. Aubault, A. Peiffer, and B. Yu. 2018. *Maximum Dissimilarity-Based Algorithm for Discretization of Metocean Data Into Clusters of Arbitrary Size and Dimension*. ASME 2018 37th International Conference on Ocean, Offshore and Arctic Engineering. https://doi.org/10.1115/OMAE2018-77977.

Manwell, J. F., J. G. McGowan, and A. L. Rogers. 2009. *Wind Energy Explained: Theory, Design and Application* (2nd ed.). John Wiley & Sons Ltd.

MARIS, BODC, IOC-IODE, IOGP. n.d.. System of Industry Metocean data for the Offshore and Research Communities (SIMORC). http://www.simorc.com/welcome.asp

Michelen, C., and R. Coe. 2015. Comparison of methods for estimating short-term extreme response of wave energy converters | IEEE Conference Publication | IEEE Xplore. *Proceedings of OCEANS 2015 - MTS/IEEE Washington*. OCEANS 2015 - MTS/IEEE Washington, Washington, DC. https://ieeexplore.ieee.org/document/7401878.

NOAA. 2009. *NDBC Handbook of Automated Data Quality Control Checks and Procedures*. U.S. Department of Commerce. https://www.ndbc.noaa.gov/publications/NDBCHandbookofAutomatedDataQualityControl2009.pdf

___. 2011. *Gulf of Mexico Data Atlas*. https://gulfatlas.noaa.gov/.

___. 2023. *JetStream Max: Bay of Fundy: The Highest Tides in the World*. https://www.noaa.gov/ocean/fundy-max.

___. 2024. *HF Radar*. The U.S. Integrated Ocean Observing System. https://ioos.noaa.gov/project/hf-radar/.

___. n.d.. *IOOS Integrated Ocean Observing System—About Us*. Accessed May 05, 2023. https://ioos.noaa.gov/about/about-us/.

NOAA National Centers for Environmental Information (NCEI). 2023. *Coastal Relief Models (CRMs)* [dataset]. https://doi.org/doi: 10.25921/5ZN5-KN44.

NOAA National Centers for Environmental Information (NCEI). 2024. *Digital Elevation Models Global Mosaic (Elevation Values)* [dataset]. https://www.ncei.noaa.gov/metadata/geoportal/rest/metadata/item/gov.noaa.ngdc.mgg.dem:999919/html.

NOAA National Data Buoy Center. 1971. *Meteorological and oceanographic data collected from the National Data Buoy Center Coastal-Marine Automated Network (C-MAN) and moored (weather) buoys* (gov. noaa.nodc:NDBC-CMANWx) [dataset]. https://www.ncei.noaa.gov/access/metadata/landing-page/bin/iso?id=gov.noaa.nodc:NDBC-CMANWx.

NOAA. n.d. "National Data Buoy Center Website - Measurement Descriptions and Units." U.S. Department of Commerce. Accessed August 20, 2024. https://www.ndbc.noaa.gov/measdes.shtml.

Santos, P., S. Creane, K. Kölle, D. Airoldi, M. Biglu, E. Cheynet, L. Frøyd, M. Hall Y.-Y. Kim, F. Lanni, X. G. Larsén, L. Lin, E. Lozon, M. B. Paskyabi, A. Yamagushi, and Y.-J. You. 2023. *Reference site conditions for floating wind arrays: Dataset of reference sites* (0.1.0) [dataset]. Zenodo. https://doi.org/10.5281/zenodo.8375736.

State of Maine. 2021. *State of Maine Offshore Wind Research Array - Application for an Outer Continental Shelf Renewable Energy Research Lease*. https://www.maine.gov/energy/sites/maine.gov.energy/files/2021-10/GEO_ResearchLeaseApplication_10121.pdf.

Steinley, Douglas. 2006. "K-means clustering: A half-century synthesis." *British Journal of Mathematical and Statistical Psychology*, *59*(1), 1–34. https://doi.org/10.1348/000711005X48266.

Stewart, G. M., A. Robertson, J. Jonkman, and M. A. Lackner. 2016. "The creation of a comprehensive metocean data set for offshore wind turbine simulations.". *Wind Energy*, *19*(6), 1151–1159. https://doi.org/10.1002/we.1881.

Tajalli Bakhsh, T., M. Monim, K. Simpson, T. Lapierre, J. Dahl, J. Rowe, and M. Spaulding. 2020. *Potential Earthquake, Landslide, Tsunami and Geo-Hazards for the U.S. Offshore Pacific Wind Farms* (p. 147). https://www.rpsgroup.com/imported-media/5565/potential-earthquake-landslide-tsunami-and-geohazards-for-the-us-offshore-pacific-wind-farms.pdf.

Tajalli Bakhsh, T., K. Simpson, T. LaPierre, K. Ware, and M. Spaulding. 2023. *Geohazard Analysis and Suitability Updates for California Floating Windfarms* (RI: U.S. Department of the Interior, Bureau of Ocean Energy Management OCS Study BOEM 2023-040; Contract No: 140M0121F0009, p. 71). https://www.rpsgroup.com/imported-media/11980/geohazard-analysis-and-suitability-updates-for-california-floating-windfarms.pdf.

Trandafir, A., J. Fisher, J. N. Fillingham, K. Smith, M. Santra, and S. Esmailzadeh. 2022. *Geological and Geotechnical Overview of the Atlantic and Gulf of Mexico Outer Continental Shelf* (BAA 140M0121R0006; p. 286). BOEM Office of Renewable Energy. https://www.boem.gov/sites/default/files/documents//BOEM-GG-DTS.pdf.

University of Maine. n.d.. "University of Maine Ocean Observing System (UMOOS)." Accessed August 16, 2023. http://gyre.umeoce.maine.edu/buoyhome.php.

Vogel, M., J. Hanson, S. Fan, G. Z. Forristall, Y. Li, R. Fratantonio, and P. Jonathan. 2016. "Efficient Environmental and Structural Response Analysis by Clustering of Directional Wave Spectra." Offshore Technology Conference. https://doi.org/10.4043/27039-MS.

Williams, S. J., M. A. Arsenault, L. J. Poppe, J. A. Reid, and C. J. Jenkins. 2006. "Surficial Sediment Character of the New York-New Jersey Offshore Continental Shelf Region; a GIS Compilation." http://pubs.usgs.gov/of/2006/1046.

Appendix A. Humboldt Metocean Details

The authors analyzed extreme wind speed values by computing the monthly maxima of each time series and then fitting a generalized extreme value distribution to those maxima. As a result, extreme values can then be read off the distribution at the desired return period probabilities. Because of the presence of suspect data, daily or subdaily peaks for wave height and current speed were computed and then fit using a Weibull distribution, which provided more consistent results. Extreme wave heights were computed by fitting a Weibull distribution to peaks from the hourly time series data using a 4-hour minimum separation between peaks. We also computed extreme current speeds by fitting a Weibull distribution to peaks from the hourly time series data using a 24-hour minimum separation between peaks. For conditional extreme values, the wave and current time series were filtered based on 2-meter-per-second (m/s) wind speed bins before doing the monthly maxima. Unconditional and conditional extreme values of wave height, wave period, and current speed for wind speed bins of every 2 m/s are provided in Table A-1.

Table A-1. Conditional Extreme Meteorological Ocean Values for Humboldt Bay

Wind Speed (m/s)	Wind Dir. (deg)	Wave Dir. (deg)	Significant Wave Height (meters [m])						Peak Wave Period (seconds [s])						Curr. Dir. (deg)	Current Speed (m/s)					
			Return Period (years)						*Return Period (years)*							*Return Period (years)*					
			1	*5*	*10*	*50*	*100*	*500*	*1*	*5*	*10*	*50*	*100*	*500*		*1*	*5*	*10*	*50*	*100*	*500*
All	339	302	8.5	9.8	10.4	11.8	12.4	13.7	16.8	18.1	18.6	19.8	20.3	21.4	84	0.92	1.09	1.15	1.28	1.33	1.44
0-2	287	295	5.4	6.9	7.6	9.1	9.8	11.4	13.4	15.2	15.9	17.4	18.1	19.5	98	0.27	0.65	0.73	0.88	0.93	1.04
2-4	301	294	6.4	8.2	8.9	10.8	11.6	13.6	14.6	16.5	17.2	18.9	19.7	21.3	89	0.55	0.81	0.89	1.06	1.12	1.25
4-6	318	296	6.8	8.4	9.1	10.8	11.6	13.3	15.0	16.7	17.4	19.0	19.6	21.0	81	0.60	0.83	0.90	1.04	1.09	1.19
6-8	330	297	7.1	8.9	9.7	11.6	12.5	14.4	15.3	17.2	18.0	19.7	20.4	21.9	84	0.63	0.86	0.93	1.08	1.13	1.24
8-10	334	300	7.0	8.6	9.3	11.0	11.8	13.5	15.2	16.9	17.6	19.2	19.8	21.2	87	0.67	0.89	0.95	1.06	1.10	1.18
10-12	340	304	6.7	8.3	9.0	10.5	11.2	12.8	15.0	16.6	17.2	18.7	19.3	20.6	79	0.70	0.89	0.94	1.03	1.06	1.12
12-14	342	309	6.4	7.6	8.1	9.3	9.8	10.9	14.6	15.9	16.4	17.6	18.0	19.0	83	0.70	0.89	0.95	1.06	1.09	1.17
14-16	345	312	6.2	7.3	7.7	8.7	9.2	10.1	14.3	15.5	16.0	17.0	17.5	18.3	81	0.64	0.87	0.94	1.07	1.12	1.22
16-18	346	310	6.1	7.1	7.5	8.4	8.7	9.6	14.2	15.3	15.8	16.7	17.0	17.8	77	0.58	0.84	0.90	1.03	1.08	1.17
18-20	346	309	6.0	7.0	7.4	8.2	8.6	9.3	14.2	15.2	15.7	16.5	16.9	17.6	77	0.51	0.83	0.90	1.03	1.07	1.15
20-22	348	309	6.0	7.1	7.6	8.6	9.0	10.0	14.1	15.4	15.8	16.9	17.3	18.3	92	0.62*	0.85	0.91	0.96	0.97	0.98
22-24	350	308	5.9	7.1	7.5	8.6	9.1	10.1	14.1	15.3	15.8	16.9	17.4	18.3	91	0.52*	0.73	0.86	0.97	0.98	0.99
24-26	167	294	6.0	7.3	7.9	9.3	9.9	11.4	14.1	15.6	16.2	17.6	18.2	19.4	149	0.34*	0.62	0.75	0.90	0.95	1.03
26-28	166	267	5.6	7.0	7.5	8.7	9.2	10.3	13.6	15.2	15.8	17.0	17.5	18.5	271	0.3*	0.58*	0.71*	0.9*	0.95*	1.05*

*Fit issues required alternative methods to fill in these data points.

Table A-2 provides 100 clusters of wind and wave conditions that represent the joint probability distribution for use in fatigue analysis.

Table A-2. Meteorological Ocean Joint Probability Fatigue Clusters for Humboldt Bay

Bin Number	Number of Data Points	Cluster Probability	Cluster Centroid					Cluster Standard Deviation				
			Wind Dir. (deg)	Wind Speed (m/s)	Wave Dir. (deg)	Wave Height (m)	Wave Period (s)	Wind Dir. (deg)	Wind Speed (m/s)	Wave Dir. (deg)	Wave Height (m)	Wave Period (s)
1	9,291	0.072158	354	11.2	334	1.93	7.4	4.6	1.8	5.4	0.41	0.9
2	8,528	0.066232	356	13.4	333	2.86	8.9	4.7	1.8	7.9	0.47	0.9
3	7,551	0.058644	354	9.8	312	1.49	7.8	5.5	2.0	4.7	0.43	1.2
4	4,735	0.036774	352	12.5	295	2.44	11.2	5.4	2.0	6.3	0.56	1.4
5	4,727	0.036712	1	7.1	287	2.01	13.1	4.8	2.1	5.6	0.58	1.0
6	4,646	0.036083	357	8.4	319	2.47	11.5	6.6	2.1	5.1	0.57	1.1
7	4,485	0.034832	351	4.9	325	1.44	8.4	7.8	1.8	5.4	0.49	1.1
8	3,935	0.030561	340	4.7	292	1.73	11.2	5.2	2.1	6.5	0.58	1.3
9	3,713	0.028837	356	8.0	284	1.29	9.4	5.7	2.1	5.1	0.43	1.3
10	3,367	0.026149	351	19.4	332	3.53	8.9	3.8	2.2	9.1	0.69	1.1
11	3,312	0.025722	15	4.4	298	1.53	10.5	5.2	1.8	6.8	0.55	1.4
12	2,380	0.018484	358	7.3	294	3.82	14.1	6.7	2.6	7.5	0.66	1.4
13	2,213	0.017187	357	8.1	353	1.82	7.9	7.2	2.4	5.0	0.56	1.2
14	2,087	0.016208	215	4.1	324	1.52	8.7	8.8	2.1	7.2	0.46	1.1
15	1,908	0.014818	178	4.0	300	1.83	11.4	6.5	2.0	6.0	0.60	1.3
16	1,776	0.013793	354	13.8	329	3.92	12.6	5.5	2.5	7.3	0.73	1.4
17	1,744	0.013545	307	3.5	286	1.96	12.1	5.9	1.9	7.0	0.65	1.6
18	1,734	0.013467	211	5.2	282	1.47	9.9	5.8	2.3	6.7	0.52	1.4
19	1,722	0.013374	178	15.3	287	2.11	11.4	5.2	1.9	6.1	0.67	1.1
20	1,607	0.012481	194	9.8	277	2.20	12.3	5.7	1.7	5.9	0.65	1.1
21	1,597	0.012403	237	3.6	292	2.03	11.8	5.9	1.9	7.2	0.68	1.3
22	1,594	0.012380	34	3.4	287	2.51	13.4	6.3	1.8	8.4	0.89	1.3
23	1,566	0.012162	352	16.6	295	3.78	13.6	5.6	2.6	6.1	0.73	1.8
24	1,552	0.012053	297	3.1	317	1.55	9.0	9.0	1.7	8.8	0.51	1.3
25	1,503	0.011673	184	8.9	328	1.67	8.6	6.6	2.8	6.5	0.52	1.3
26	1,442	0.011199	14	5.6	290	2.27	16.7	6.4	2.4	6.5	0.72	1.6
27	1,431	0.011114	346	6.0	289	1.87	16.4	6.2	2.8	5.7	0.62	1.6
28	1,424	0.011059	201	4.5	285	1.91	14.2	6.7	2.2	5.7	0.59	1.2
29	1,393	0.010819	356	7.1	245	1.09	15.2	6.6	2.7	5.9	0.41	1.6
30	1,350	0.010485	314	8.9	309	3.15	11.8	7.0	2.6	8.8	0.66	1.3
31	1,341	0.010415	182	12.4	293	2.40	14.6	5.6	2.1	6.8	0.67	1.2
32	1,286	0.009988	183	9.1	295	1.39	8.8	7.0	2.7	5.7	0.47	1.4
33	1,252	0.009724	173	18.4	293	3.28	14.1	6.0	2.0	6.5	0.64	1.5
34	1,250	0.009708	166	10.5	295	2.32	12.1	6.8	2.0	6.4	0.64	1.1
35	1,233	0.009576	47	3.2	319	1.72	9.5	9.4	1.8	7.6	0.65	1.6
36	1,228	0.009537	178	5.0	268	1.59	11.0	6.2	2.2	6.0	0.63	1.5
37	1,211	0.009405	272	3.8	281	1.68	10.2	7.3	2.2	7.1	0.63	1.7
38	1,157	0.008986	138	3.2	282	1.73	12.5	7.6	1.9	7.2	0.71	1.7
39	1,154	0.008962	178	15.4	264	3.47	13.2	6.4	2.2	5.8	0.71	1.4

Bin Number	Number of Data Points	Cluster Probability	Cluster Centroid					Cluster Standard Deviation				
			Wind Dir. (deg)	Wind Speed (m/s)	Wave Dir. (deg)	Wave Height (m)	Wave Period (s)	Wind Dir. (deg)	Wind Speed (m/s)	Wave Dir. (deg)	Wave Height (m)	Wave Period (s)
40	1,139	0.008846	203	6.9	292	3.48	12.8	6.0	2.3	6.7	0.57	1.2
41	1,071	0.008318	179	13.8	259	1.94	8.8	5.6	2.4	6.4	0.55	1.5
42	1,064	0.008263	169	4.7	291	3.87	14.4	7.1	2.2	7.9	0.79	1.5
43	994	0.007720	358	10.6	317	2.88	16.1	6.0	2.4	7.5	0.75	1.7
44	934	0.007254	359	5.9	252	1.43	9.8	9.5	2.6	8.7	0.61	1.6
45	933	0.007246	181	13.6	285	4.36	16.3	6.2	2.7	7.9	0.72	1.6
46	913	0.007091	317	4.4	295	3.98	14.2	7.0	2.1	7.7	0.76	1.6
47	867	0.006733	355	7.5	212	1.08	15.4	5.8	2.5	5.5	0.31	1.5
48	847	0.006578	258	6.3	319	2.84	11.6	7.8	3.1	7.3	0.75	1.5
49	800	0.006213	125	3.2	317	1.67	9.4	9.9	2.1	7.9	0.52	1.5
50	762	0.005918	79	2.4	291	2.16	14.1	7.1	1.4	8.2	0.87	1.9
51	762	0.005918	225	12.7	286	3.76	12.3	7.1	2.7	9.0	0.74	1.5
52	751	0.005833	271	4.2	294	3.18	14.6	6.6	2.5	7.2	0.80	1.5
53	737	0.005724	167	16.5	201	2.27	7.0	7.1	2.4	8.2	0.52	1.3
54	729	0.005662	172	23.4	275	4.39	14.3	6.5	2.8	7.7	0.79	1.8
55	706	0.005483	183	8.1	292	2.18	18.4	8.2	3.6	8.0	0.75	1.5
56	634	0.004924	112	3.0	297	3.28	13.1	7.9	1.8	9.2	0.85	1.6
57	615	0.004776	212	9.8	250	2.48	9.6	7.9	2.8	8.0	0.82	1.5
58	608	0.004722	170	21.1	271	2.98	10.1	5.9	2.6	7.6	0.60	1.6
59	605	0.004699	273	8.7	279	3.98	12.3	7.6	3.1	8.7	0.73	1.4
60	605	0.004699	202	5.9	320	2.32	13.4	7.9	2.8	5.4	0.69	1.5
61	601	0.004668	62	2.4	270	1.49	10.7	9.5	1.3	9.1	0.61	1.6
62	585	0.004543	169	21.8	204	2.99	7.8	6.4	2.0	7.4	0.55	1.0
63	552	0.004287	162	9.8	266	4.11	14.1	8.2	2.6	7.4	0.85	1.4
64	548	0.004256	180	15.4	328	2.89	10.0	7.1	2.6	8.6	0.68	1.8
65	526	0.004085	167	11.8	239	2.13	10.3	7.5	2.3	6.8	0.74	1.4
66	523	0.004062	219	5.5	286	4.50	15.4	7.6	2.5	8.6	0.77	1.5
67	485	0.003767	186	7.8	243	1.36	15.0	8.1	3.5	6.7	0.61	1.3
68	484	0.003759	135	10.0	288	2.46	15.9	7.4	3.6	7.6	0.74	2.0
69	434	0.003371	306	11.4	316	5.50	14.1	9.2	3.0	9.6	0.76	1.5
70	428	0.003324	355	6.6	340	2.09	13.8	8.0	2.6	7.7	0.81	1.4
71	406	0.003153	241	4.0	285	2.10	16.8	9.5	2.5	8.6	0.69	1.8
72	382	0.002967	187	17.4	229	3.28	10.3	8.1	2.4	7.4	0.70	1.4
73	354	0.002749	251	9.7	298	5.44	15.2	8.0	3.2	9.0	0.80	1.4
74	351	0.002726	224	3.7	218	0.96	14.9	9.1	2.0	11.1	0.30	1.6
75	341	0.002648	189	12.3	208	1.54	5.8	7.7	3.1	8.8	0.47	1.4
76	340	0.002641	168	21.9	238	3.87	10.8	6.8	2.6	5.8	0.70	1.5
77	285	0.002213	305	3.7	235	1.23	14.1	9.5	2.3	7.9	0.58	2.1
78	279	0.002167	24	3.2	218	0.95	15.1	8.1	1.5	9.2	0.37	1.7
79	275	0.002136	247	5.6	242	1.74	8.6	11.0	3.0	10.4	0.75	1.5

Bin Number	Number of Data Points	Cluster Probability	Cluster Centroid					Cluster Standard Deviation				
			Wind Dir. (deg)	Wind Speed (m/s)	Wave Dir. (deg)	Wave Height (m)	Wave Period (s)	Wind Dir. (deg)	Wind Speed (m/s)	Wave Dir. (deg)	Wave Height (m)	Wave Period (s)
80	242	0.001879	175	6.4	207	1.04	15.1	8.9	3.8	6.9	0.29	1.7
81	240	0.001864	169	27.3	194	4.11	8.6	5.8	2.6	7.3	0.75	1.1
82	230	0.001786	326	4.0	317	2.42	17.2	8.9	2.0	9.1	0.83	2.3
83	204	0.001584	138	6.8	230	1.93	9.4	9.3	3.6	9.5	0.70	1.6
84	185	0.001437	171	27.8	245	5.25	11.7	6.5	2.8	10.4	1.14	1.9
85	169	0.001313	359	7.5	177	1.07	14.3	6.9	2.7	7.5	0.34	1.8
86	167	0.001297	204	13.8	274	6.88	16.4	11.0	3.8	10.2	0.92	1.6
87	137	0.001064	101	2.5	240	1.28	14.1	11.3	1.7	8.5	0.61	2.0
88	122	0.000947	320	3.1	190	0.95	14.8	11.5	1.7	10.2	0.28	1.8
89	86	0.000668	358	8.2	147	1.05	16.5	7.8	2.5	10.3	0.30	1.8
90	65	0.000505	351	6.6	72	0.99	15.5	13.9	2.7	12.1	0.30	2.0
91	58	0.000450	193	8.5	157	1.15	16.5	11.2	4.2	10.9	0.39	2.1
92	40	0.000311	166	5.6	344	2.32	17.5	12.6	4.2	10.2	1.00	1.9
93	38	0.000295	101	2.3	189	0.95	15.0	11.7	1.7	9.5	0.35	2.0
94	34	0.000264	274	14.4	310	8.71	16.3	15.0	4.3	8.0	0.93	1.5
95	29	0.000225	359	9.9	13	2.55	20.2	4.7	3.5	12.4	0.83	2.3
96	17	0.000132	219	4.7	33	1.09	13.2	13.8	1.8	9.5	0.28	3.4
97	8	0.000062	169	18.9	176	4.13	17.5	7.0	4.7	18.7	0.93	2.3
98	5	0.000039	184	9.7	67	1.73	19.1	9.3	4.5	11.6	0.59	1.2
99	3	0.000023	138	4.0	68	1.01	13.6	7.5	0.7	8.6	0.05	1.1
100	1	0.000008	166	28.0	95	4.26	17.4	0.0	0.0	0.0	0.00	0.0

Appendix B. Morro Bay Metocean Details

Analysis of extreme wind speed values was done by computing the monthly maxima of each time series and then fitting a generalized extreme value distribution to those maxima. Extreme values can then be read off the distribution at the desired return period probabilities. Because of the presence of suspect data, daily or subdaily peaks for wave height and current speed were computed and then fit using a Weibull distribution, which provided more consistent results. We then computed extreme wave heights by fitting a Weibull distribution to peaks from the hourly time series data using a 4-hour minimum separation between peaks. Extreme current speeds were computed by fitting a Weibull distribution to peaks from the hourly time series data using a 24-hour minimum separation between peaks. For conditional extreme values, the wave and current time series were filtered based on 2-meter-per-second (m/s) wind speed bins before doing the monthly maxima. Unconditional and conditional extreme values of wave height, wave period, and current speed for wind speed bins of every 2 m/s are provided in Table B-1.

Table B-1. Conditional Extreme Meteorological Ocean Values for Morro Bay

Wind Speed (m/s)	Wind Dir. (deg)	Wave Dir. (deg)	Significant Wave Height (meters [m]) Return Period (years)						Peak Wave Period (seconds [s]) Return Period (years)						Curr. Dir. (deg)	Current Speed (m/s) Return Period (years)					
			1	*5*	*10*	*50*	*100*	*500*	*1*	*5*	*10*	*50*	*100*	*500*		*1*	*5*	*10*	*50*	*100*	*500*
All	321	300	6.9	8.5	9.2	10.7	11.3	12.7	15.7	17.5	18.2	19.6	20.1	21.3	45	0.68	0.81	0.87	0.99	1.04	1.16
0-2	255	294	4.6	5.9	6.4	7.7	8.3	9.5	12.8	14.5	15.2	16.6	17.2	18.5	130	0.43	0.52	0.56	0.63	0.66	0.71
2-4	295	293	5.2	6.8	7.5	9.2	10.0	11.8	13.6	15.6	16.4	18.2	18.9	20.5	121	0.51	0.63	0.68	0.78	0.82	0.91
4-6	314	291	5.5	7.3	8.1	10.2	11.2	13.5	14.0	16.2	17.1	19.2	20.0	22.0	107	0.51	0.62	0.66	0.76	0.80	0.90
6-8	320	293	5.6	7.4	8.3	10.2	11.1	13.3	14.2	16.3	17.2	19.2	20.0	21.9	75	0.52	0.67	0.74	0.91	0.99	1.19
8-10	323	297	5.6	7.1	7.8	9.3	9.9	11.3	14.2	16.0	16.7	18.2	18.8	20.1	52	0.53	0.65	0.70	0.82	0.87	0.97
10-12	325	302	5.5	7.0	7.7	9.2	9.9	11.4	14.1	15.9	16.6	18.1	18.8	20.3	34	0.53	0.61	0.64	0.71	0.73	0.77
12-14	326	308	5.7	7.1	7.7	9.1	9.7	11.0	14.3	16.0	16.7	18.1	18.6	19.9	20	0.53	0.58	0.60	0.63	0.63	0.65
14-16	326	312	5.9	7.2	7.8	8.9	9.4	10.5	14.6	16.1	16.7	17.9	18.4	19.4	13	0.57	0.67	0.71	0.78	0.81	0.87
16-18	327	315	5.9	7.1	7.6	8.6	9.0	9.8	14.5	16.0	16.5	17.5	17.9	18.7	9	0.57	0.67	0.71	0.79	0.81	0.87
18-20	328	317	5.9	7.2	7.7	8.6	9.0	9.8	14.6	16.1	16.6	17.6	18.0	18.8	7	0.55	0.62	0.65	0.68	0.69	0.71
20-22	330	317	6.0	7.4	7.9	9.0	9.5	10.4	14.7	16.3	16.8	18.0	18.4	19.3	4	0.51	0.59	0.61	0.66	0.67	0.70
22-24	331	310	6.4	8.0	8.6	10.0	10.6	11.8	15.2	16.9	17.6	19.0	19.5	20.6	12	0.47	0.52	0.53	0.54	0.55	0.55
24-26	173	231	6.8	8.0	8.5	9.6	10.0	11.0	15.6	17.0	17.5	18.6	19.0	19.9	31						
26-28	150	163																			

Table B-2 provides 100 clusters of wind and wave conditions that represent the joint probability distribution for use in fatigue analysis.

Table B-2. Meteorological Ocean Joint Probability Fatigue Clusters for Morro Bay

			Cluster Centroid					Cluster Standard Deviation				
Bin Number	Number of Data Points	Cluster Probability	Wind Dir. (deg)	Wind Speed (m/s)	Wave Dir. (deg)	Wave Height (m)	Wave Period (s)	Wind Dir. (deg)	Wind Speed (m/s)	Wave Dir. (deg)	Wave Height (m)	Wave Period (s)
1	11,555	0.082763	325	8.3	316	1.80	9.3	4.9	1.6	6.0	0.45	1.1
2	9,930	0.071124	326	13.7	322	2.21	7.3	3.6	1.3	5.9	0.41	1.2
3	7,589	0.054356	308	4.0	314	1.70	9.9	7.2	1.6	6.6	0.46	1.3
4	7,403	0.053024	323	5.1	292	1.90	12.8	6.0	1.8	6.1	0.56	1.5
5	6,889	0.049342	328	17.7	325	2.55	7.1	2.8	1.4	5.7	0.40	1.1
6	6,838	0.048977	326	13.3	309	2.54	10.5	4.8	1.4	5.7	0.50	1.2
7	6,178	0.044250	327	9.3	302	2.15	13.2	5.5	1.3	5.1	0.47	1.3
8	4,681	0.033528	331	10.7	306	3.52	14.2	5.4	1.7	6.2	0.53	1.3
9	4,386	0.031415	327	10.8	324	1.67	6.1	4.2	1.5	6.4	0.31	1.0
10	4,047	0.028987	330	6.8	300	2.55	17.5	7.5	2.4	7.4	0.79	1.7
11	3,895	0.027898	266	2.9	298	1.90	12.2	7.7	1.6	9.6	0.57	2.4
12	3,738	0.026773	352	4.1	311	2.22	11.5	8.1	1.8	5.7	0.68	1.9
13	3,345	0.023959	340	10.1	317	2.71	11.0	5.1	1.5	5.6	0.49	1.2
14	3,259	0.023343	331	15.0	316	3.71	12.3	4.3	1.2	5.6	0.47	1.4
15	3,186	0.022820	327	12.0	281	2.12	12.9	5.2	1.8	5.7	0.55	1.6
16	3,170	0.022705	301	5.7	300	3.14	14.3	7.6	2.4	7.2	0.79	1.7
17	2,584	0.018508	317	5.9	200	1.32	15.2	4.5	1.6	6.3	0.34	1.7
18	2,315	0.016581	319	6.8	251	1.40	14.2	7.7	2.3	6.8	0.39	2.1
19	2,297	0.016452	167	3.3	311	1.74	10.2	6.5	1.7	6.9	0.49	1.2
20	2,255	0.016151	215	2.4	303	1.84	11.3	7.2	1.3	8.4	0.53	1.9
21	1,839	0.013172	321	7.7	173	1.32	14.0	5.5	2.0	6.0	0.32	1.7
22	1,830	0.013107	329	18.2	322	3.99	9.9	3.6	1.5	4.6	0.49	1.0
23	1,776	0.012721	151	3.8	288	2.40	14.6	6.2	1.8	7.6	0.86	1.9
24	1,735	0.012427	323	9.9	214	1.41	14.8	5.3	1.5	6.0	0.34	1.6
25	1,675	0.011997	330	17.8	304	2.95	11.4	3.7	1.4	5.7	0.44	1.5
26	1,620	0.011603	357	3.6	282	1.86	13.9	7.2	1.8	7.8	0.67	2.0
27	1,594	0.011417	180	4.5	298	2.23	13.5	5.5	2.1	6.5	0.66	1.4
28	1,512	0.010830	124	3.8	309	1.91	10.7	7.5	2.2	5.9	0.58	1.5
29	1,422	0.010185	96	4.0	293	2.14	15.2	7.1	2.1	7.9	0.76	2.4
30	1,361	0.009748	62	2.9	307	1.83	10.9	9.4	1.9	8.3	0.57	1.6
31	1,211	0.008674	289	3.5	197	1.31	14.9	7.1	1.5	11.1	0.30	1.6
32	1,201	0.008602	330	14.8	316	2.87	15.3	4.2	1.7	5.5	0.57	1.4
33	1,188	0.008509	155	8.2	269	1.81	11.5	6.2	2.0	8.3	0.53	1.7
34	1,078	0.007721	329	14.9	291	3.08	16.5	4.5	2.0	5.7	0.66	1.7
35	1,057	0.007571	326	12.8	187	1.76	15.8	4.9	2.0	5.5	0.43	1.6
36	1,034	0.007406	192	5.4	263	1.90	11.6	8.6	2.8	7.8	0.63	2.1
37	1,033	0.007399	126	4.9	274	1.62	13.1	7.9	2.4	7.7	0.54	1.8
38	1,033	0.007399	231	6.3	292	3.08	14.2	7.5	2.4	8.5	0.75	1.9
39	1,022	0.007320	45	3.0	294	2.43	15.7	8.7	1.7	9.2	0.89	2.2

Bin Number	Number of Data Points	Cluster Probability	Cluster Centroid					Cluster Standard Deviation				
			Wind Dir. (deg)	Wind Speed (m/s)	Wave Dir. (deg)	Wave Height (m)	Wave Period (s)	Wind Dir. (deg)	Wind Speed (m/s)	Wave Dir. (deg)	Wave Height (m)	Wave Period (s)
40	971	0.006955	330	18.5	309	4.86	12.9	4.6	1.7	5.8	0.55	1.6
41	940	0.006733	149	9.9	290	2.61	14.9	6.8	1.7	6.5	0.79	2.0
42	896	0.006418	189	4.1	287	2.81	17.1	8.5	2.3	8.2	1.11	2.0
43	736	0.005272	321	13.2	302	5.02	15.4	8.4	2.3	7.4	0.63	1.7
44	697	0.004992	341	4.0	192	1.42	15.4	6.7	1.9	9.4	0.36	2.0
45	684	0.004899	330	21.1	322	3.25	8.3	3.4	1.1	4.9	0.42	1.0
46	669	0.004792	186	11.7	285	2.98	13.2	6.7	2.1	7.3	0.69	1.8
47	589	0.004219	327	10.1	342	1.94	15.4	5.8	2.4	11.4	0.60	2.2
48	502	0.003596	327	14.5	231	1.99	16.2	4.6	2.2	7.9	0.49	1.7
49	477	0.003417	150	4.8	207	1.31	14.2	8.0	2.5	9.0	0.34	1.8
50	473	0.003388	261	9.7	277	2.72	10.8	9.1	2.8	9.8	0.67	1.9
51	435	0.003116	263	6.6	292	5.28	16.0	12.8	3.2	8.8	1.25	1.9
52	415	0.002972	205	3.5	220	1.38	14.9	10.6	2.3	8.8	0.40	1.8
53	384	0.002750	178	3.3	179	1.41	14.8	8.2	2.0	8.3	0.40	1.8
54	361	0.002586	242	2.5	187	1.39	14.0	8.5	1.5	10.7	0.41	2.3
55	359	0.002571	152	15.8	162	2.67	7.0	6.9	1.9	5.6	0.53	1.0
56	350	0.002507	325	11.6	148	1.58	15.6	5.4	1.8	6.9	0.40	1.8
57	278	0.001991	159	12.3	250	2.56	14.3	8.2	2.0	7.8	0.72	2.1
58	250	0.001791	98	10.0	300	2.97	14.5	8.8	2.1	8.3	0.78	2.4
59	239	0.001712	308	9.8	261	2.02	8.4	8.4	3.0	9.0	0.69	1.3
60	201	0.001440	87	3.1	204	1.31	14.6	9.3	2.2	12.4	0.41	2.4
61	189	0.001354	159	17.1	276	3.71	14.4	7.6	2.3	5.8	0.56	1.6
62	178	0.001275	146	9.3	320	1.79	12.6	7.4	2.0	10.3	0.48	1.7
63	177	0.001268	209	11.0	308	2.26	12.0	8.3	2.1	8.8	0.54	1.6
64	175	0.001253	315	5.3	137	1.54	17.3	8.7	2.4	10.0	0.53	2.2
65	166	0.001189	233	13.6	283	4.41	14.6	8.9	2.2	8.6	1.01	2.0
66	163	0.001167	26	2.8	189	1.37	14.4	8.4	1.9	12.2	0.43	2.2
67	162	0.001160	189	10.8	177	2.91	7.8	9.8	2.8	9.1	0.84	1.3
68	155	0.001110	134	5.9	164	1.35	14.8	9.8	2.8	8.1	0.34	1.6
69	150	0.001074	139	10.4	170	1.92	6.5	12.4	2.5	10.3	0.62	1.7
70	147	0.001053	162	15.5	198	2.90	7.4	8.3	2.2	6.6	0.66	1.2
71	143	0.001024	151	20.5	163	3.96	8.2	7.2	1.5	5.3	0.59	0.9
72	131	0.000938	159	15.4	299	2.90	14.1	7.3	1.7	6.4	0.62	1.5
73	101	0.000723	225	12.4	214	3.13	8.6	9.6	3.2	11.8	0.91	1.4
74	92	0.000659	324	7.6	102	1.32	14.9	7.1	1.9	14.0	0.33	1.8
75	90	0.000645	151	15.8	237	2.88	9.7	10.3	2.7	6.6	0.56	1.2
76	86	0.000616	333	22.7	319	6.39	12.2	4.0	1.4	4.9	0.77	1.3
77	78	0.000559	327	12.6	84	1.70	16.1	4.8	2.2	12.0	0.48	2.2
78	77	0.000552	171	15.8	273	5.79	15.6	9.5	3.8	9.1	0.80	1.6
79	59	0.000423	147	22.0	185	4.55	9.1	4.6	1.7	6.7	0.60	0.5

Bin Number	Number of Data Points	Cluster Probability	Cluster Centroid					Cluster Standard Deviation				
			Wind Dir. (deg)	Wind Speed (m/s)	Wave Dir. (deg)	Wave Height (m)	Wave Period (s)	Wind Dir. (deg)	Wind Speed (m/s)	Wave Dir. (deg)	Wave Height (m)	Wave Period (s)
80	54	0.000387	330	17.4	139	2.23	16.9	4.8	1.8	7.4	0.44	1.3
81	46	0.000329	144	5.8	109	1.91	18.1	12.4	2.4	12.2	0.68	2.6
82	43	0.000308	163	10.8	118	2.79	14.8	7.9	2.6	8.6	0.87	1.2
83	43	0.000308	142	11.7	136	1.75	5.0	9.7	3.0	9.1	0.41	0.6
84	32	0.000229	167	23.9	167	4.24	7.8	4.2	1.4	5.0	0.53	0.7
85	30	0.000215	174	16.6	111	4.05	14.8	12.1	2.3	8.7	0.85	1.1
86	23	0.000165	221	4.1	99	1.60	16.1	13.2	2.2	16.4	0.68	2.2
87	21	0.000150	123	19.7	277	3.93	16.8	4.2	2.3	13.3	0.68	2.1
88	19	0.000136	189	21.7	196	3.84	7.9	5.7	1.7	10.1	0.57	0.9
89	15	0.000107	59	2.6	115	1.47	16.1	11.3	1.4	16.9	0.64	2.0
90	15	0.000107	314	14.9	194	2.64	9.2	5.6	2.2	7.7	0.87	1.2
91	15	0.000107	223	15.4	105	7.04	19.3	4.5	1.8	3.1	1.01	1.3
92	14	0.000100	149	26.5	164	5.38	9.4	2.5	1.0	6.0	0.40	0.7
93	10	0.000072	327	14.0	133	2.69	9.0	1.9	2.3	7.1	0.77	1.8
94	10	0.000072	286	9.1	184	4.21	8.7	6.2	3.0	9.0	1.57	1.0
95	10	0.000072	140	26.2	153	4.24	8.4	3.1	1.5	4.8	0.36	0.4
96	9	0.000064	218	6.2	108	6.18	15.9	12.2	1.5	4.4	1.00	1.1
97	9	0.000064	156	13.7	111	1.95	19.7	9.0	2.1	10.4	0.59	1.8
98	7	0.000050	328	17.5	73	3.05	8.9	1.8	2.3	14.6	0.61	2.2
99	4	0.000029	203	20.7	116	7.07	16.1	6.5	0.5	5.7	0.76	1.0
100	1	0.000007	132	29.8	266	3.70	16.0	0.0	0.0	0.0	0.00	0.0

Appendix C. Gulf of Maine Metocean Details

The team analyzed extreme values by fitting a generalized extreme distributions to the monthly maxima of each relevant time series. For conditional extreme values, the wave and current time series were filtered based on 2-meters-per-second (m/s) wind speed bins before doing the monthly maxima. Unconditional and conditional extreme values of wave height, wave period, and current speed for wind speed bins of every 2 m/s are provided in Table C-1.

Table C-1. Conditional Extreme Meteorological Ocean Values for the Gulf of Maine

Wind Speed (m/s)	Wind Dir. (deg)	Wave Dir. (deg)	Significant Wave Height (meters [m])						Peak Wave Period (seconds [s])						Curr. Dir. (deg)	Current Speed (m/s)					
			Return Period (years)						*Return Period (years)*							*Return Period (years)*					
			1	*5*	*10*	*50*	*100*	*500*	*1*	*5*	*10*	*50*	*100*	*500*		*1*	*5*	*10*	*50*	*100*	*500*
All	253	134	7.1	9.2	10.0	11.9	12.6	14.2	12.2	13.9	14.5	15.8	16.2	17.2	44	0.71	0.88	0.94	1.11	1.18	1.34
0-2	141	118	2.6	3.4	3.8	4.5	4.8	5.5	7.4	8.5	8.9	9.7	10.0	10.7	45	0.52	0.65	0.70	0.80	0.84	0.92
2-4	240	116	3.2	4.1	4.5	5.3	5.6	6.4	8.2	9.3	9.7	10.5	10.9	11.6	48	0.56	0.66	0.70	0.76	0.79	0.83
4-6	286	120	3.6	4.6	4.9	5.8	6.1	6.9	8.7	9.8	10.2	11.0	11.3	12.0	44	0.60	0.69	0.73	0.79	0.81	0.85
6-8	284	118	4.0	5.2	5.6	6.6	7.0	7.9	9.2	10.4	10.8	11.8	12.1	12.8	47	0.59	0.67	0.70	0.75	0.76	0.79
8-10	284	117	4.3	5.4	5.8	6.7	7.0	7.8	9.5	10.6	11.0	11.8	12.1	12.8	44	0.62	0.74	0.78	0.88	0.91	0.98
10-12	289	115	4.6	5.7	6.2	7.1	7.4	8.1	9.8	11.0	11.4	12.2	12.5	13.1	44	0.62	0.74	0.79	0.88	0.91	0.98
12-14	269	116	4.7	5.6	5.9	6.5	6.7	7.1	9.9	10.8	11.1	11.6	11.8	12.1	44	0.61	0.74	0.79	0.90	0.94	1.03
14-16	267	122	5.1	6.2	6.6	7.4	7.7	8.3	10.3	11.4	11.8	12.5	12.7	13.2	42	0.57	0.66	0.69	0.74	0.75	0.78
16-18	245	117	5.1	6.1	6.4	6.9	7.1	7.5	10.3	11.3	11.5	12.1	12.2	12.5	52	0.60	0.76	0.83	0.98	1.03	1.16
18-20	241	109	5.4	6.4	6.7	7.3	7.5	7.8	10.6	11.6	11.9	12.4	12.5	12.8	46	0.54	0.67	0.72	0.83	0.87	0.95
20-22	231	109	5.8	7.1	7.6	8.4	8.7	9.2	11.0	12.2	12.6	13.2	13.5	13.9	56	0.53	0.70	0.77	0.91	0.97	1.11
22-24	218	101	6.1	7.4	7.9	8.7	9.0	9.5	11.3	12.5	12.8	13.5	13.7	14.1	49	0.47	0.59	0.63	0.72	0.75	0.81
24-26	183	101	6.3	7.3	7.6	8.0	8.2	8.4	11.5	12.3	12.6	13.0	13.1	13.3	61	0.44	0.59	0.66	0.80	0.86	0.99
26-28	181	93	6.9	7.9	8.2	8.7	8.8	9.0	12.0	12.9	13.1	13.5	13.6	13.7	57	0.43	0.62	0.70	0.90	0.99	1.20

Table C-2 provides 100 clusters of wind and wave conditions that represent the joint probability distribution for use in fatigue analysis.

Table C-2. Metocean Joint Probability Fatigue Clusters for the Gulf of Maine

Bin Number	Number of Data Points	Cluster Probability	Cluster Centroid					Cluster Standard Deviation				
			Wind Dir. (deg)	Wind Speed (m/s)	Wave Dir. (deg)	Wave Height (m)	Wave Period (s)	Wind Dir. (deg)	Wind Speed (m/s)	Wave Dir. (deg)	Wave Height (m)	Wave Period (s)
1	2,956	0.034218	229	6.5	136	0.83	7.7	5.7	2.5	5.5	0.34	1.4
2	2,366	0.027388	195	8.3	140	0.88	7.8	6.0	2.7	6.8	0.38	1.4
3	2,282	0.026416	270	7.8	137	0.87	6.4	6.8	2.9	7.8	0.34	1.4
4	2,238	0.025906	227	14.7	146	1.17	6.3	6.9	2.5	5.2	0.40	1.3
5	2,026	0.023452	261	5.6	120	0.99	9.8	5.9	2.5	6.3	0.48	1.6
6	2,005	0.023209	168	4.6	128	0.79	7.9	6.8	2.2	7.0	0.33	1.4
7	1,791	0.020732	312	11.9	277	1.52	5.3	6.8	2.5	7.7	0.46	0.8
8	1,788	0.020697	299	6.9	137	1.08	9.1	6.0	2.8	7.5	0.53	1.5
9	1,745	0.020200	323	5.6	127	0.83	6.7	7.4	2.6	8.3	0.32	1.6
10	1,662	0.019239	207	15.3	178	1.25	5.1	6.0	2.2	6.1	0.42	1.0
11	1,662	0.019239	216	5.1	110	0.83	7.5	7.3	2.1	7.3	0.36	1.7
12	1,660	0.019216	124	4.6	119	0.97	9.3	6.2	2.4	7.7	0.51	1.7
13	1,606	0.018591	319	17.3	302	2.47	6.3	6.5	2.5	7.2	0.57	0.8
14	1,597	0.018486	327	8.6	299	1.17	4.7	9.0	2.5	7.7	0.35	0.7
15	1,589	0.018394	1	6.3	111	1.18	10.8	6.0	2.6	6.7	0.57	1.6
16	1,555	0.018000	14	5.8	136	0.88	8.0	7.1	2.8	5.5	0.41	1.4
17	1,525	0.017653	45	5.3	119	1.02	9.6	6.0	2.4	6.9	0.46	1.7
18	1,522	0.017618	341	10.8	139	1.01	7.5	8.0	2.8	8.0	0.45	1.5
19	1,480	0.017132	180	15.4	149	1.29	5.6	6.9	2.8	7.0	0.51	1.3
20	1,427	0.016518	219	11.6	113	1.02	10.5	6.9	2.6	6.7	0.45	1.4
21	1,397	0.016171	242	10.0	223	1.16	4.8	8.8	2.5	7.2	0.48	1.0
22	1,392	0.016113	231	15.1	205	1.62	5.5	6.6	2.1	6.2	0.62	1.0
23	1,353	0.015662	323	5.8	110	1.17	11.0	5.6	2.5	7.4	0.62	1.7
24	1,351	0.015639	89	5.2	124	0.92	7.0	6.9	2.4	6.9	0.42	1.6
25	1,293	0.014967	336	13.6	315	1.78	5.4	7.5	2.0	6.6	0.45	0.7
26	1,256	0.014539	271	14.7	137	2.18	9.3	7.8	2.7	6.7	0.82	2.0
27	1,251	0.014481	188	8.7	182	0.88	4.7	8.3	2.6	9.8	0.34	1.4
28	1,225	0.014180	64	8.0	75	1.20	5.6	6.2	2.5	8.2	0.43	1.3
29	1,221	0.014134	137	9.6	139	1.07	5.6	8.2	2.8	8.4	0.42	1.6
30	1,198	0.013868	237	9.6	183	0.92	4.8	8.1	2.5	6.6	0.32	1.0
31	1,176	0.013613	206	22.6	162	2.00	6.4	7.4	2.6	6.3	0.59	0.9
32	1,170	0.013544	278	12.8	255	1.78	5.6	7.0	2.4	6.1	0.49	0.9
33	1,157	0.013393	226	20.1	183	1.83	6.0	6.3	2.1	7.1	0.65	1.0
34	1,133	0.013115	225	12.8	113	1.06	5.9	7.8	2.6	7.6	0.45	1.5
35	1,091	0.012629	175	5.5	108	0.95	11.1	8.0	2.4	6.1	0.45	1.5
36	1,058	0.012247	68	6.5	150	0.96	7.9	7.8	3.0	8.5	0.49	1.8
37	1,057	0.012235	344	9.7	338	1.26	4.8	8.8	2.7	6.8	0.40	0.8
38	1,019	0.011796	35	9.1	38	1.21	5.0	7.6	2.8	6.3	0.44	1.0
39	983	0.011379	232	6.0	106	0.97	12.4	7.9	2.6	8.4	0.51	1.8

Bin Number	Number of Data Points	Cluster Probability	Cluster Centroid					Cluster Standard Deviation				
			Wind Dir. (deg)	Wind Speed (m/s)	Wave Dir. (deg)	Wave Height (m)	Wave Period (s)	Wind Dir. (deg)	Wind Speed (m/s)	Wave Dir. (deg)	Wave Height (m)	Wave Period (s)
40	970	0.011228	19	7.5	109	1.00	5.9	8.5	3.0	7.0	0.43	1.4
41	943	0.010916	181	10.8	108	1.15	7.9	6.9	2.5	6.3	0.46	1.8
42	914	0.010580	277	7.5	273	1.06	4.6	8.0	2.2	9.0	0.35	0.8
43	910	0.010534	356	12.4	17	1.66	5.5	8.3	1.9	7.0	0.46	0.9
44	889	0.010291	277	12.2	105	1.56	8.8	8.4	2.7	7.7	0.74	2.0
45	882	0.010210	50	13.9	65	2.22	6.7	8.4	2.1	8.1	0.52	1.1
46	872	0.010094	106	13.4	110	1.95	6.5	7.9	2.6	8.1	0.58	1.4
47	849	0.009828	293	11.1	223	1.57	5.8	8.4	2.8	6.8	0.56	1.2
48	842	0.009747	25	10.3	107	2.53	11.4	8.0	2.6	7.6	0.89	1.7
49	838	0.009700	289	5.1	99	1.16	10.8	6.2	2.4	8.5	0.68	2.1
50	782	0.009052	203	18.3	120	1.99	8.8	8.0	2.5	8.5	0.78	1.7
51	770	0.008913	106	7.0	81	1.06	5.4	7.2	2.6	8.6	0.44	1.3
52	758	0.008774	266	15.2	186	1.75	6.4	7.2	2.7	8.0	0.71	1.3
53	746	0.008635	82	5.9	111	1.29	11.7	8.0	2.8	7.9	0.78	1.8
54	736	0.008520	297	18.2	272	2.97	7.1	7.7	2.8	5.9	0.66	1.0
55	716	0.008288	333	12.6	128	1.99	11.8	8.9	2.7	8.0	0.82	1.7
56	703	0.008138	1	9.9	67	1.55	6.2	6.8	2.8	7.7	0.58	1.2
57	697	0.008068	9	7.3	11	0.96	4.5	7.3	2.3	8.0	0.30	0.9
58	667	0.007721	146	18.2	129	2.08	7.1	7.2	2.8	9.5	0.64	1.6
59	631	0.007304	59	13.7	122	2.36	8.6	7.5	2.7	10.0	0.77	1.6
60	618	0.007154	330	11.1	86	1.77	9.2	7.1	2.6	8.4	0.75	1.9
61	585	0.006772	27	6.5	69	1.19	7.0	6.5	2.6	7.5	0.52	1.9
62	554	0.006413	195	6.2	136	1.04	12.7	9.3	2.9	8.9	0.51	1.8
63	554	0.006413	171	27.1	145	3.41	8.1	7.8	3.2	10.2	0.95	1.2
64	541	0.006262	319	7.7	196	0.97	5.7	10.4	3.2	10.5	0.38	1.5
65	523	0.006054	284	18.7	230	3.08	7.3	9.7	2.8	7.7	0.81	1.0
66	522	0.006043	255	6.2	162	1.01	8.8	8.7	2.7	8.4	0.44	1.7
67	508	0.005880	47	19.9	74	3.75	8.5	7.9	2.6	7.9	0.73	0.9
68	499	0.005776	7	16.4	80	3.19	8.7	7.9	2.4	8.3	0.63	1.6
69	490	0.005672	328	6.4	45	0.98	5.5	9.0	3.0	10.0	0.41	1.6
70	480	0.005556	133	5.2	169	0.84	8.4	10.1	2.6	8.3	0.46	2.0
71	430	0.004978	232	10.3	125	2.84	10.8	8.3	2.9	8.7	0.90	1.6
72	430	0.004978	359	18.3	15	2.78	6.7	8.7	2.1	9.2	0.60	0.9
73	343	0.003970	215	14.1	151	1.83	11.3	9.3	2.4	7.8	0.87	1.6
74	338	0.003913	163	5.0	79	0.87	5.7	9.6	2.6	9.5	0.46	1.5
75	309	0.003577	35	6.9	180	0.84	6.6	11.0	3.2	10.8	0.33	1.7
76	308	0.003565	12	22.3	60	4.20	8.6	7.8	2.7	8.9	0.74	1.2
77	307	0.003554	98	17.7	120	3.43	8.6	7.1	2.7	8.7	0.86	1.5
78	305	0.003531	169	11.4	107	3.24	11.7	10.7	3.7	8.8	1.12	1.4
79	304	0.003519	228	21.2	144	3.83	10.0	10.2	3.1	10.0	0.93	1.6

Bin Number	Number of Data Points	Cluster Probability	Cluster Centroid					Cluster Standard Deviation				
			Wind Dir. (deg)	Wind Speed (m/s)	Wave Dir. (deg)	Wave Height (m)	Wave Period (s)	Wind Dir. (deg)	Wind Speed (m/s)	Wave Dir. (deg)	Wave Height (m)	Wave Period (s)
80	272	0.003149	43	19.2	103	5.20	12.7	9.3	3.3	7.2	0.83	1.9
81	262	0.003033	6	7.0	162	1.18	11.3	10.0	3.0	9.3	0.50	1.9
82	236	0.002732	121	24.0	117	4.07	8.9	8.7	3.1	7.9	0.92	1.4
83	166	0.001922	112	13.9	63	2.11	6.6	11.9	3.0	7.3	0.68	1.2
84	135	0.001563	288	8.5	292	1.37	8.1	8.3	3.1	10.1	0.70	2.1
85	129	0.001493	260	4.5	36	0.96	5.8	13.2	2.9	13.3	0.66	1.8
86	128	0.001482	90	26.9	98	6.03	10.5	9.4	3.8	7.4	0.80	1.1
87	123	0.001424	330	9.4	300	1.27	9.5	8.4	3.1	10.1	0.43	1.5
88	123	0.001424	34	28.1	73	6.52	11.0	10.3	2.9	7.9	1.06	1.4
89	109	0.001262	341	24.7	337	4.18	7.7	7.8	3.4	11.8	0.83	1.0
90	98	0.001134	223	5.6	296	0.75	4.3	12.6	2.9	13.3	0.38	1.2
91	70	0.000810	68	6.1	357	1.00	5.3	10.3	3.1	15.0	0.54	2.3
92	63	0.000729	127	7.3	15	1.22	5.6	13.1	4.6	11.5	0.64	1.4
93	57	0.000660	234	8.1	224	0.86	10.2	8.7	2.2	10.6	0.43	1.3
94	37	0.000428	315	23.5	125	2.87	10.5	10.5	3.5	9.8	0.95	2.9
95	30	0.000347	166	10.2	88	0.72	15.9	11.7	4.0	16.6	0.22	1.8
96	14	0.000162	141	7.1	231	0.65	8.9	6.0	3.4	14.6	0.26	5.0
97	6	0.000069	181	8.2	280	0.58	16.9	12.6	4.0	18.3	0.11	1.9
98	2	0.000023	180	35.7	360	6.01	9.5	0.0	1.6	0.0	0.12	0.5
99	1	0.000012	340	8.6	78	0.32	25.0	0.0	0.0	0.0	0.00	0.0
100	1	0.000012	286	2.4	188	0.29	25.0	0.0	0.0	0.0	0.00	0.0

Appendix D. Gulf of Mexico Metocean Details

The team analyzed extreme values by using the fitting method, which provided the most reasonable results for each parameter. Extreme wind speeds were then computed by fitting a generalized extreme value distribution to the monthly maxima. Extreme wave heights were computed by fitting a Weibull distribution to peaks from the hourly time series data using a 4-hour minimum separation between peaks. Extreme current speeds were computed by fitting a Weibull distribution to peaks from the hourly time series data using a 24-hour minimum separation between peaks (the current speed data excluded values exceeding 1.5 meters per second [m/s]). For conditional extreme values, the wave and current time series were filtered based on 2-m/s wind speed bins before doing the monthly maxima. Unconditional and conditional extreme values of wave height, wave period, and current speed for wind speed bins of every 2 m/s are provided in Table D-1.

Table D-1. Conditional Extreme Meteorological Ocean Values for the Gulf of Mexico

Wind Speed (m/s)	Wind Dir. (deg)	Wave Dir. (deg)	Significant Wave Height (meters [m]) Return Period (years)						Peak Wave Period (seconds [s]) Return Period (years)						Curr. Dir. (deg)	Current Speed (m/s) Return Period (years)					
			1	*5*	*10*	*50*	*100*	*500*	*1*	*5*	*10*	*50*	*100*	*500*		*1*	*5*	*10*	*50*	*100*	*500*
All	125	111	4.9	5.8	6.1	6.8	7.0	7.4	10.1	11.1	11.4	11.9	12.1	12.5	68	1.02	1.33	1.45	1.73	1.84	2.10
0-2	144	126	2.0	2.6	2.9	3.5	3.8	4.4	6.5	7.5	7.8	8.6	8.9	9.6	52	0.55*	0.69	0.84	1.09	1.18	1.34
2-4	131	123	2.6	3.2	3.4	3.9	4.1	4.5	7.3	8.2	8.5	9.1	9.3	9.7	62	0.55	0.92	1.05	1.33	1.44	1.69
4-6	131	121	3.0	3.8	4.2	5.0	5.4	6.3	7.9	9.0	9.4	10.3	10.7	11.5	69	0.69	1.01	1.13	1.38	1.49	1.72
6-8	131	119	3.2	3.9	4.1	4.7	4.9	5.4	8.2	9.0	9.3	9.9	10.2	10.6	70	0.76	1.08	1.21	1.48	1.59	1.83
8-10	136	116	3.6	4.3	4.6	5.2	5.5	6.0	8.7	9.5	9.9	10.5	10.7	11.2	69	0.81	1.13	1.24	1.45	1.53	1.70
10-12	133	112	3.8	4.6	4.9	5.5	5.7	6.1	9.0	9.9	10.2	10.8	11.0	11.4	66	0.75	1.10	1.21	1.42	1.50	1.66
12-14	119	98	4.2	4.9	5.2	5.8	6.0	6.3	9.4	10.2	10.5	11.0	11.2	11.6	63	0.59	1.01	1.14	1.39	1.48	1.67
14-16	75	95	4.4	5.0	5.3	5.7	5.8	6.1	9.6	10.3	10.5	11.0	11.1	11.3	60	0.59*	0.96	1.12	1.34	1.41	1.54
16-18	24	80	4.6	5.2	5.3	5.6	5.7	5.9	9.8	10.4	10.6	10.9	11.0	11.1	50	0.59*	0.69	0.91	1.26	1.38	1.61
18-20	340	65	4.8	5.6	5.9	6.3	6.5	6.8	10.0	10.9	11.1	11.6	11.7	12.0	55	0.59*	0.69	0.75	1.11	1.22	1.46
20-22	352	82	5.0	5.9	6.2	6.7	6.9	7.2	10.3	11.2	11.4	11.9	12.1	12.4	61	0.59*	0.69*	0.75*	1.11*	1.22*	1.46*

*Fit issues required alternative methods to fill in these data points.

Table D-2 provides 100 clusters of wind and wave conditions that represent the joint probability distribution for use in fatigue analysis.

Table D-2. Meteorological Ocean Joint Probability Fatigue Clusters for the Gulf of Mexico

Bin Number	Number of Data Points	Cluster Probability	Cluster Centroid					Cluster Standard Deviation				
			Wind Dir. (deg)	Wind Speed (m/s)	Wave Dir. (deg)	Wave Height (m)	Wave Period (s)	Wind Dir. (deg)	Wind Speed (m/s)	Wave Dir. (deg)	Wave Height (m)	Wave Period (s)
1	7,900	0.053529	163	6.9	162	0.88	5.2	4.8	1.6	6.2	0.25	1.0
2	7,430	0.050345	163	11.1	149	1.58	6.3	5.4	1.6	4.9	0.33	0.8
3	6,709	0.045459	139	9.1	130	1.25	6.0	5.8	1.6	4.9	0.30	1.0
4	6,239	0.042275	118	5.5	109	0.82	6.0	5.5	1.8	5.7	0.27	1.3
5	6,155	0.041705	155	5.2	122	0.78	5.8	6.2	1.6	6.1	0.28	1.3
6	4,929	0.033398	164	9.7	119	1.47	6.8	5.9	1.7	5.9	0.36	1.1
7	4,893	0.033154	180	10.6	178	1.49	6.0	6.7	1.6	5.8	0.34	0.9
8	4,746	0.032158	188	5.3	156	0.81	5.4	6.4	1.9	6.2	0.31	1.0
9	4,292	0.029082	129	4.6	149	0.71	5.5	7.0	1.6	6.5	0.26	1.1
10	4,056	0.027483	189	5.9	193	0.74	4.7	6.6	1.8	5.9	0.24	0.9
11	3,835	0.025985	44	9.7	56	1.60	6.2	6.7	1.4	6.7	0.31	0.8
12	3,784	0.025640	65	5.6	92	0.92	6.2	6.1	1.8	6.1	0.30	1.2
13	3,318	0.022482	89	6.4	108	1.13	7.1	5.2	1.9	6.3	0.35	1.3
14	3,272	0.022171	156	14.4	135	2.32	7.5	6.5	1.9	7.2	0.44	0.9
15	3,227	0.021866	122	5.4	76	0.80	5.4	7.2	1.9	5.8	0.30	1.2
16	3,221	0.021825	141	10.4	96	1.60	7.0	6.7	1.8	6.3	0.39	1.1
17	3,166	0.021452	43	5.7	54	0.88	5.2	5.9	1.8	7.0	0.28	0.9
18	2,905	0.019684	88	8.9	78	1.52	6.4	6.6	1.9	6.5	0.43	1.1
19	2,895	0.019616	34	4.6	107	0.84	6.9	6.3	1.8	7.5	0.33	1.2
20	2,891	0.019589	173	5.2	96	0.86	6.7	7.1	2.0	6.2	0.36	1.3
21	2,806	0.019013	85	4.5	132	0.79	6.1	7.5	1.9	6.8	0.32	1.1
22	2,717	0.018410	137	8.5	155	1.38	6.6	6.9	1.7	6.2	0.32	1.0
23	2,604	0.017644	81	5.5	55	0.84	5.0	6.2	1.9	6.9	0.32	0.9
24	2,252	0.015259	145	4.7	192	0.60	4.9	8.5	1.9	7.3	0.24	0.9
25	2,198	0.014893	209	3.9	121	0.68	6.5	8.1	1.7	7.7	0.31	1.2
26	2,196	0.014880	16	9.7	24	1.40	5.4	7.4	1.7	6.4	0.32	0.7
27	2,137	0.014480	25	13.1	37	2.19	6.7	7.0	1.4	6.4	0.32	0.7
28	2,010	0.013619	115	8.5	105	1.72	7.7	5.9	1.7	7.0	0.36	1.2
29	1,901	0.012881	201	8.8	139	1.52	6.9	7.2	2.0	8.3	0.47	1.0
30	1,786	0.012102	55	8.7	95	1.85	8.0	6.5	1.8	6.3	0.38	1.1
31	1,776	0.012034	178	15.0	170	2.60	7.5	6.6	1.9	7.0	0.48	0.8
32	1,766	0.011966	235	4.4	186	0.71	5.0	8.6	1.9	10.0	0.34	1.1
33	1,650	0.011180	356	14.0	355	2.18	6.1	7.6	1.9	7.3	0.41	0.6
34	1,628	0.011031	359	5.2	43	0.83	5.1	10.6	2.0	7.9	0.30	0.9
35	1,505	0.010198	50	13.2	71	2.63	7.6	8.3	1.6	6.7	0.40	0.7
36	1,486	0.010069	207	9.4	206	1.22	5.4	7.8	1.6	7.8	0.34	1.0
37	1,396	0.009459	350	8.1	346	1.03	4.4	9.9	2.5	8.0	0.40	0.9
39	1,370	0.009283	4	11.1	55	1.87	6.8	7.9	1.8	6.7	0.41	0.7
40	1,084	0.007345	19	16.6	39	3.00	7.6	7.5	1.6	7.7	0.35	0.6

Bin Number	Number of Data Points	Cluster Probability	Cluster Centroid					Cluster Standard Deviation				
			Wind Dir. (deg)	Wind Speed (m/s)	Wave Dir. (deg)	Wave Height (m)	Wave Period (s)	Wind Dir. (deg)	Wind Speed (m/s)	Wave Dir. (deg)	Wave Height (m)	Wave Period (s)
41	1,024	0.006938	319	9.3	305	1.20	4.8	9.0	2.4	9.1	0.40	0.8
42	1,020	0.006911	32	10.3	105	1.51	7.5	6.9	1.9	6.8	0.43	1.2
43	1,018	0.006898	4	8.2	99	1.70	8.5	7.1	2.0	6.1	0.46	1.6
44	984	0.006667	292	3.4	153	0.69	6.0	9.8	1.9	9.5	0.37	1.1
45	938	0.006356	344	4.7	93	0.77	6.7	7.6	2.1	7.0	0.31	1.3
46	935	0.006335	142	4.8	104	1.35	9.1	7.3	1.7	6.3	0.45	1.6
47	935	0.006335	124	13.2	116	2.39	7.8	8.1	1.9	8.3	0.47	1.0
48	909	0.006159	256	5.8	131	1.11	7.0	7.6	2.5	9.1	0.46	1.2
49	864	0.005854	65	3.8	174	0.64	5.5	10.3	2.0	8.1	0.33	1.0
50	836	0.005665	330	14.6	314	2.31	6.2	7.1	1.9	7.7	0.44	0.6
51	779	0.005278	3	3.7	154	0.70	5.9	9.5	1.8	9.6	0.36	1.1
52	767	0.005197	263	6.0	253	0.71	4.2	9.7	2.0	11.1	0.30	0.8
53	719	0.004872	283	3.0	95	0.68	6.5	9.0	1.6	12.1	0.36	1.5
54	718	0.004865	152	7.7	63	1.15	5.9	8.2	1.9	7.5	0.40	1.0
55	690	0.004675	314	5.7	111	1.36	8.0	6.9	2.4	8.3	0.56	1.3
56	684	0.004635	352	3.2	115	0.84	7.8	7.3	1.5	5.8	0.39	1.4
57	591	0.004005	29	9.0	145	1.34	7.0	8.5	2.4	9.0	0.45	1.0
58	573	0.003883	339	8.5	137	1.18	7.1	7.9	2.0	7.4	0.41	1.0
59	539	0.003652	195	4.9	234	0.54	4.1	10.6	2.0	8.5	0.21	0.8
60	491	0.003327	48	5.3	8	0.75	4.2	9.4	2.0	8.7	0.33	0.9
61	468	0.003171	341	18.4	338	3.20	7.2	8.1	1.7	9.1	0.45	0.5
62	421	0.002853	232	3.9	72	0.76	5.9	9.8	2.6	10.3	0.53	1.5
63	413	0.002798	199	13.3	201	2.51	7.5	6.7	2.0	9.0	0.41	0.9
64	398	0.002697	121	4.1	36	0.65	4.6	8.2	2.1	9.2	0.38	0.8
65	382	0.002588	179	3.3	49	0.47	4.3	9.2	1.6	11.8	0.27	1.3
66	310	0.002101	337	13.6	123	2.20	8.6	9.5	2.5	9.1	0.55	1.2
67	261	0.001768	300	7.8	184	1.41	6.7	9.9	2.8	9.7	0.54	1.1
68	251	0.001701	316	5.6	236	0.71	4.5	9.6	2.8	12.0	0.36	0.9
69	241	0.001633	297	15.1	273	2.39	6.6	12.6	2.7	10.5	0.61	1.0
70	238	0.001613	120	10.2	162	2.59	9.2	8.5	2.6	7.8	0.55	1.4
71	237	0.001606	21	15.2	90	3.59	9.6	9.2	1.8	5.4	0.60	1.5
72	210	0.001423	221	4.4	106	1.51	9.9	10.1	2.3	6.6	0.59	1.8
73	176	0.001193	342	14.1	178	2.04	7.6	10.3	2.7	11.7	0.59	1.1
74	170	0.001152	258	4.1	343	0.55	3.6	14.4	1.8	12.7	0.39	1.8
75	167	0.001132	241	12.2	193	2.01	6.8	8.2	2.9	12.4	0.49	0.9
76	144	0.000976	46	8.0	103	3.48	12.3	14.3	2.5	7.4	0.52	2.0
77	127	0.000861	270	9.9	141	2.70	8.6	10.5	3.4	10.1	0.65	1.1
78	97	0.000657	13	4.3	231	0.56	4.8	8.4	2.2	14.1	0.28	1.6
79	96	0.000650	83	3.4	226	0.45	4.5	10.6	1.9	11.2	0.18	1.3
80	89	0.000603	22	20.8	52	3.97	8.4	9.1	2.6	8.1	0.45	0.6

Bin Number	Number of Data Points	Cluster Probability	Cluster Centroid					Cluster Standard Deviation				
			Wind Dir. (deg)	Wind Speed (m/s)	Wave Dir. (deg)	Wave Height (m)	Wave Period (s)	Wind Dir. (deg)	Wind Speed (m/s)	Wave Dir. (deg)	Wave Height (m)	Wave Period (s)
81	76	0.000515	98	15.3	130	4.66	10.7	6.6	2.8	10.3	0.76	1.0
82	73	0.000495	164	5.8	328	1.10	4.8	13.1	3.1	12.4	0.50	1.4
83	56	0.000379	57	5.3	110	1.42	14.0	11.1	2.0	5.6	0.61	2.4
84	52	0.000352	160	22.7	157	4.03	8.9	8.7	3.1	13.9	0.72	0.9
85	46	0.000312	154	15.2	47	2.53	7.8	11.3	3.4	13.4	0.56	1.1
86	38	0.000257	51	16.4	136	4.17	11.4	7.3	3.2	6.4	0.86	1.5
87	35	0.000237	192	17.2	221	3.48	8.5	11.5	2.3	14.2	0.67	1.2
88	29	0.000196	142	10.0	146	5.32	10.6	9.7	2.7	13.6	0.98	1.2
89	25	0.000169	330	20.4	75	5.30	10.1	8.2	2.4	8.7	0.53	2.0
90	25	0.000169	81	4.5	295	0.71	6.4	10.1	2.7	9.1	0.38	3.3
91	17	0.000115	286	23.8	46	2.82	8.3	10.9	4.6	7.9	0.58	0.6
92	16	0.000108	130	5.1	104	0.99	20.9	13.3	1.6	9.1	0.36	3.5
93	14	0.000095	113	4.0	271	0.85	14.9	12.7	2.6	9.7	0.41	3.0
94	7	0.000047	62	5.0	268	0.82	23.1	10.3	1.8	7.3	0.40	3.1
95	7	0.000047	152	5.4	279	1.17	23.6	10.6	1.2	3.8	0.28	2.3
96	7	0.000047	98	3.4	19	0.75	11.7	14.8	1.5	10.2	0.26	2.1
97	6	0.000041	183	2.9	301	0.79	19.6	13.0	1.3	22.2	0.22	1.4
98	5	0.000034	298	3.0	269	0.48	15.3	11.2	0.8	12.9	0.09	3.0
99	4	0.000027	173	6.0	222	0.78	16.2	2.9	0.9	15.1	0.24	2.9
100	3	0.000020	39	25.8	252	4.23	7.9	1.0	4.7	8.4	0.25	0.6

Appendix E. Turbulence Intensity Recommendations for Humboldt Bay and the Gulf of Maine

Turbulence intensity values were recommended by Santos et al. (2023) for Humboldt Bay and the Gulf of Maine. These values are conditioned on wind speed and are shown in Table E-1 and Table E-2.

Table E-1. Turbulence Intensity Recommendations for Humboldt Bay From Santos et al. (2023)

Wind Speed (meters per second [m/s])	Turbulence Intensity
0-2	0.4224
2-4	0.1380
4-6	0.0878
6-8	0.0706
8-10	0.0628
10-12	0.0590
12-14	0.0571
14-16	0.0560
16-18	0.0553
18-20	0.0550
20-22	0.0547
22-24	0.0544
24-26	0.0544
26-28	0.0541
28-30	0.0541
30-32	0.0541
32-34	0.0537
34-36	0.0529

Table E-2. Turbulence Intensity Recommendations for Gulf of Maine From Santos et al. (2023)

Wind Speed (m/s)	Turbulence Intensity
0–2	0.4168
2–4	0.1363
4–6	0.0867
6–8	0.0697
8–10	0.0620
10–12	0.0583
12–14	0.0564
14–16	0.0554
16–18	0.0548
18–20	0.0544
20–22	0.0542
22–24	0.0540
24–26	0.0538
26–28	0.0536
28–30	0.0535
30–32	0.0533
32–34	0.0535
34–36	0.0536
36–38	0.0538
38–40	0.0540

Appendix F. Metocean Data: Data Source Overview per Site and Data Coverage

Lists of meteorological ocean (metocean) data sources are shown in the following tables, including time ranges and links to respective sources. It should be noted that the duration of the time range is not necessarily equal to the length of the actual time series. Furthermore, there might be data gaps, due to missing measurement data.

Table F-1. Humboldt Bay: Metocean Data Sources

Region	Data Type	Data Source	Time Range		
			Start	End	Duration (years)
Humboldt Bay	Main metocean data (waves)	National Data Buoy Center (NDBC) station 46022	1982	2022	41
	Secondary metocean data (waves)	NDBC station 46244	2010	2022	13
	Wind data	National Offshore Wind dataset (NOW-23)	2000	2022	23
	Ocean currents	High Frequency Radar Network (HFRNet)	2012	2023	12
	Ocean currents	NDBC station 44032 (E01), University of Maine Ocean Observing System (UMOOS)	2001	2022	22

Table F-2. Morro Bay: Metocean Data Sources

Region	Data Type	Data Source	Time Range		
			Start	End	Duration (years)
Morro Bay	Main metocean data (waves)	NDBC station 46028	1983	2022	40
	Secondary metocean data (waves)	NDBC station 46244	2010	2022	13
	Wind data	NOW-23	2000	2022	23
	Ocean currents	HFRNet	2012	2023	12

Table F-3. Gulf of Maine: Metocean Data Sources

Region	Data Type	Data Source	Time Range		
			Start	End	Duration
Gulf of Maine	Main metocean data (waves)	NBDC station 44005	1978	2022	45
	Secondary metocean data (waves)	NBDC station 44098	2008	2022	15
	Wind data	NOW-23	2000	2020	21
	Ocean currents	NDBC station 44032 (E01), UMOOS	2001	2022	22

Table F-4. Gulf of Mexico: Metocean Data Sources

Region	Data Type	Data Source	Time Range		
			Start	End	Duration
Gulf of Mexico	Main metocean data (waves)	NDBC station 42019	1990	2022	33
	Wind data	NOW-23	2000	2020	21
	Ocean currents	NDBC station 42049 (TABS W)	2010	2020	11

Table F-5. Data Coverage per Metocean Parameter Dataset

	Dataset	Humboldt Bay		Morro Bay		Gulf of Maine		Gulf of Mexico	
Years	Start year	2000							
	End year	2020							
	Covered Years	21	100.00%	21	100.00%	21	100.00%	21	100.00%
Parameters	WDIR10m	21.00	100.00%	21.00	100.00%	21.00	100.00%	21.00	100.00%
	WSPD10m	21.00	100.00%	21.00	100.00%	21.00	100.00%	21.00	100.00%
	WDIR150m	21.00	100.00%	21.00	100.00%	21.00	100.00%	21.00	100.00%
	WSPD150m	21.00	100.00%	21.00	100.00%	21.00	100.00%	21.00	100.00%
	MWD	12.71	60.51%	15.94	75.91%	11.55	55.00%	16.85	80.26%
	WVHT	19.74	93.98%	18.32	87.25%	18.56	88.37%	17.09	81.39%
	DPD	19.71	93.86%	18.32	87.25%	18.56	88.36%	16.97	80.83%
	CDIR	5.35	25.49%	8.46	40.28%	16.31	77.66%	6.72	31.99%
	CSPD	5.35	25.48%	8.45	40.24%	16.32	77.72%	6.72	31.98%
	ATMP10m	21.00	100.00%	21.00	100.00%	21.00	100.00%	21.00	100.00%
	WTMP	15.87	75.59%	18.97	90.34%	15.31	72.88%	15.64	74.46%

Please refer to Table 1. List of Metocean Parameters Considered in the metocean1h File, section 2.1.4 for further information on parameters.

Appendix G. Metocean Data: Content of Raw Data

The content of the provided raw data from the considered sources is listed follows.

G.1 National Data Buoy Center

The following content of raw data was copied from the National Data Buoy Center (NDBC) at https://www.ndbc.noaa.gov/faq/measdes.shtml:

Standard Meteorological Data (h)

WDIR	Wind direction (the direction the wind is coming from in degrees clockwise from true N) during the same period used for WSPD.
WSPD	Wind speed (m/s) averaged over an eight-minute period for buoys and a two-minute period for land stations. Reported Hourly.
GST	Peak 5 or 8 second gust speed (m/s) measured during the eight-minute or two-minute period. The 5 or 8 second period can be determined by payload
WVHT	Significant wave height (meters) is calculated as the average of the highest one-third of all the wave heights during the 20-minute sampling period
DPD	Dominant wave period (seconds) is the period with the maximum wave energy.
APD	Average wave period (seconds) of all waves during the 20-minute period
MWD	The direction from which the waves at the dominant period (DPD) are coming. The units are degrees from true North, increasing clockwise, with North as 0 (zero) degrees and East as 90 degrees
PRES	Sea level pressure (hPa). For C-MAN sites and Great Lakes buoys, the recorded pressure is reduced to sea level using the method described in NWS Technical Procedures Bulletin 291 (11/14/80). (labeled BAR in Historical files)
ATMP	Air temperature (Celsius)
WTMP	Sea surface temperature (Celsius). For buoys the depth is referenced to the hull's waterline
DEWP	Dewpoint temperature taken at the same height as the air temperature measurement.
VIS	Station visibility (nautical miles). Note that buoy stations are limited to reports from 0 to 1.6 nmi.
TIDE	The water level in feet above or below Mean Lower Low Water (MLLW).

Ocean Current Data (a)

DEP01, DEP02, …	The distance from the sea surface to the middle of the depth cells, or bins, measured in meters.
DIR01, DIR02, ...	The direction the ocean current is flowing toward. 0-360 degrees, 360 is due north, 0 means no measurable current.
SPD01, SPD02, ...	The speed of the ocean current measured in cm/s.

Further information: https://www.ncei.noaa.gov/access/metadata/landing-page/bin/iso?id=gov.noaa.nodc:NDBC-CMANWx

Station ID: Five-digit WMO Station Identifier, used since 1976. IDs can be reassigned to future deployments within the same 1-degree square (https://www.ndbc.noaa.gov/faq/staid.shtml).

Hull descriptions: https://www.ndbc.noaa.gov/faq/hull.shtml

Tidal: https://tidesandcurrents.noaa.gov/datum_options.html#MLLW

Wave measurements: https://www.ndbc.noaa.gov/faq/wave.shtml

Wind averaging: https://www.ndbc.noaa.gov/faq/wndav.shtml.

The data are easily accessible via the main website: https://www.ndbc.noaa.gov/ or https://www.ncei.noaa.gov/access/metadata/landing-page/bin/iso?id=gov.noaa.nodc:NDBC-CMANWx. However, without using suitable Python scripts, it is a lot of manual work. The data are available as one single file per year, data type and station, leading to more than 100 files per buoy.

The measurement accuracy (+/-) of different NDBC sensors is defined in Table G-1 (National Oceanic and Atmospheric Administration 2009).

Table G-1. NDBC Measurement Accuracy

Measurement	NDBC Accuracy
Air Temperature	0.09 degrees (deg) Celsius (C)
Water Temperature	0.08 deg. Celsius (°C)
Dew Point	0.31 (°C)
Wind Direction	9.26 deg
Wind Speed	0.55 meters per second
Sea-Level Pressure	0.07 hectopascal
Wave Height	0.2 m
Wave Period	1 s
Wave Direction	10 deg

It should be noted that although the measurement buoy is accessible via NDBC, many stations are operated by different parties, leading to deviations regarding the measurement accuracy, provided amount, and quality of data.

G.2 National Offshore Wind dataset

The HDF5 output files contain the following variables:

- Planetary boundary layer height (meters [m])
- Pressure at 0 m, 100 m, 200 m, and 300 m (pascals)
- Temperature at 2-, 10-, and 20-m intervals between 20 and 300 m, 400 and 500 m (°C)
- Wind direction at 10- and 20-m intervals between 20 and 300 m, and 400 and 500 m (°from north)
- Wind speed at 10-and 20-m intervals between 20 and 300 m and 400 and 500 m (m s-1)
- Friction velocity at 2 m (m s-1)
- Sea surface temperature (°C)
- Skin temperature (°C)
- Surface heat flux (watts / m^2)
- Relative humidity at 2 m (%)
- Inverse Monin-Obukhov length (m-1)
- Roughness length (m).

Additional information located at https://www.osti.gov/biblio/1821404.

G.3 HFRNet - Scripps Institution of Oceanography / NOAA

The HFRNET dataset provides the following parameters:

- time = date/time
- lat = latitude
- lon = longitude
- dopx = longitudinal dilution of precision
- dopy = latitudinal dilution of precision
- hdop = horizontal dilution of precision
- number_of_radials (count) = number of contributing radials
- number_of_sites (count) = number of contributing radars
- u (m s-1) = surface_eastward_sea_water_velocity = surface_eastward_sea_water_velocity
- v (m s-1) = surface_northward_sea_water_velocity = surface_northward_sea_water_velocity.

The dataset can be accessed via two different servers:

NOAA (https://www.ncei.noaa.gov/access/metadata/landing-page/bin/iso?id=gov.noaa.nodc:NDBC-HFRadarRTVector): This server provides the data structure in regions and time steps, meaning that each hour of data is saved in one single file per region. There is another way to access this server, which delivers the time series in the required format; however, it contains a few days of data only.

Scripps Institution of Oceanography (https://hfrnet-tds.ucsd.edu/thredds/catalog.html): The data can be accessed at one location and the entire time series (20 years) can be downloaded. This format is required for the metocean analysis; however, we have often experienced connectivity issues when accessing the server.

Appendix H. List of Public Site Condition Data Sources

Below we have listed helpful publicly available site condition data sources, including those that were not used in the present work.

Table H-1. Meteorological and Oceanographical Public Site Condition Data Sources

Source	Link
National Data Buoy Center (NDBC)	https://www.ncei.noaa.gov/access/metadata/landing-page/bin/iso?id=gov.noaa.nodc:NDBC-CMANWx
National Offshore Wind dataset (NOW-23)	https://www.osti.gov/biblio/1821404
Scripps Institution of Oceanography (High Frequency Radar Network)	https://www.ncei.noaa.gov/access/metadata/landing-page/bin/iso?id=gov.noaa.nodc:NDBC-HFRadarRTVector https://cordc.ucsd.edu/projects/hfrnet/
European Centre for Medium Range Weather Forecasts 5 Reanalysis (ERA5)	https://cds.climate.copernicus.eu/cdsapp#!/dataset/reanalysis-era5-single-levels?tab=overview
U.S. Army Corps of Engineers Wave Information Study	https://wisportal.erdc.dren.mil/

Table H-2. Bathymetry Public Site Condition Data Sources

Source	Link
General Bathymetric Chart of the Oceans (GEBCO)	https://www.gebco.net/
National Centers for Environmental Information (NCEI) Coastal Relief Model	https://www.ncei.noaa.gov/products/coastal-relief-model
National Centers for Environmental Information (NCEI) Digital Elevation Model Global Mosaic	https://www.ncei.noaa.gov/metadata/geoportal/rest/metadata/item/gov.noaa.ngdc.mgg.dem:999919/html#

Table H-3. Soil Conditions

Source	Link
usSEABED: Offshore surficial-sediment database for samples collected within the U.S. Exclusive Economic Zone	https://www.usgs.gov/data/usseabed-offshore-surficial-sediment-database-samples-collected-within-united-states-exclusive#connect
International Ocean Discovery Program (IODP)	https://www.iodp.org/

Table H-4. Other Helpful Sources

Source	Link
Marine Cadastre	https://marinecadastre.gov/
Gulf of Mexico Atlas	New: https://gulfatlas.noaa.gov/ Old: https://www.ncei.noaa.gov/maps/DataAtlas_1985/atlas.html
California Offshore Wind Energy Gateway	https://caoffshorewind.databasin.org/
Mid-Atlantic Regional Council on the Ocean	https://www.midatlanticocean.org/
Northeastern Regional Association of Coastal Ocean Observing Systems	https://www.neracoos.org/

Appendix I. Additional Metocean Analysis Information

This appendix gives further information on the methods and equation we applied to estimating extreme return period based on the giving time series, as described in section 2.2.1.

For the Weibull fit to all peaks, the authors identified the peaks from the entire time series (with a threshold for minimum spacing) and then fit a Weibull distribution to all of them. This approach uses the most data but includes some that may not be relevant to the high return period extremes. This approach can be modified to fit the tail of the distribution to prioritize the high return period data points.

A block maxima approach (Eq. 1) involves dividing the data into regular blocks (such as monthly or yearly), finding the maxima of each block, then performing a generalized extreme value fit to these maxima (DNV GL 2018; Michelen and Coe 2015). It provides a more direct estimation of extremes, but typically has fewer data points to use so it can be less robust for shorter datasets.

$$G(y) = exp\left(-\left[1+\xi\left(\frac{y-\mu}{\sigma}\right)\right]^{-1/\xi}\right) \; if \; \xi \neq 0$$

$$G(y) = exp\left(-exp\left(-\frac{y-\mu}{\sigma}\right)\right) \; if \; \xi = 0 \qquad (1)$$

where:

μ = the location

σ = the scale

ξ = the shape parameter (DNV GL 2018).

The shapes of the distribution change depending on the parameter ξ:

- $\xi = 0$ Gumbel distribution
- $\xi > 0$ Frechet distribution
- $\xi < 0$ Weibull distribution.

The peaks-over-threshold (POT) approach considers all peaks above a chosen threshold value, and fits a Pareto distribution to them. The idea is to extract time series that are long enough to be considered an extreme event (DNV GL 2018). The results can be sensitive to the choice of threshold, which is subjective.

$$G(y) = 1 - \left[1 + \xi\left(\frac{y-u}{\sigma}\right)\right]^{-\frac{1}{\xi}} \; with\; \sigma > 0, y > u \; and \; 1 + \xi\left(\frac{y-u}{\sigma}\right) > 0 \quad (2)$$

Also, in this case, the shapes of the distribution change depending on the parameter ξ:

- ξ = 0 Exponential distribution
- ξ > 0 Pareto distribution
- ξ < 0 Beta distribution.

Appendix J. Soil Conditions: usSEABED Data Content

The list of all parameters (Conservation Biology Institute 2020; Buczkowski et al. 2020) included in the US9_ONE file is as follows. However, it should be noted that not all parameters are available for all locations.

Latitude	Latitude coordinate at sample location
Longitude	Longitude coordinate at sample location
WaterDepth	Water depth at sample location
ObsvnTop	Measured sub-bottom depth information for each point or subsample (top)
ObsvnBot	Measured sub-bottom depth information for each point or subsample (bottom)
LocnName	Location name
DataSetKey	Dataset key (relational link)
LocnKey	Location key (relational link)
ObsvnKey	Sample key (relational link)
Device	Device
DataTypes	Data types
Gravel	Gravel grain size fraction in percentage
Sand	Sand grain size fraction in percentage
Mud	Mud grain size fraction in percentage
Clay	Clay grain size fraction in percentage
Grainsze	Phi characteristic grain size
Sorting	Phi grain size dispersion moment measure standard deviation sorting only
Facies	Seabed class, facies with the maximum fuzzy-membership value > 30%
FacMshp	Class membership, fuzzy membership (%) above class (facies)
FolkCde	Flok code grain size classification
RckMshp	Rock membership, fuzzy membership (%) reflecting percent exposure of rock
VegMshp	Vegetation membership, fuzzy membership reflecting abundance of seaweed and seagrass
Carbonate	Carbonate, including finest to coarsest sampled fractions
MunslColr	Munsell color code
OrgCarbn	Organic carbon in the sample
lShearStr	Undrained compressive shear strength, Log10 KiloPascals
Porosity	Void volume
PWaveVel	Compressional wave velocity
Roughness	A coded output representing the V:H of the roughness element with the greatest aspect ratio
lCritShStr	Critical shear strength
GeolAge	Geological age
ObsvnDetai	Observation details
Key	Key
ObsvnDate	Observation date
DateSrc	Date information

Appendix K. Soil Conditions: usSEABED Analysis Information

This appendix gives more insights how we processed usSEABED data, described in section 2.3.3. The goal is to select and process several usSEABED data points and to estimate representative soil conditions for a larger area. Most locations contain information about the grain size as Krumbein phi scale and the soil classification according to the Folk's classification scheme.

All existing usSEABED data points within a square with a user-defined side length and the target location as center (e.g., offshore wind lease area center) are selected based on the geographical coordinates. The normed distance ($d_{i,norm}$) to the center location is calculated and used to weight the respective data point, w_i, with 1.0 for the closest data point and 0 for the most distant one. Then, the soil ratios for gravel, sand, and mud (in percent) are calculated by first calculating the distance-weighted values per data point, then computing the average per ratio across all data points. The last step involves scaling the ratios so that the sum is again 100%.

First, the weighting factor, w_i, is calculated as follows and used for the calculation of the grain size and the soil for gravel, sand, and mud:

$$w_i = 1 - d_{i,norm}\,, w \in [0,1] \tag{1}$$

The grain size, φ, is calculated with the weighted average:

$$\varphi = \frac{\sum_{i=1}^{N} \varphi_i \cdot w_i}{\sum_{i=1}^{N} w_i} \tag{2}$$

The ratios of each data point are multiplied with the weighting factor, leading to weighted ratios, $r_{ij,w}$:

$$r_{ij,w} = r_{ij} \cdot w_i \tag{3}$$

Then, the weighted mean values (rows i) per ratio (columns j) $\overline{r_{j,w}}$ over all data points are calculated. Afterward, a scaling factor needs to be applied to ensure that the sum of gravel, sand, and mud add to 100%:

$$\overline{r_j} = \frac{\sum_{i=1}^{N} \overline{r_{ij,w}}}{N_j} \cdot \frac{100}{\sum_{j=1}^{M} \overline{r_{j,w}}} \tag{4}$$